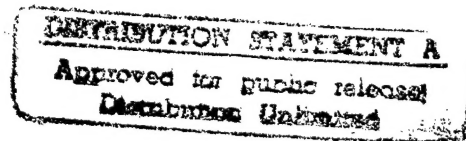VOLUME III
SYSTEMS PHASE

CHAPTER 2
NAVIGATION SYSTEMS

19970117 023

MARCH 1988
USAF TEST PILOT SCHOOL
EDWARDS AFB, CALIFORNIA

Table of Contents

9.1 INTRODUCTION

The development of highly accurate, self-contained inertial navigation systems (INS) has been one of the major engineering accomplishments of the past 50 years. It has taken the combined efforts of hundreds of engineers of all types as well as physicists, mathematicians, metallurgists, skilled craftsmen, and managers to bring inertial navigation to its present advanced state; however, the principles upon which it is based are actually quite simple.

In the simplest terms, an INS is a system which uses Newton's laws of motion and a set of initial conditions to continuously determine the velocity, position, and attitude of the vehicle in which it is contained. The INS differs from other types of navigation systems in that it is completely self-contained, requiring no external references such as radio links, radar contact with the surface of the earth, or measurement of the vehicle's velocity through the air or water. An INS gives the military an accurate non-emitting, unjammable navigation system requiring no ground-based or airborne support. This text presents inertial navigation system principles of operation, error analysis, and flight test techniques.

9.1.1 Fundamental Concepts.

Prior to starting our study of Inertial Navigation Systems and their basic components, it is appropriate to review some fundamental concepts.

From Newtonian physics, recall that a body at rest tends to remain at rest, and a body in motion tends to remain in uniform linear motion unless acted upon by an external force.

Newton's use of the term "at rest" eventually came under heavy criticism. In 1905, Einstein published his paper on the special theory of relativity which shattered the premise of "absolute motion." The new view of things is that nothing is at rest. The body that had been previously defined as being stationary was, in reality, only sharing a velocity with some other object and its coordinate system, all of which was being recorded by an observer who was also going along for the ride (whether the observer was aware of it or not).

The primary measuring device in an inertial navigation system, the accelerometer, bears out the theory. It makes no distinction between "at

rest" and any other fixed velocity. On the other hand, the accelerometer makes a disturbing distinction between truly fixed velocities and those that we like to think of as fixed, but which are, actually, only fixed speeds along curved paths (and all paths are curved, inertially speaking). Velocity is a vector quanitity made up of speed and direction. Therefore, if direction is changing, velocity is changing.

Velocity is a description of a state of motion, a time-rate-of-change of position. A change of velocity—that is, a change in either the magnitude (speed) or the direction of motion—is an acceleration. A body accelerates (changes its state of motion) when, and only when, acted upon by an external force. The body resists changes in its state of motion due to the property of matter known as inertia.

The inertial force displayed by a body under a given rate of acceleration provides a measure of that body known as its mass. Mass is equal to force divided by acceleration.

In the development of an inertial navigation system we are primarily interested in Newton's Second Law. This law states that the acceleration (rate of change of velocity) of a body is directly proportional to the force acting upon the body and is inversely proportional to the mass of the body; i.e., the resultant force is proportional to the acceleration applied to the mass:

$$\bar{F}_I = \frac{d}{dt}(m\, \dot{\bar{r}}_I) \qquad (9.1)$$

where

$\bar{F}_I$ = the force measured in the inertial reference system.

m = mass

$\dot{\bar{r}}_I$ = the velocity vector in the inertial reference system

9.1.2 Coordinate Systems.

For navigation, we are more interested in position and velocity than in acceleration. From calculus, acceleration, velocity, and displacement are related as follows:

$$\dot{\bar{r}}_{P/I} = \int \ddot{\bar{r}}_{P/I}\; dt$$
$$\bar{r}_{P/I} = \iint \ddot{\bar{r}}_{P/I}\; dt\; dt \quad \text{or} \quad \int \dot{\bar{r}}_{P/I}\; dt$$

9.2

where

$\dot{\bar{r}}_{p/I}$ = velocity of the vehicle with respect to inertial space

$\bar{r}_{p/I}$ = displacement of the vehicle with respect to inertial space

These relationships are shown in Figure 9.1 for a simplified one-dimensional case. Of course, for navigation we want to know our velocity and position in terms of earth-based coordinates, not inertial coordinates. A coordinate transformation is therefore necessary. We also have to understand that what the accelerometer senses is total inertial acceleration, not just the acceleration of the aircraft in an earth-based reference frame. Initially then, our task will be to identify an inertial reference frame which we can relate to a navigationally-useful earth-based frame.

ACCELERATION

VELOCITY

DISPLACEMENT
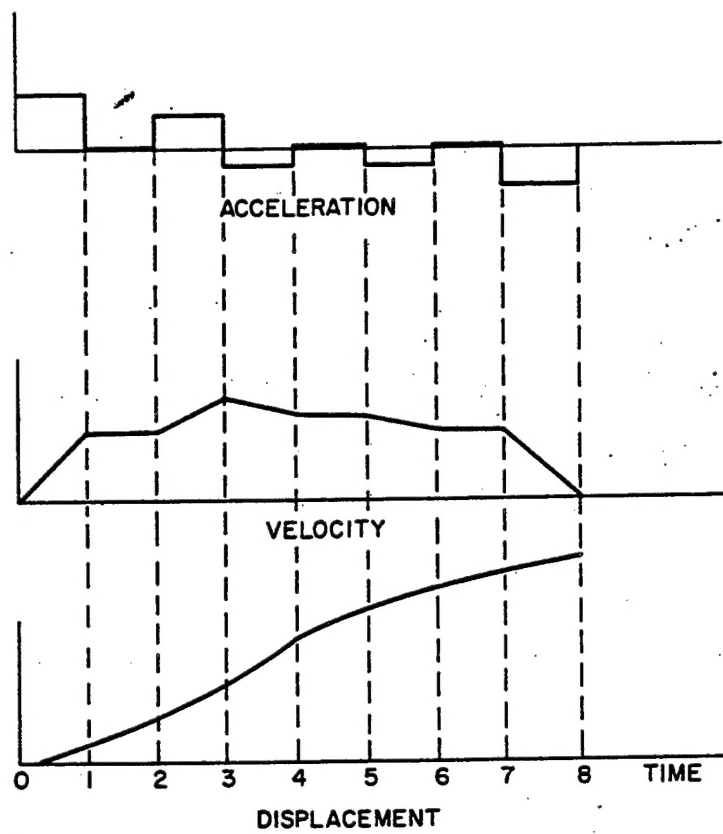
TIME

FIGURE 9.1 ONE-DIMENSIONAL TIME INTEGRAL OF ACCELERATION

9.4

It would appear to be most rigorous to use a coordinate system which is at rest or in a state of uniform motion with respect to the distant galaxies (the so-called "fixed stars") and arbitrarily define this as inertial space. (Actually, these stars may rotate at a rate not in excess of 3×10^{-11} degrees per hour. Such a small rate can be neglected in the navigational problem and in fact cannot be measured with existing instruments.)

A coordinate system could also be selected with its origin at the center of the sun and which is nonrotating with respect to the fixed stars. The motion of the vehicle with respect to the planets could be readily defined in such a system. However, the system would be quite unsatisfactory for describing satellite motion around the earth since the uncertainty in the knowledge of the astronomical unit (the mean distance between the earth and the sun) might be greater than the perturbations in the orbit due to earth oblateness, atmospheric drag, etc.

A less rigorous, but still good, approximation is to utilize an "inertial" coordinate system which is centered at the earth with one axis along the earth's rotation vector but which is not rotating with respect to the fixed stars. The inaccuracy of this coordinate system results from the orbital motion of the earth about the sun and from the precession and the nutation of the earth's spin axis caused by the gravitational torques of sun and moon. The advantage of this system is that it provides a coordinate system residing on the celestial body which exerts the strongest gravitational attraction of the vehicle.

A significant criterion in the location and orientation of a coordinate system is the ease with which measurements can be related between two or more bodies. The measurements are normally related by means of Euler angles which can become quite involved if several angular transformations are required.

Some of the most common types of reference frames used when discussing inertial navigation systems are explained below. (Refer to Figure 9.2.)

1. True Inertial Frame - The true inertial frame is, strictly speaking, the only reference frame in which Newton's Laws of Motion are valid. It consists of a set of mutually perpendicular axes that neither accelerate nor rotate with respect to inertial space.

2. Reference Inertial Frame. One axis lies along the north polar axis, the other two lie in the equatorial plane forming the right-hand set. The origin remains fixed at the center of the earth. Approximates the True Inertial Frame neglecting the earth's revolution around the sun and the motion of the solar system.

3. Geographic Frame. Origin at the inertial navigation system location. This is also called the local navigation frame. Three axes represent north, east, and down (perpendicular to the reference ellipsoid).

(1) Reference Inertial Frame

(2) Earth Frame
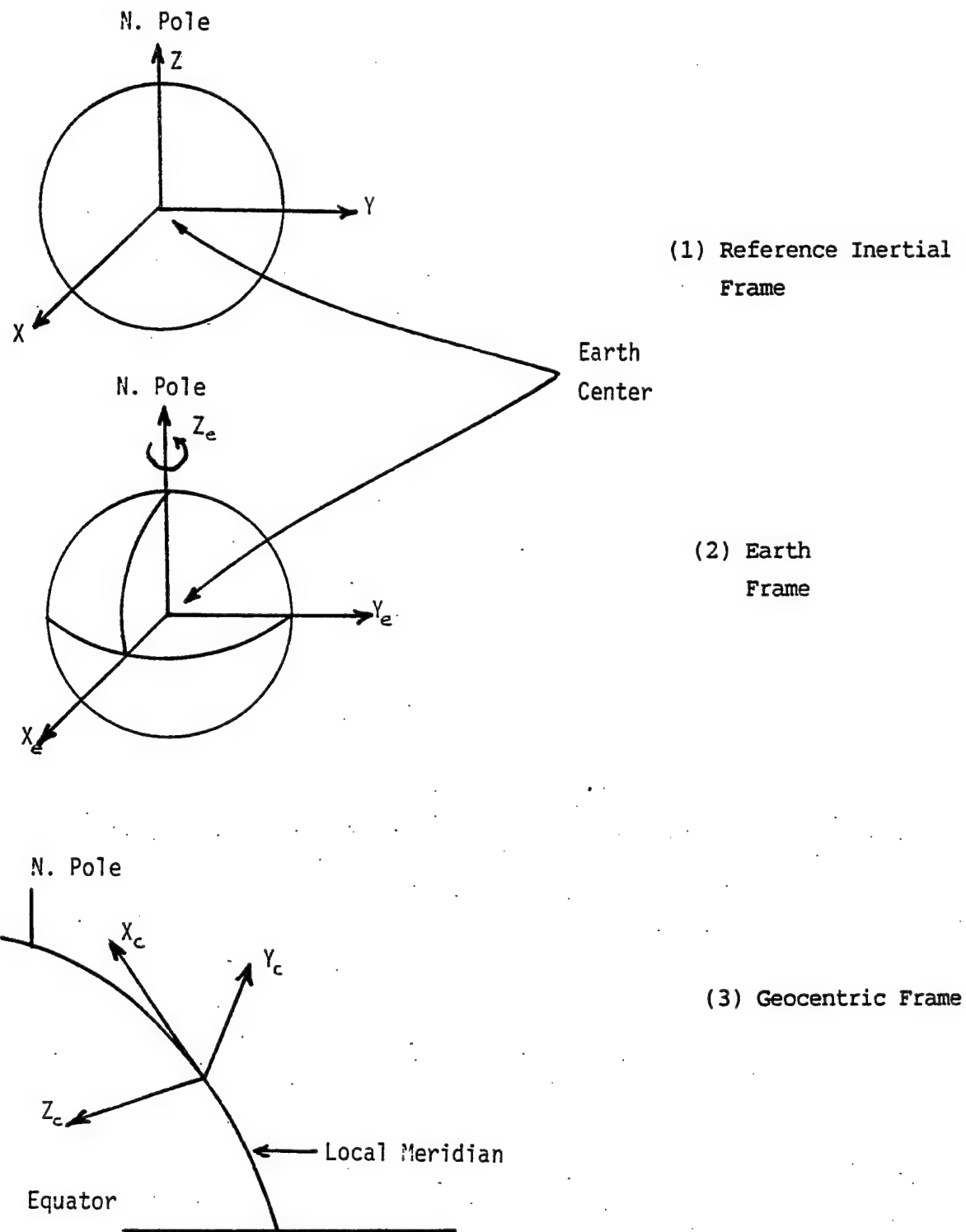
(3) Geocentric Frame

FIGURE 9.2   COORDINATE FRAME GEOMETRY

9.7

4. Geocentric Frame. Origin at the inertial navigation system location, coincident with the geographic frame. The three axes are: x_c, local meridian, y_c, east; z_c, down.

5. Earth Frame. Origin at earth's center of mass. Axes are fixed to the earth and are coincident with the reference inertial axes at time $t = 0$.

6. Body Frame. The roll, pitch and yaw axes of the aircraft. This frame is fixed to the vehicle.

9.1.3 INS Mathematics.

The development of a mathematical expression for the acceleration sensed by INS accelerometers is important because it is the basis by which the real world system must operate. The situation can be described as shown in Figure 9.3: The platform, p, is located in the earth reference frame by position vector $\bar{r}_{p/E}$. The earth is located in inertial space with position vector $\bar{r}_{E/I}$ and rotates about its north-south axis with angular velocity $\omega_{E/I}$.

$$\bar{r}_{p/I} = \bar{r}_{E/I} + \bar{r}_{p/E}$$
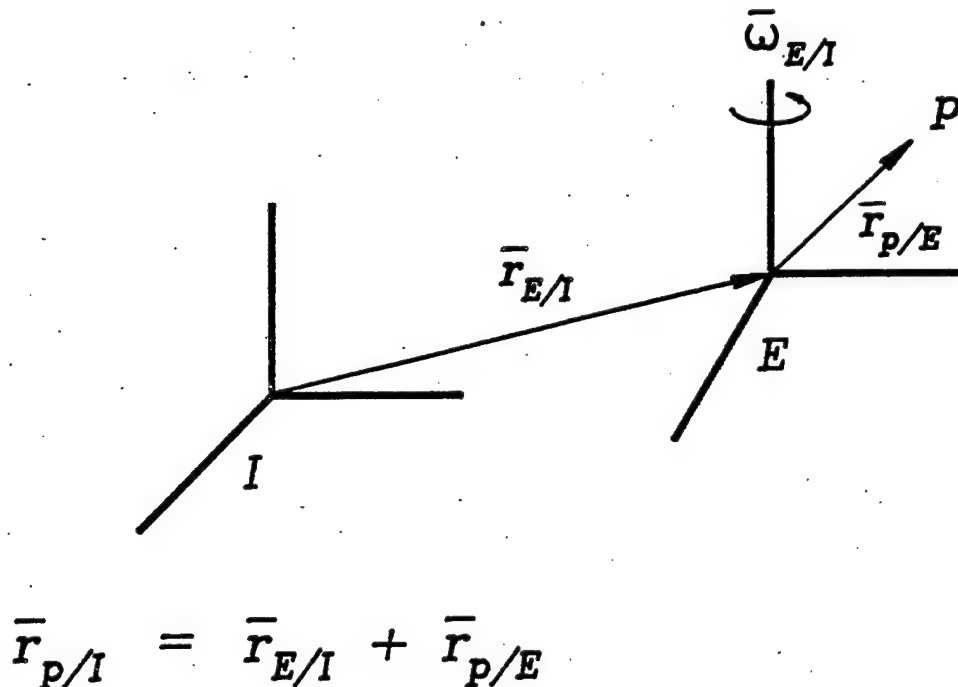
FIGURE 9.3. RELATIONSHIPS BETWEEN INS REFERENCE FRAMES

A useful expression for the quantity measured by the accelerometers can now be derived. Recall from Ops Math that when a position vector in one reference frame (B) is differentiated with respect to another reference frame (C), the resulting expression is:

$$\frac{d\,\bar{r}_{p/B}}{dt}\bigg|_{C} = \dot{\bar{r}}_{p/B} + (\bar{\omega}_{B/C} \times \bar{r}_{p/B}) \tag{9.2}$$

$\bar{r}_{p/B}$ = position vector measured in reference frame B

$\dot{\bar{r}}_{p/B}$ = time derivative of position vector measured with respect to reference frame B

$\bar{\omega}_{B/C}$ = rotation of frame C with respect to frame B (i.e., as viewed from frame B)

The position vector of our navigation system, $\bar{r}_{p/I}$, can be differentiated with respect to the inertial frame as

$$\frac{^I d}{dt}\,\bar{r}_{p/I} = \frac{^I d}{dt}\,\bar{r}_{E/I} + \frac{^I d}{dt}\,\bar{r}_{p/E}$$

From (9.2), the second term is

$$\frac{^I d}{dt}\,\bar{r}_{p/E} = \dot{\bar{r}}_{p/E} + (\bar{\omega}_{E/I} \times \bar{r}_{p/E})$$

then

$$\frac{^I d}{dt}\,\bar{r}_{p/I} = \dot{\bar{r}}_{E/I} + \dot{\bar{r}}_{p/E} + (\bar{\omega}_{E/I} \times \bar{r}_{p/E})$$

9.9

This expression can be differentiated once again with respect to the inertial frame

$$\frac{^{I}d^2}{dt^2} \, \bar{r}_{P/I} = \frac{^{I}d}{dt} \, \dot{\bar{r}}_{E/I} + \frac{^{I}d}{dt} \, \dot{\bar{r}}_{P/E} + \frac{^{I}d}{dt} \, (\bar{\omega}_{E/I} \times \bar{r}_{P/E}) \qquad (9.3)$$

Again using (9.2)

$$\frac{^{I}d}{dt} \, \dot{\bar{r}}_{P/E} = \ddot{\bar{r}}_{P/E} + (\bar{\omega}_{E/I} \times \dot{\bar{r}}_{P/E}) \qquad (9.4)$$

From the chain rule for differentiation,

$$\frac{^{I}d}{dt} \, (\bar{\omega}_{E/I} \times \bar{r}_{P/E}) = \frac{^{I}d}{dt} \, (\bar{\omega}_{E/I} \times \bar{r}_{P/E}) + (\bar{\omega}_{E/I} \times \frac{^{I}d}{dt} \, \bar{r}_{P/E})$$

$$= \dot{\bar{\omega}}_{E/I} \times \bar{r}_{P/E} + \bar{\omega}_{E/I} \times (\dot{\bar{r}}_{P/E} + \dot{\bar{\omega}}_{E/I} \times \bar{r}_{P/E})$$

$$= (\dot{\bar{\omega}}_{E/I} \times \bar{r}_{P/E}) + (\bar{\omega}_{E/I} \times \dot{\bar{r}}_{P/E}) + (\bar{\omega}_{E/I} \times \bar{\omega}_{E/I} \times \bar{r}_{P/E}) \qquad (9.5)$$

Combining (9.3), (9.4), and (9.5), and introducing the variable $\bar{A}$ to represent acceleration,

$$\bar{A} = \frac{^{I}d^2}{dt^2} \, \bar{r}_{P/I} = \ddot{\bar{r}}_{E/I} = \ddot{\bar{r}}_{P/E} + (\bar{\omega}_{E/I} \times \dot{\bar{r}}_{P/E})$$

$$+ (\dot{\bar{\omega}}_{E/I} \times \bar{r}_{P/E}) + (\bar{\omega}_{E/I} \times \dot{\bar{r}}_{P/E}) + (\bar{\omega}_{E/I} \times \bar{\omega}_{E/I} \times \bar{r}_{P/E})$$

9.10

which can be rewritten

$$\bar{A}_I = \bar{A}_{E/I} + \bar{A}_{p/E} + (\bar{\omega}_{E/I} \times \bar{V}_{p/E}) + (\dot{\bar{\omega}}_{E/I} \times \bar{r}_{p/E})$$

$$+ (\bar{\omega}_{E/I} \times \bar{V}_{p/E}) + (\bar{\omega}_{E/I} \times \bar{\omega}_{E/I} \times \bar{r}_{p/E})$$

We can reasonably assume that the earth's rate of rotation is constant, and eliminate one term, yielding

$$\bar{A} = \bar{A}_I = \bar{A}_{p/E} + 2(\bar{\omega}_{E/I} \times \bar{V}_{p/E}) + (\bar{\omega}_{E/I} \times \bar{\omega}_{E/I} \times \bar{r}_{p/E})$$

This important result expresses a good approximation of the acceleration sensed by the accelerometers in an inertial navigation system. Notice that the acceleration which we measure is $(\bar{A}_{p/E})_E$, that is, the acceleration of the platform in the earth reference frame. The other terms represent centripetal and Coriolis accelerations, which result from operating in a non-inertial frame. An expression for $(\bar{A}_{p/E})_E$ can be obtained by noting that it is the acceleration of the vehicle with respect to inertial space less the mass attraction of gravity at the platform:

$$\bar{A}_{p/E} = \bar{A}_I - 2(\bar{\omega}_{E/I} \times \bar{V}_{p/E}) - (\bar{\omega}_{E/I} \times \bar{\omega}_{E/I} \times \bar{r}_{p/E}) \tag{9.6}$$

9.1.4 Geometry of the Earth.

With our Earth reference we position ourselves in terms of latitude and longitude. The shape of the earth is sometimes approximated as a sphere with a diameter of about 7927 miles. The principle geometry is shown in Figure 9.4, where

9.11

L = longitude

λ = latitude

A better approximation for the earth's shape is an ellipsoid of rotation, symmetrical to the earth's spin axis, called a <u>reference ellipsoid</u>. Several reference ellipsoids are in use. The international reference (Hayford ellipsoid) has the following parameters:

Equatorial radius:

$$R_e = 20,926,428 \text{ feet}$$

Polar radius:

$$R_p = 20,855,969 \text{ feet.}$$

Ellipticity:

$$\varepsilon = \frac{R_e - R_p}{R_e} = \frac{1}{297}$$
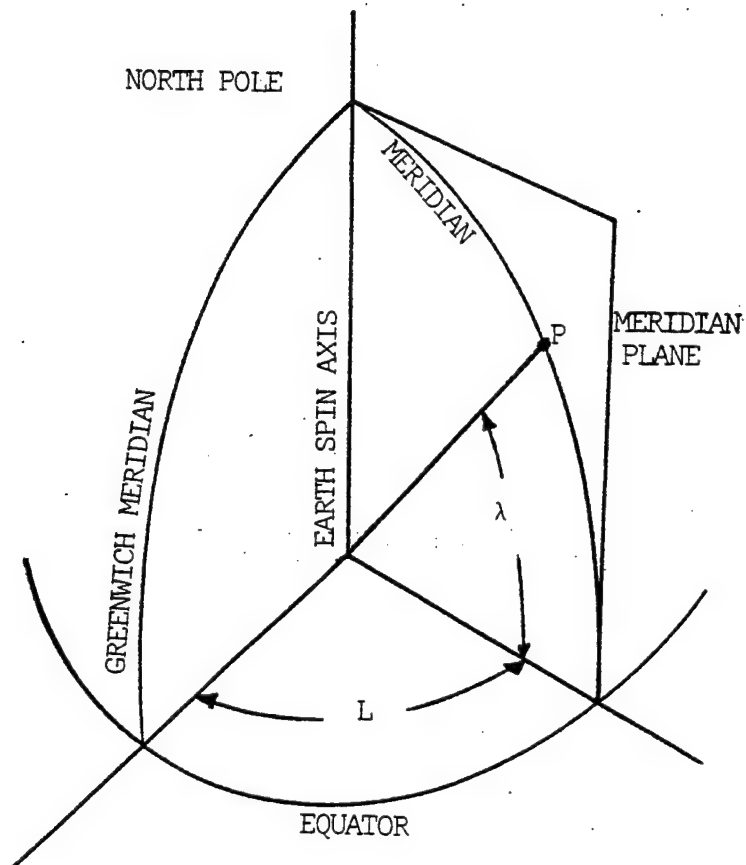
FIGURE 9.4 GEOMETRY OF THE EARTH

The definitions given for the spherical earth also apply to the reference ellipsoid except the definition of latitude. The difference can be seen in Figure 9.5, which shows a cross-section of one section of the ellipsoid. The plane of the figure is a meridian plane.

9.13
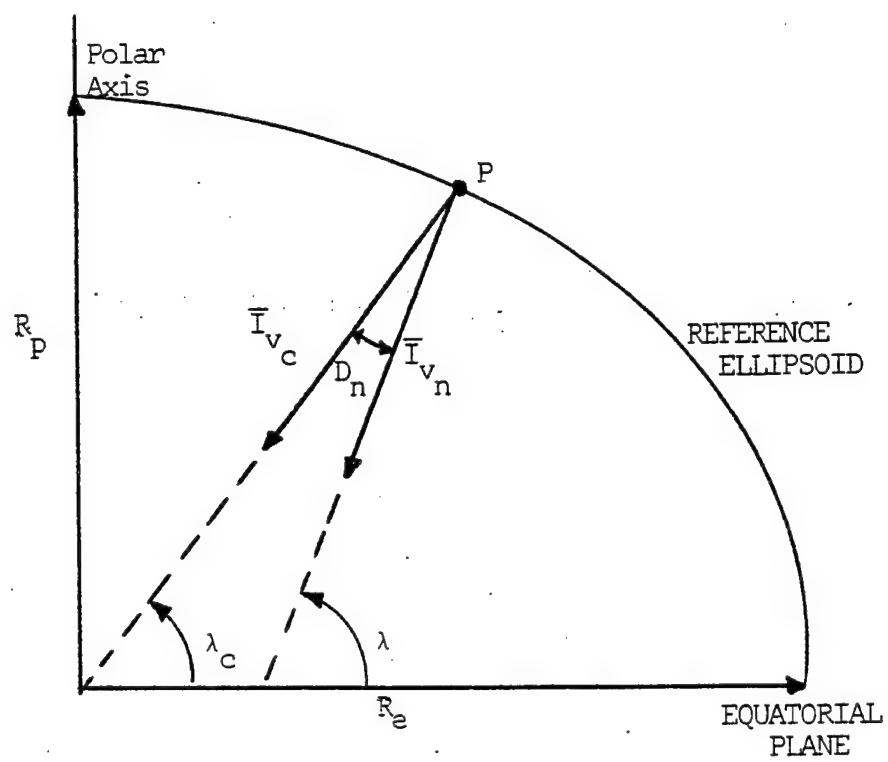
FIGURE 9.5   MEASUREMENT OF LATITUDE

9.14

Point P is a point on the reference ellipsoid.

Definitions:

Geocentric Vertical, $\bar{I}_{vc}$: unit vector directed from point P toward the earth's center.

Geographic Vertical, $\bar{I}_{vn}$: unit vector normal to the surface of the reference ellipsoid. This also defines the direction of the z-axis of the navigation frame.

Geocentric Latitude, λ_c : The angle in the meridian plane between the direction of $\bar{I}_{vc}$ and the equatorial plane.

Geographic Latitude, λ : The angle in the meridian plane between the direction of $\bar{I}_{vn}$ and the equatorial plane. This is the latitude used on most maps.

9.15

Deviation of the Normal, D_η : The angle between $\bar{I}_{vc}$ and $\vec{I}_{vn}$.
Analytically, D_η is given by

$$D_\eta = \lambda - \lambda_c$$

An approximate expression for D_η is given by

$$D_\eta = \varepsilon \sin 2\lambda$$

Using this equation, D_η can be shown to have a maximum value of about 12 arc sec at a latitude of 45 degrees.

9.2 ACCELEROMETERS

The fundamental component of any INS is the accelerometer. Its function is to sense acceleration along its input axis and to provide a proportional electrical output.

The operation of accelerometers is based on Newton's First Law of Motion: A body at rest tends to remain at rest and a body in motion tends to remain in motion. The basic form of the inertial accelerometer consists of a slug (often called a proof mass or test mass) of known mass which is movable in a frictionless slide bearing in a frame and constrained toward null by two equal springs (see Figure 9.6). The presence of acceleration or gravitational force along the frame axis will cause the slug to move against the springs. Deflection, δ, of the slug is the measure of acceleration, and an electrical pick-off (not shown) produces a signal proportional to acceleration.

Typically, three accelerometers are orthogonally mounted on a gyrostabilized element. This configuration is able to sense velocity changes in any direction.
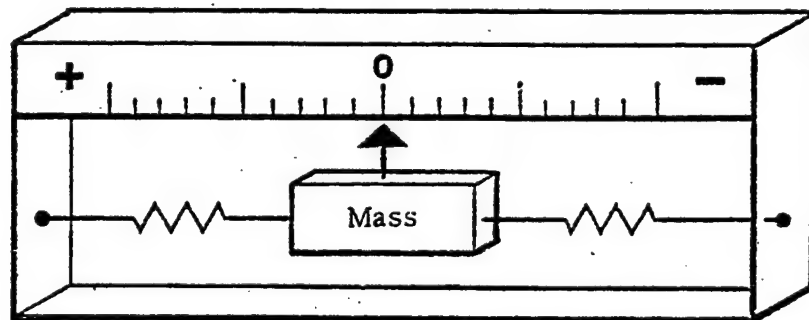
FIGURE 9.6. SIMPLE ACCELEROMETER

9.2.1 The Single Axis Accelerometer

As shown above accelerometers are devices which are capable of measuring acceleration (via inertia). They come in a large variety of shapes and sizes and range from simple mechanical instruments with direct visual readout to highly sophisticated electromechanical precision instruments costing many thousands of dollars each. Whatever their size or complexity, they all work on the same basic principle, that of measuring the inertial "pushing back" of a known mass in response of externally applied forces.

The accelerometer is made up of two primary mechanical parts: a case and a mass (Figure 9.7). The mass is suspended within the case in a manner which permits some amount of restricted movement between the two parts.
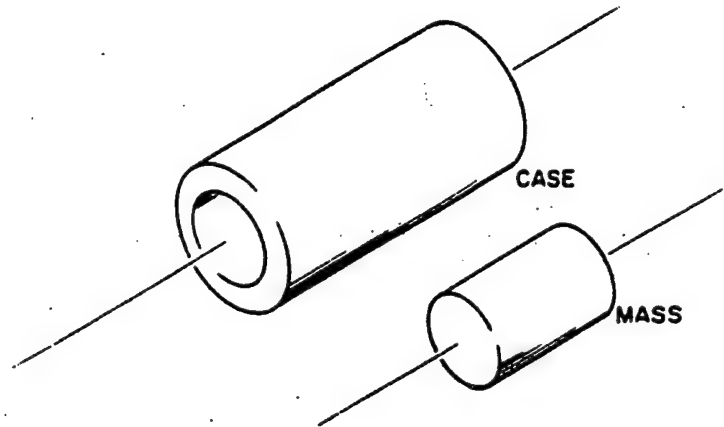
FIGURE 9.7 TWO PRIMARY ACCELEROMETER PARTS

For the sake of illustration, we can imagine a simplified accelerometer constructed of a cylindrical section of tubing and a piston (Figure 9.8). The piston will be free to move longitudinally within the cylindrical case but will be restrained by a pair of centering springs. It is this restrained mass which will be expected to display its inertia.

9.18
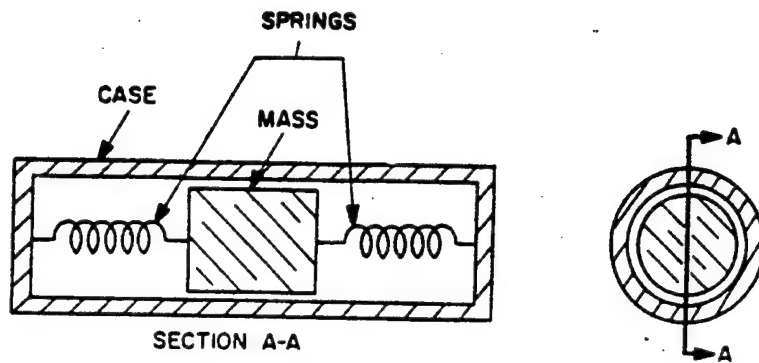
FIGURE 9.8.   SIMPLE ACCELEROMETER (CROSS SECTION)

The mass has a neutral, or null, position within the case where it resides when no external force is acting upon the case—when the accelerometer is not accelerating (Figure 9.9).
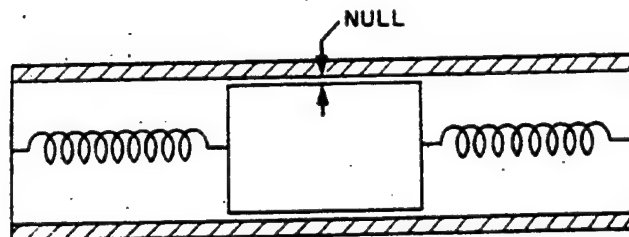
FIGURE 9.9.   ACCELEROMETER (ZERO ACCELERATION)

9.19

It can be seen intuitively that this accelerometer registers the largest displacement in response to those forces applied parallel to the longitudinal axis of the case, the axis along which the relative motion of the two parts takes place. This direction of maximum sensitivity defines the sensitive axis, sometimes called the input axis, of any accelerometer.

Another common acceleration configuration is one having a pendulous mass. Displacement increments in the pendulous accelerometer are angular rather than linear.
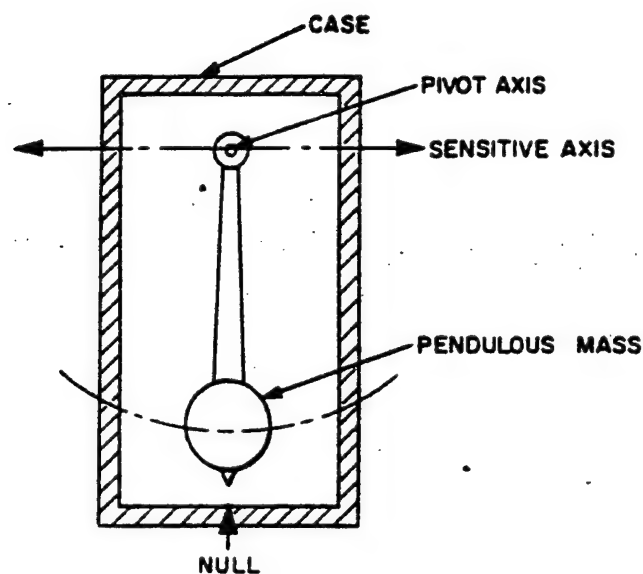
FIGURE 9.10. SIMPLIFIED PENDULOUS ACCELEROMETER

9.20

If an accelerometer produces a true measure of acceleration to a computer, the computer can be relied upon to produce accurate information about the amount of movement the accelerometer has undergone along its sensitive axis. This is an important point. A single axis accelerometer measures only those accelerations paralleling its input axis.

In addition, the centering springs present a linearity problem. If an input is built up in the form of equal increments, the displacement of the mass will build up in correspondingly diminishing increments until the expansion-contraction limits of the springs are reached (Figure 9.11).
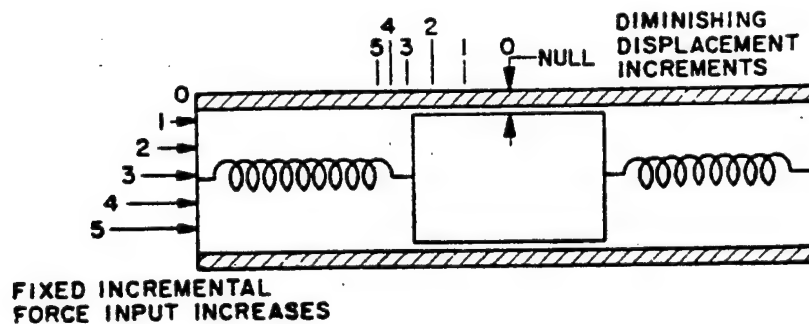
FIGURE 9.11. ACCELEROMETER NONLINEARITY

The pendulous accelerometer shares this shortcoming even if gravity-null is substituted for the centering springs (Figure 9.12).
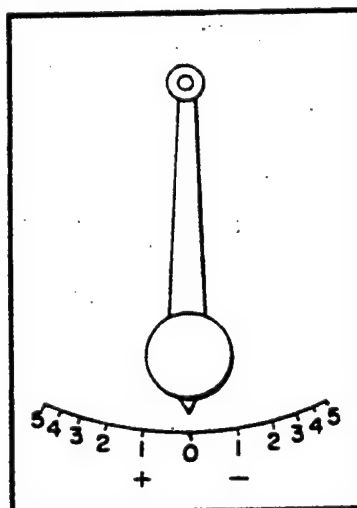
FIGURE 9.12. PENDULOUS ACCELEROMETER NONLINEARITY

9.21

The pendulous accelerometer carries another liability. An accelerometer's sensitive axis is defined by the direction in which the accelerometer is the most sensitive. In the pendulous accelerometer, that direction is perpendicular to the arm of the pendulum (and lying in the plane of rotation). This means that the sensitive axis actually moves when the mass is off the null position, a factor known as sensitive axis shift. At the same time that the pendulous accelerometer becomes less sensitive to forces along its original sensitive axis (when at null), it becomes sensitive to forces at right angles to its original input axis. It's measuring accelerations not assigned to it, a condition known as cross-coupling error.

Fortunately, the same accelerometer mechanization which minimizes nonlinearity also reduces the amount of input axis shift. The scheme is called force-rebalancing or torque-rebalancing. The theory behind the principle is this: take the demodulated amplified accelerometer output signal and use it to drive electromagnets; position the electromagnets in the case to interact with permanent magnets on the accelerometer mass to return the mass toward the null point; after the current has passed through these torquers, drop it across a resistance to develop an analog voltage of acceleration (Figure 9.13).
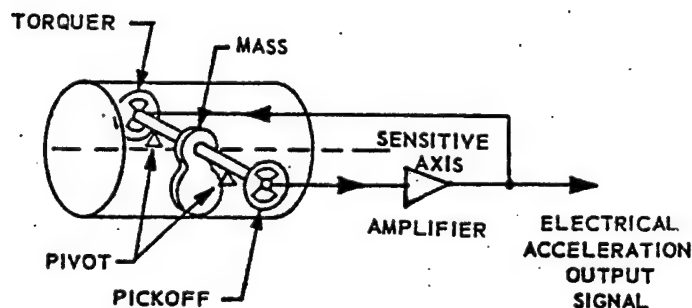
FIGURE 9.13. A SIMPLE FORCE REBALANCING PENDULOUS ACCELEROMETER

9.22

9.2.2 The Two-Axis Measuring Device.

The most direct solution to measuring the forces at right angles to a single axis accelerometer (those lying in its insensitive plane) is to point another accelerometer in that direction. Mounting two accelerometers on a common mounting base with their axes 90 degrees apart creates a functional two axis accelerometer. The two axes of this new device form a rectangular coordinate system defining a plane (Figure 9.14). Any change of motion in that plane will be sensed by one or the other or both accelerometers, each one responsible for one of the two components of that change.
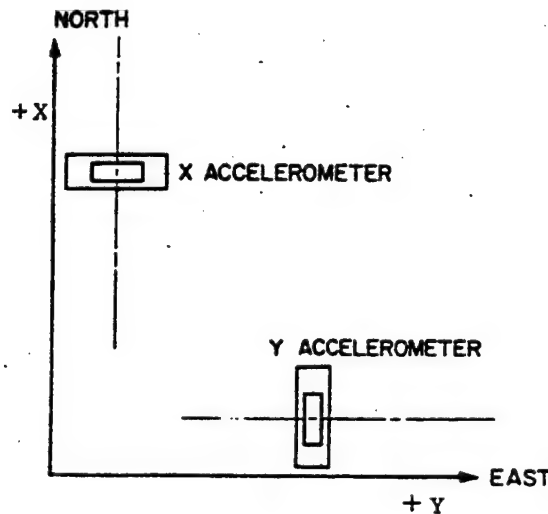
FIGURE 9.14. RECTANGULAR COORDINATE SYSTEM

9.23
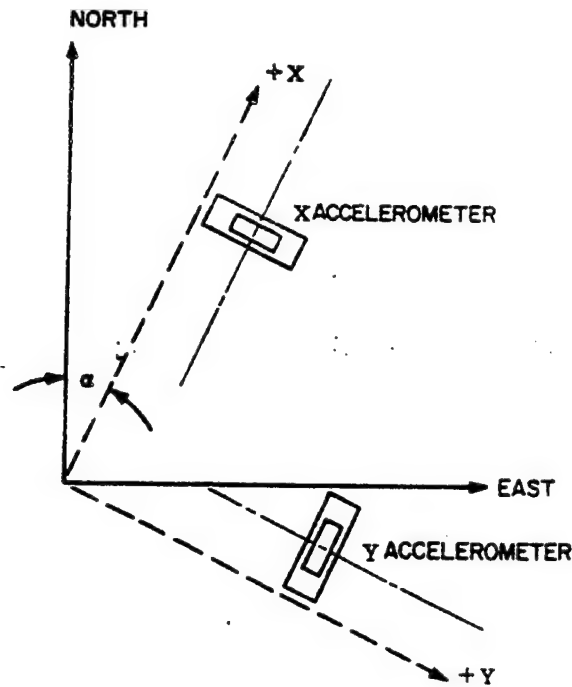
FIGURE 9.15. ROTATED REFERENCE COORDINATES WITH WANDER ANGLE, α

Maintaining a specific angular relationship between the reference and the terrestrial coordinate axes requires a virtually faultless angular stability on the part of both systems.

If parallelism is the required condition, the reference system must be rotated at precisely the same rate at which the earth rotates (relative to "fixed" celestial reference points). The parallel coordinate system appears identical to the rectangular coordinate system depcited in figure 9.14. If the relationship is a variable one (where a "wander angle", alpha, exists as in Figure 9.15), the stability requirements are no less stringent.

It may appear that the angle between the X axis and North (even if it's zero as in the parallel systems) is a measure of where the accelerometer axis is relative to the known north coordinate. But, as far as the operator of a vehicle is concerned, just the opposite is true (i.e., the angle is a measure of where North is with respect to the vehicle). Generally, all other attitude reference indicators in a vehicle carrying an inertial navigation system use the inertial system as the prime reference. In short, the computed alpha angle is measured back from the X axis to provide the estimate of direction North. Alpha had best not be a random variable.

Here, then, is the need. We have a pair of accelerometers on a common mounting base. This assembly must be suspended in a moving vehicle and,

9.24

despite vehicle movement, remain angularly fixed or rotated at a very precise
angular rate. The only known device which displays this sort of angular
stability is a gyroscope—a rapidly rotating mass. More on gyros in Section
9.3.

9.2.3 Accelerometer Characteristics.

The desired characteristics of all accelerometers are essentially the
same. First, you want the instrument to have a low threshold of sensitivity.
This will allow for sensing the smallest acceleration possible. Quality
modern day instruments can sense accelerations as low as .000001 g as compared
to the human body which is limited to about .05 g sensitivity.

An accelerometer should have a wide range of sensitivity. This will
allow for sensing very small accelerations and very large accelerations on the
same instrument. Typical accelerometers can sense as little as $\pm$ .01 g and as
much as $\pm$ 25 g. Accelerometers require a linear output response so the output
will vary in direct proportion to the input. High resolution (the ability to
detect small increments of change in acceleration) is another essential
element for an accelerometer.

9.2.3.1 Accelerometer Performance Parameters and Error Sources.
As discussed
above we want the accelerometer to furnish an output signal directly
proportional to the input acceleration. In practice, however, the output of
an accelerometer is not a perfect representation of the acceleration input.
Instead, there is an error associated with the output which arises from any of
several sources. These accelerometer errors (Figure 9.16) may be classified
as follows:
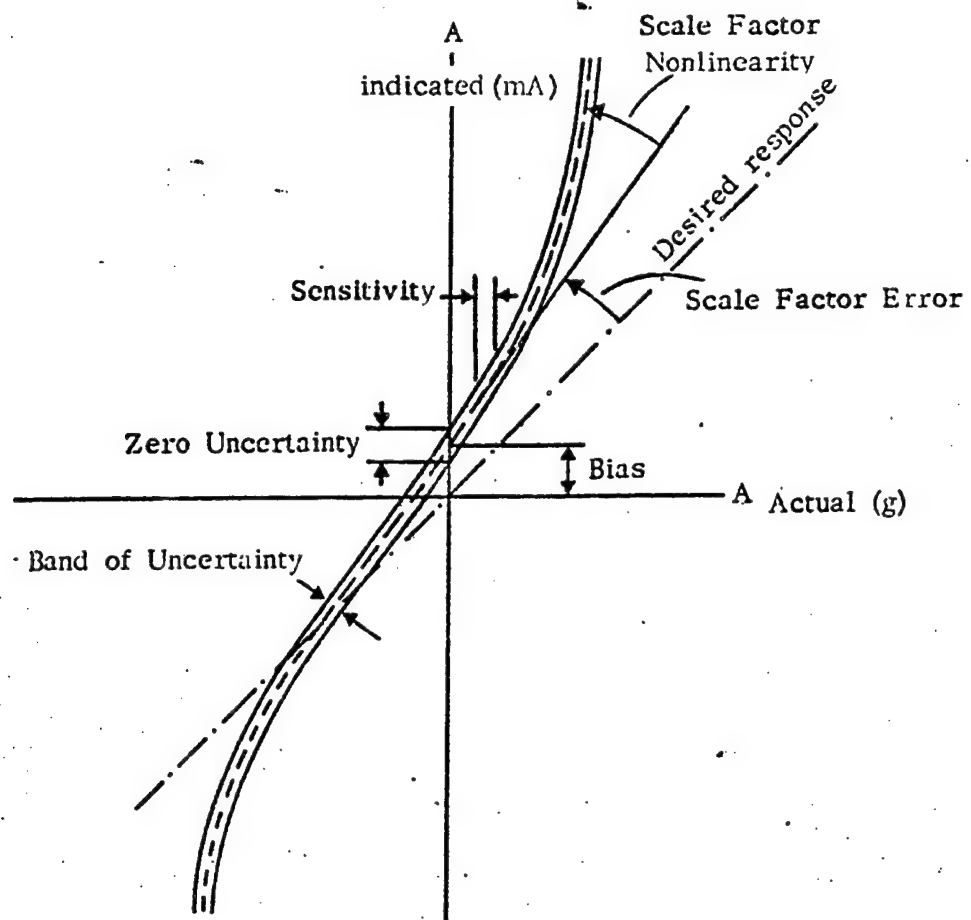
FIGURE 9.16. ACCELEROMETER ERROR DEPICTION

9.2.3.1.1 Bias Errors.

9.2.3.1.1.1 Threshold. Threshold is the minimum acceleration input which causes an accelerometer electrical output. Many inertial applications require a threshold of 1×10^{-6}g or better.

9.2.3.1.1.2 Sensitivity. The sensitivity is the minimum change in acceleration input causing a change in accelerometer electrical output. It is usually assumed that the incremental change is made from an arbitrary, but relatively large input compared to the incremental change.

9.2.3.1.1.3 Bias. Bias is the accelerometer electrical output under conditions of no acceleration input, and is due to the residual internal forces acting on the proof mass after it has been electrically or mechanically zeroed. Bias is expressed by an equivalent error in g's and is usually acceptable if less than 1×10^{-4}g. Frequently it is convenient to express the error in micro g's. An INS can be designed to compensate for known accelerometer bias, provided the bias is stable to within 1×10^{-4}g based on a continuous plot of day-to-day bias over a period of one year.

9.2.3.1.1.4 Zero Uncertainty. Zero uncertainty, also referred to as null uncertainly, is the angle equivalent to the maximum variation in accelerometer output under conditions of zero acceleration input. It is caused by misalignment of the accelerometer mounting pad with the vertical datum with zero feedback current in the circuit. Errors greater than 0.1 millirad amps (20 arc secs) are generally not acceptable for an INS.

9.2.3.1.1.5 Zero Stability. Zero stability, also referred to as null stability, is the random drift of the accelerometer output at zero acceleration input. This drift is caused mainly by fluctuations in bias compensation, but could also be caused by mechanical instabilities. Typical values for an INS are of the order of $\pm$ 10 arc secs, or about one half of the maximum error of 20 arc secs for zero position.

9.2.3.1.2 Scale Factor Errors. The proportionality constant relating the accelerometer input and output is known as the scale factor. This constant has units of

$$\text{VOLTS} \Big/ \text{FT/SEC}^2, \quad \frac{\text{VOLTS}}{g}, \quad \frac{\text{AMP}}{g'} \Big/ \frac{\text{PULSES/SEC}}{g}, \quad \text{ETC}$$

depending on the instrument design.

An uncertainty or shift in the value of the scale factor causes a steady state error in the indicated acceleration. Such an error is proportional to the actual applied acceleration. Thus a scale factor error causes an error in the accelerometer output only when an acceleration is being measured.

9.2.3.1.3 Scale Factor Nonlinearity. In some accelerometer designs, the scale factor itself is not a constant for all ranges of applied acceleration. For example, a nonlinear spring might cause the scale factor itself to vary with acceleration. This type error is known as scale factor nonlinearity, and if not compensated can lead to errors in indicated acceleration which are proportional to the square (or higher power) of the actual acceleration.

9.2.3.1.4 Time Lag. The inertia of a proof mass or a pendulum prevents it from responding instantaneously to changes in acceleration. Instead, it lags such changes, thus causing temporary transient errors in the indicated acceleration. These errors are time dependent and are transient in nature, existing for a short time after any change in acceleration.

9.2.3.1.5 Dynamic Errors. There are two dynamic errors inherent in even a 'perfect' pendulous accelerometer.

9.2.3.1.5.1 Cross Coupling. The accelerometer is sensitive to accelerations along an axis perpendicular to the pendulous axis. If the instrument is subject to accelerations, the acceleration sensed along the input axis will be ax (Figure 9.17) where:

$$A = ax \cos \theta + ay \sin \theta$$

or if θ is small

$$A = ax + ay \, \theta$$

The instrument should be measuring ax, and the term ay θ is thus an error in measurement. This error can be kept small by keeping the gain on the feedback loop high, to keep θ small.
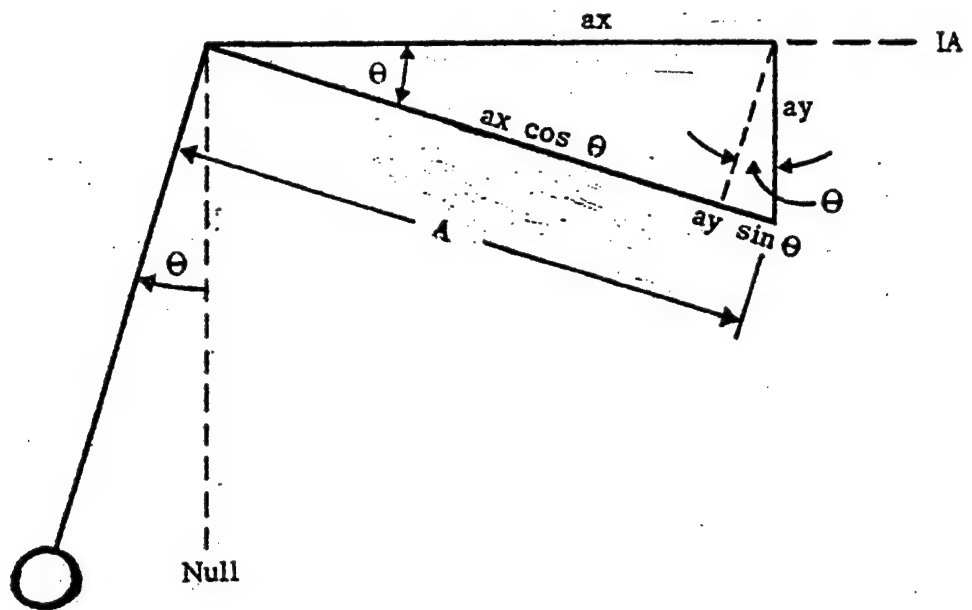
FIGURE 9.17. CROSS COUPLING

9.2.3.1.5.2 Vibropendulosity. This is a source error related
to cross coupling. When the accelerometer is operated in a vibration
environment below the natural frequency of the accelerometer loop, components
of vibration may act along the input axis and perpendicular to the input axis.
This will cause the accelerometer to oscillate about its null.

9.3 GYROSCOPES

The second major element of an INS is the gyroscope. Gyro behavior often impresses the uninitiated as some form of subtle trickery (as witness the continuing prevalence of toy gyros in "novelty shop" surroundings). The spinning wheel appears to adopt a new and peculiar set of laws governing its response to all external forces, including gravity. This response manifests itself in a way which has been traditionally categorized as a pair of gyro characteristics: (1) rigidity (gyroscopic inertia) and (2) precession. But a little thoughtful analysis of what happens when a wheel spins will show that this mass, too, conforms normally to Newton's set of rules governing motion.

9.3.1 Gyroscope Characteristics

9.3.1.1 Rigidity (Inertia). Gyroscopic inertia may be defined as that characteristic whereby the axis about which a wheel turns tends to maintain a fixed direction in inertial space. The amount by which a gyro physically resists those torques tending to realign its spin axis can be increased by any or all of three means: (1) increasing the rate of spin, (2) increasing the mass of the rotor, or (3) increasing the radius of the rotor.

All three are factors governing the size of a quantity called angular momentum, H. As H increases, gyroscopic rigidity increases. Due to size and weight limitations, it is current practice to lean heavily toward increased RPM as a means of increasing H.

9.3.1.2 Precession. Precession is a gyro response characteristic. To precess is to precede, to go before. The term seems to describe the movement of the gyro when it is subjected to torquing forces. To illustrate (Figure 9.18), imagine a wheel with its plane of rotation in this page and its spin axis perpendicular to the page. We'll impart a spin velocity to the wheel and indicate the direction of rotation. If a downward force is applied at any point (indicated by an X) on the rim of the wheel, the greatest amount of downward movement will be at another point (0) on the rim 90 degrees away from the point of application and in the direction of spin (hence the concept of "ahead of", or "before"). The amount of precession resulting from a given torque force decreases as $\bar{H}$ increases.
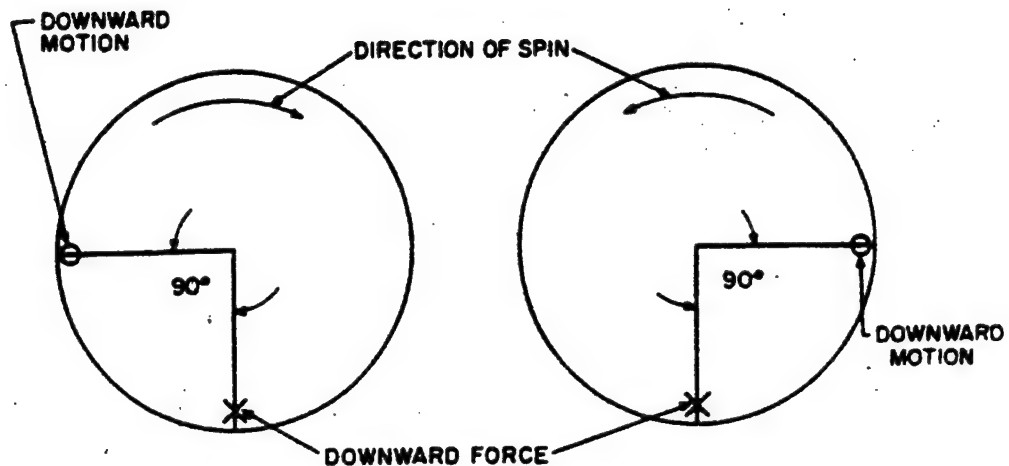
FIGURE 9.18. GYROSCOPIC PRECESSION

9.3.1.3 <u>Application to INS</u>. The characteristic of the gyro that makes it so
useful in INS systems is rigidity. At the same time because of its
characteristic of precession, the gyro can have very precise torques applied
to it to cause a precise amount of precession. So the gyro can be spun up
with a certain alignment relative to inertial space and then this alignment
can be maintained by always applying the right amount of precession to the
gyro. Gyros are then used to provide an inertial reference system for
measuring acceleration, velocity, and position. The gyros themselves are
acting as angular motion sensors.

Conventional gyros have had extensive application in missiles and/or
aircraft. In a conventional gyro the spinning mass (called a rotor or spin
motor) may be supported either by a framework of gimbals or by a gas bearing.
The gimbals or gas bearings provide freedom of rotation of the mass about
several axes. In the gimballed gyro, bearings are mounted in each gimbal
providing for spin of the rotor and also for rotation of the mass
perpendicular to its spin axis. The rotors of conventional gyros are normally
driven by electricity.

9.31

Conventional gyros may be classified in two subcategories according to the degrees of freedom through which the rotor can turn or by the angular measurement which the gyro can make. A single degree of freedom gyroscope is one which is free to rotate about one axis normal to its spin axis. Similarly, a two degree of freedom gyro is free to rotate about two axes each normal to its spin axis. A two degree of freedom gimballed gyro is depicted in Figure 9.19.

Since a gyro spin axis does not move in space and is isolated by means of gimbals or a gas bearing from its case, a gyro can be used to measure angular motion between the rotor and the case. Depending upon the configuration of the gyro, this measurement may be angular rate, angular displacement or the integral of angular displacement.
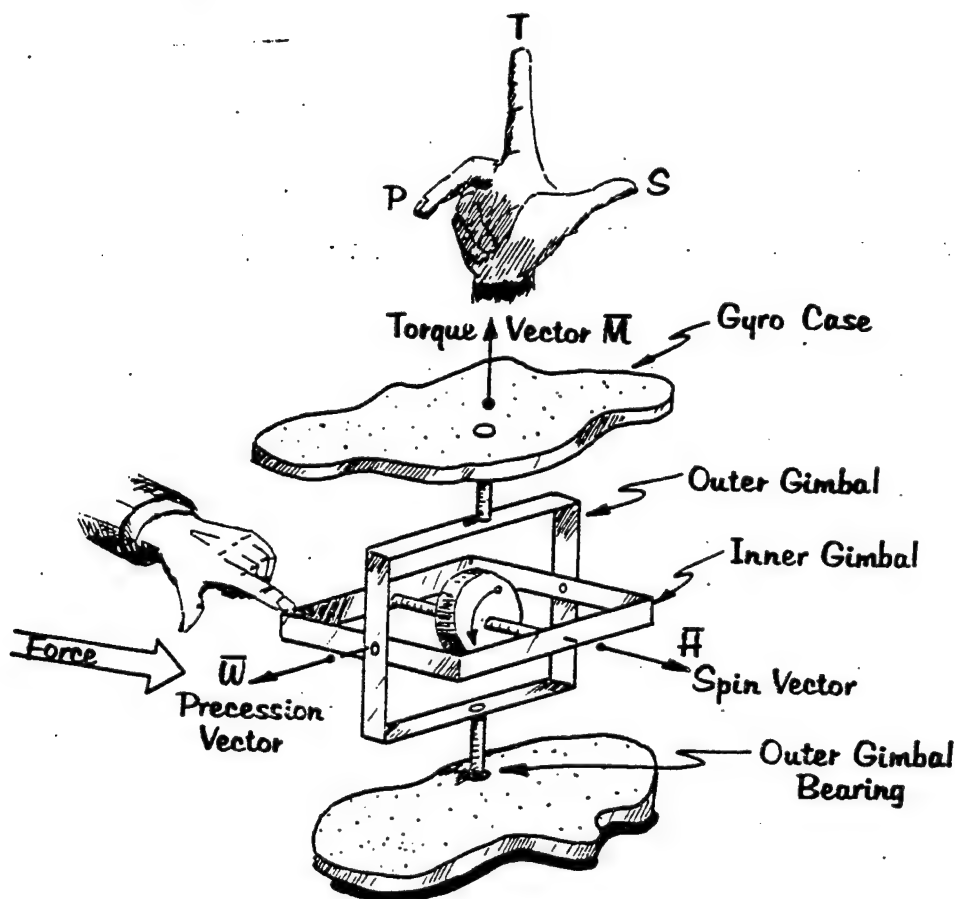
FIGURE 9.19. PRECESSION OF A TWO DEGREE OF FREEDOM GIMBALLED GYRO

9.32

9.3.2 Gyroscopic Theory

For those that lack a basic understanding about gyrodynamics and wish to be exposed to the theory of gyros the following section is written. If you accept those ideas presented in the introduction to this section, then skip the following discussion on gyroscopic theory and move on to the discussion of gyro classification.

Theoretically, there is a simpler means of establishing a stable reference frame than using a gyroscopic device. In theory, an inertial frame of reference about three axes could be established by a body that is "perfectly" supported. An example of such an apparatus might be a massive ball supported in a frictionless socket as shown if Figure 9.20.

The practical obstacle to such a device arises from the fact that significant disturbing torques will inevitably be present. These unwanted torques are caused by unbalance, imperfect geometry of the ball or the bearing, friction and other causes. A _torque impulse_ (torque x time) represented by a vector $\bar{T}t$ imparts an angular momentum increment identical to

$$\bar{T}t = \Delta \bar{H} = I\,\bar{\omega} \tag{9.7}$$

where I is the moment of inertia of the ball.
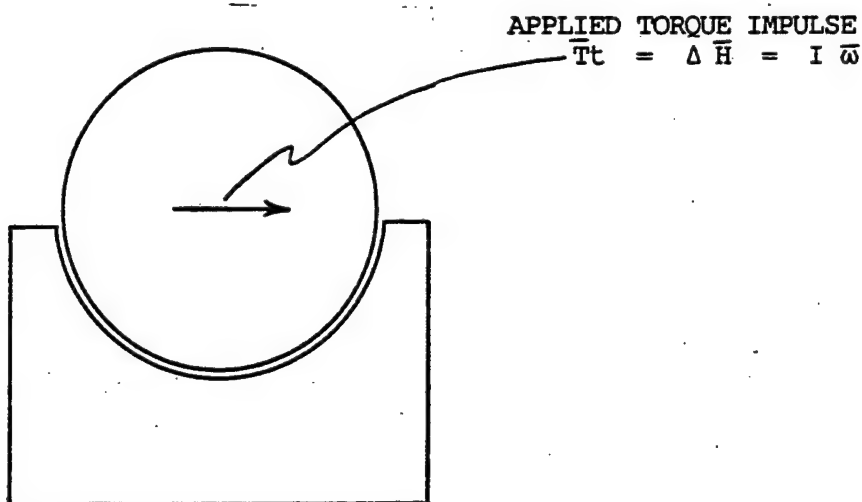
FIGURE 9.20 INERTIAL FRAME CREATED BY A BALL AND FRICTIONLESS SOCKET

9.33

If the ball is spun about the vertical axis a very large angular
momentum H is imparted to it. Then an incremental disturbing torque Tt is
added vectorially to the built-in angular momentum resulting in an angular
deflection ω_t, but not in a cumulative error. These vectors are shown in
Figure 9.21.
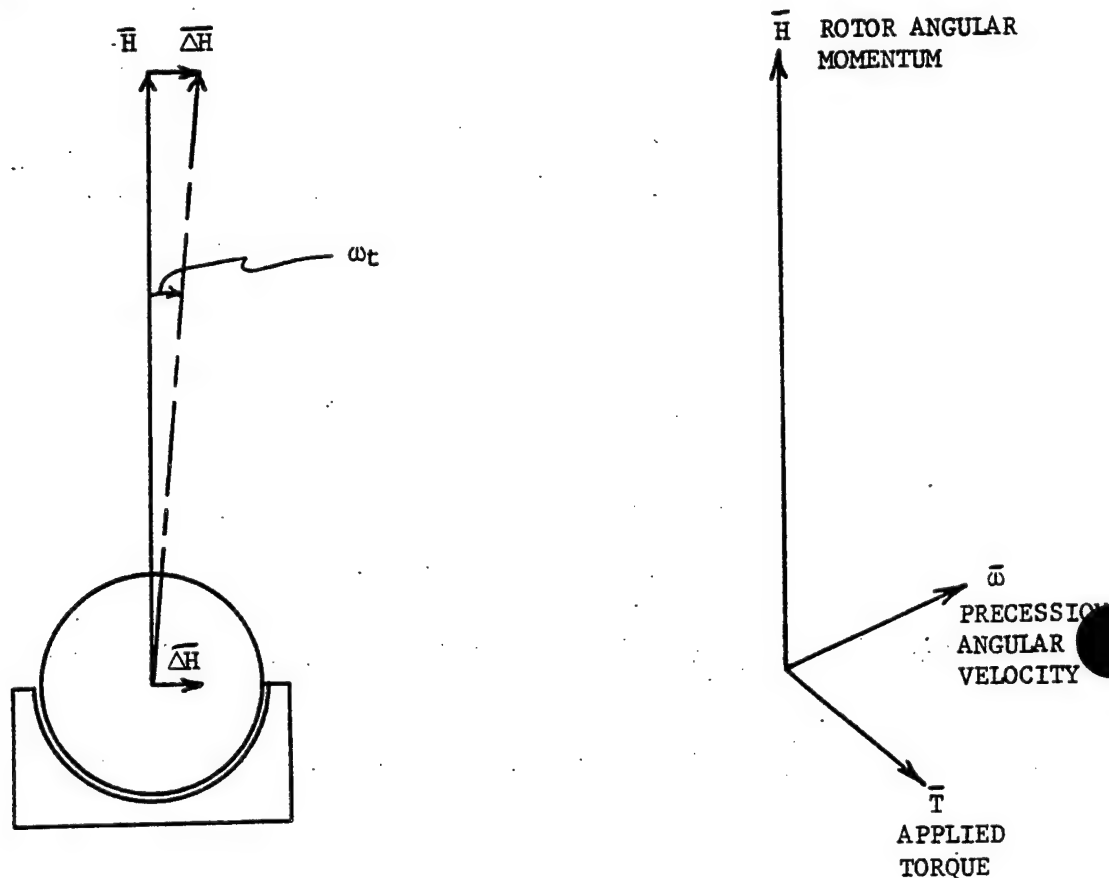
FIGURE 9.21 GYRO VECTORS

Spinning the ball has made a gyro out of the device. This behavior
represents obedience of the gyro to Newton's second law expressed as a cross
product in rotational form as

$$\overline{T}t = \overline{\omega}_t \times \overline{H} \tag{9.8}$$

where

$\overline{T}t$ = Applied torque

9.34

$\overline{H}$ = Rotor angular momentum

$\overline{\omega}_t$ = Angular velocity of precession

$\overline{H}$ = I $\overline{\omega}_s$

I = Rotor moment of inertia

$\overline{\omega}_s$ = Rotor angular spin rate

The gyro's rotation imparts three curious properties to the device:
   a. It has made the rotor stiff, or rigid against angular deflections
       (rigidity in space).
   b. If a torque is applied about an axis which is transverse to the spin
       axis, the rotor turns about a third axis which is at right angles to
       the others (precession).
   c. On removing the torque, the rotation (precession) ceases—unlike the
       case of an ordinary wheel and axle where the wheel keeps on rotating
       after the torque impulse is removed.

These phenomena, all somewhat surprising when first encountered, are
consequences of the laws of motion. Figure 9.19 depicted these actions. The
direction of rotational vectors such as spin, torque, and precession can be
shown by means of the right hand rule. If the curve of the fingers of the
closed right hand point in the direction of rotation, the thumb extended will
point along the axis of rotation. For gyro work it is convenient to let the
thumb, forefinger, and middle finger represent the spin, torque, and
precession axes respectively.

The law of precession is a reversible one. Just as a torque input
results in an angular velocity output, an angular velocity input results in a
torque output along the corresponding axis.

The manipulation of the restraints acting upon the rotating body converts
it into a usable reference instrument. These restraints are either torques or
angular freedom limiters for the spin axis. Gyro design then becomes a matter
of properly choosing these restraints to make the instrument do a specified

job. Rate, rate integrating, and integrating are the three general gyro
classifications. A more complete explanation will follow.

As an example of the right hand rule, the spin vector illustrated in
Figure 9.19 is to the right because the thumb points that way when the fingers
are closed about the direction of rotor spin. If the right hand rule for gyro
precession is applied to this gyro, it is evident that the gyroscope will
precess in a counterclockwise direction if viewed from the left (along the
inner gimbal axis).

9.3.2.1 Gyro Axes. As previously discussed, three gyro axes are significant
in describing gyro operation: the torque axis, the spin axis, and the preces-
sion axis. These are also commonly referred to as input (torque), spin, and
output (precession).

The direction of these axes is shown in Figure 9.22 and is such that the
spin axis rotated into the input axis gives the output axis direction by the
right hand rule.
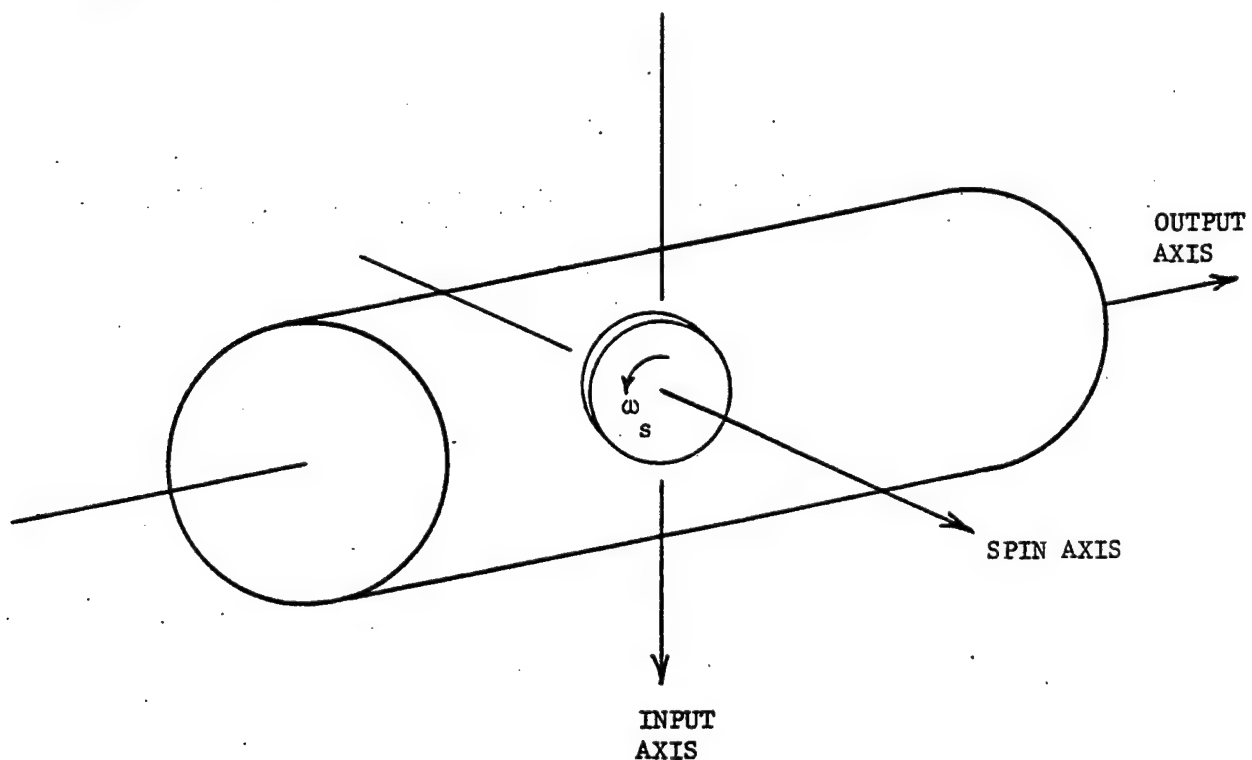
FIGURE 9.22. GYRO REFERENCE AXES

9.36

9.3.2.2 <u>Gyro Classification</u>. A gyro is generally classified by the degrees of freedom that it possesses. A single degree of freedom gyro is one that is restrained so that it is free to precess about just one axis (single degree of freedom gyros can be further classified as rate gyros, rate integrating gyros, and integrating gyros). A two degree of freedom gyro is one that is free to rotate about two axes, not counting its spin axis. Two degree of freedom gyros are also known as displacement gyros.

The gyroscope depicted in Figure 9.23 is a single degree of freedom gyro because it is free to precess only about the z axis. Notice that its operation depends on the phenomena of gyro precession. Two degree of freedom gyros are used to measure vehicle angular displacement in both guidance and control systems. Their operation depends on the phenomena of the gyro rotor's stability in inertial space. A two degree of freedom gyro is depicted in Figure 9.24. If both of the sets of bearings (i.e., the bearings along the x and z axes) are frictionless, then there can be no torques translated to the rotor. Therefore, the rotor will remain fixed in space. The gyro case is again mounted rigidly to the structure of the vehicle. Since the rotor is fixed with respect to inertial space, when the vehicle rotates there will be relative motion between the rotor and the case. This motion may once again be measured by use of position pick-offs. As seen in Figure 9.24, angular displacement can be sensed only about two axes (y and z). Consequently, two gyros with two degrees of freedom are required to measure rotation about three axes. This provides a redundant measurement about one axis.

The vertical (attitude) gyro and the directional gyro which are found <u>in</u> <u>most airplanes are examples of two degree of freedom gyros used for flight</u> <u>control systems</u>. The vertical gyro is mounted with its spin axis up and therefore senses deviation of the airplane in roll or pitch. The directional gyro is mounted with its spin axis horizontal and senses deviations in yaw (roll sensing is available but not used in this application).

Since the earth is continuously rotating there must be a method for torquing a vertical gyro so that it remains aligned along the local vertical. Otherwise, it would tend to remain fixed in inertial space. This is commonly done by means of a pendulous reference such as a plumb bob which is mounted directly on a gimbal, say the outer gimbal in Figure 9.24. (The figure must be rotated 90 degrees so that when viewed for this application, the direction of the x or spin axis points to the top of the page.) When this gimbal is not

horizontal, a signal is generated by the pendulous reference. The signal is used to torque the gyro electrically until the outer gimbal is horizontal, thereby making the spin axis vertical.
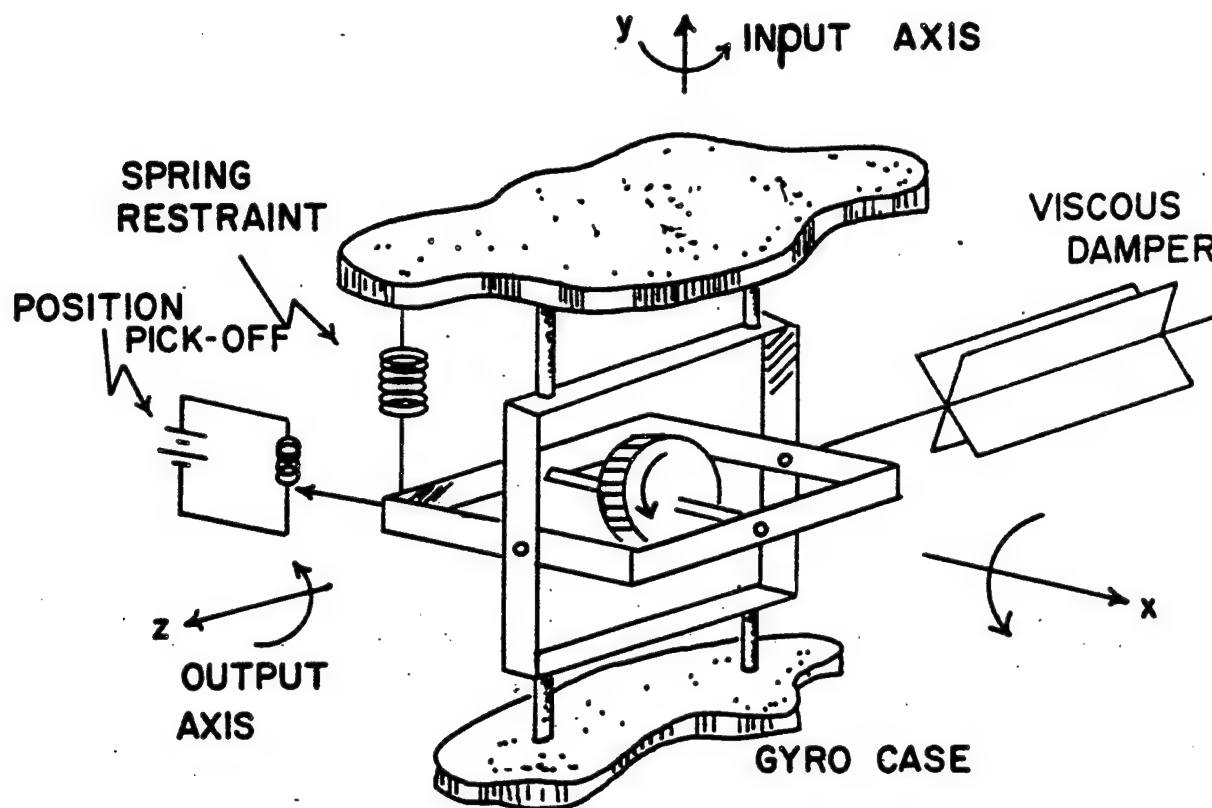
FIGURE 9.23. SINGLE DEGREE OF FREEDOM RESTRAINED GYRO
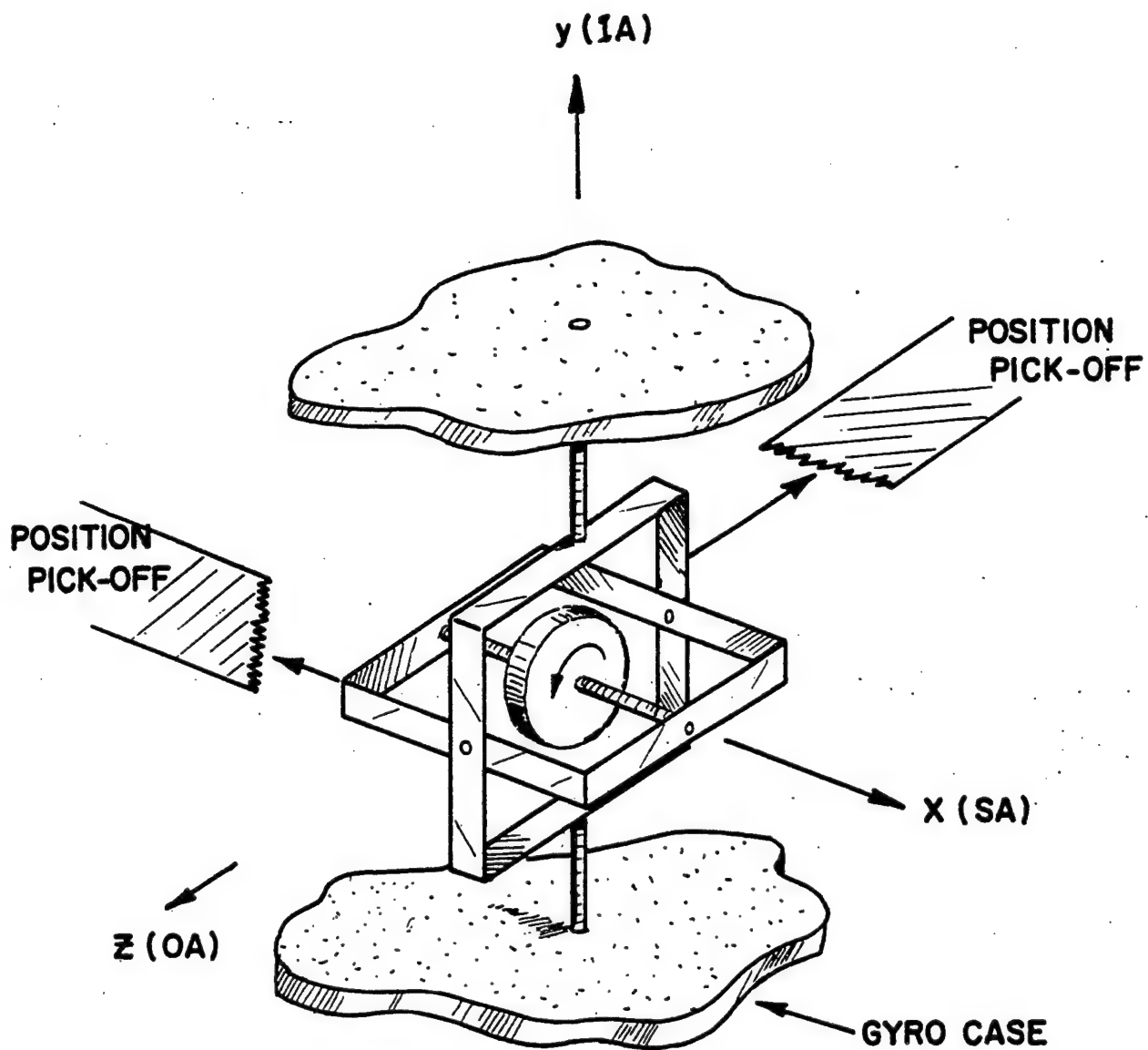
FIGURE 9.24. TWO DEGREE OF FREEDOM GYRO

Table 9.1 below gives a comparison between Single Degree of Freedom gyros (SDF) and Two Degree of Freedom gyros (TDF).

PROPERTY	SDF	TDF
Number required in INS platform	3	2 (one redundant axis)
Gyro Gain	Normally controlled by fluid viscosity	Nil (output=input)
Cross-Coupling	Limited input axis movement minimizes cross-coupling	No cross-coupling
Vehicle movement detection capability	Detected by input axis movement	Detected by gimbal axis movement
Accuracy	0.003°/hr - 0.1°/hr	Same as SDF

TABLE 9.1.   COMPARISON OF SDF AND TDF GYROS

9.3.2.3 Conventional Gyro Design. The spinning mass (rotor) of a precision gyro is normally located inside a cylinder or sphere which has been filled with an inert gas such as nitrogen. The cylinder or sphere is constrained to rotate about one or two axes by bearings. One axis may be an input axis for gyro torquing or output axis for gyro precession. It is evident that the output of the gyro will be significantly affected by output axis torques. Uncertainty in these torques will affect the accuracy of a guidance or control system. Consequently, the cylinder or sphere (called the float) containing the rotor is frequently floated in a fluid in order to minimize the load and thus the torque on the gimbal bearings of the output axis (see Figure 9.25). For most high accuracy gyros one hundred percent flotation is achieved using high viscosity florocarbons. Silicone is normally used for rate gyros. Beryllium is often used as primary material for the float and the rotor because of its low density, ruggedness and thermal stability.

The flotation fluid performs an additional function of providing damping about the output axis. The viscosity of the fluid will change with temperature. Consequently, most high accuracy floated gyros are heated to very close tolerances (within one degree Fahrenheit) at all times to maintain

constant damping. Other types of gyros utilize a change in temperature to mechanically control the damping. If the temperature increases, the viscosity decreases and the fluid expands. This expansion is utilized to mechanically decrease the damping gap between the float and the case and therefore compensate for the lower viscosity. The net result is a nearly constant damping factor. However, such control generally provides less gyro accuracy than that achieved by fluid temperature control.

The rotor angular momentum is a significant factor in gyro design. A high angular momentum is desirable in order to minimize the effect of output axis torques and improve the gyro response (gain). Angular momentum is normally expressed in $gm - cm^2/sec$. Typical values of angular momentum range from 10^4 to 10^7 $gm - cm^2/sec$. Gyro rotors are normally supported by ball or gas bearings. Examples of rotor spinup techniques include the use of AC hysteresis motors, DC motors, or an air blast directed at the rim of the rotor.

The single degree of freedom gyro depicted in Figure 9.25 shows a signal generator at one end and a torque generator at the other end of the float. This is a HIG type gyro which stands for Hermetic Integrating Gyro. This type of gyro is often used in missile control systems and inertial guidance systems. In the HIG gyro, jewel bearings are used to provide low friction centering of the float about the output axis. Other types of gyros utilize gas or liquid bearings and two degree of freedom floated gyros often utilize gyro torsion wires to provide centering of the float.

A typical two degree of freedom gyro is depicted in Figure 9.26. Such a gyro has an obvious advantage in that only two gyros are required to establish a reference system. In addition, precise viscous damping is not as critical as for the single degree of freedom gyro since in theory no damping is required for gyro operation. However, a two degree of freedom gyro is subject to certain additional drift errors which are caused by cross coupling of drifts between the two sensing axes. In addition to centering the float and the gimbal ring, the torsion wires carry electrical current to activate the rotor and the electromagnets in the float which are used for pick-offs and torquing. Note that since there are two orthogonal sensing axes, there are two orthogonal pick-offs and two torquers. Normally, these two functions are combined in one unit, a gyro requiring two of these, each containing a pick-off and a torquer.

9.41

Another type of two degree of freedom gyro that has found extensive application is the gas bearing free rotor (or gimbal—less) gyro depicted in Figure 9.27. The spherical rotor is supported by viscous drag forces which are generated when it turns inside the case. Helium or hydrogen is normally used to provide the gas bearing. The moment of inertia of the rotor is made large by the inclusion of a conducting flange which also acts as the rotor of an induction motor. Therefore, no external connections between the rotor and the case are necessary. It is necessary to hold the rotor and the case in close alignment. When the case moves with respect to the inertially fixed rotor, the relative movement is sensed by four capacitive pick-offs. The resulting signal is amplified and transmitted to torquers which apply a torque by means of electrostatic or induction forces in order to precess the gyro back into alignment with the case. This same signal, which is proportional to the angular motion of the vehicle, is transmitted to the guidance system.
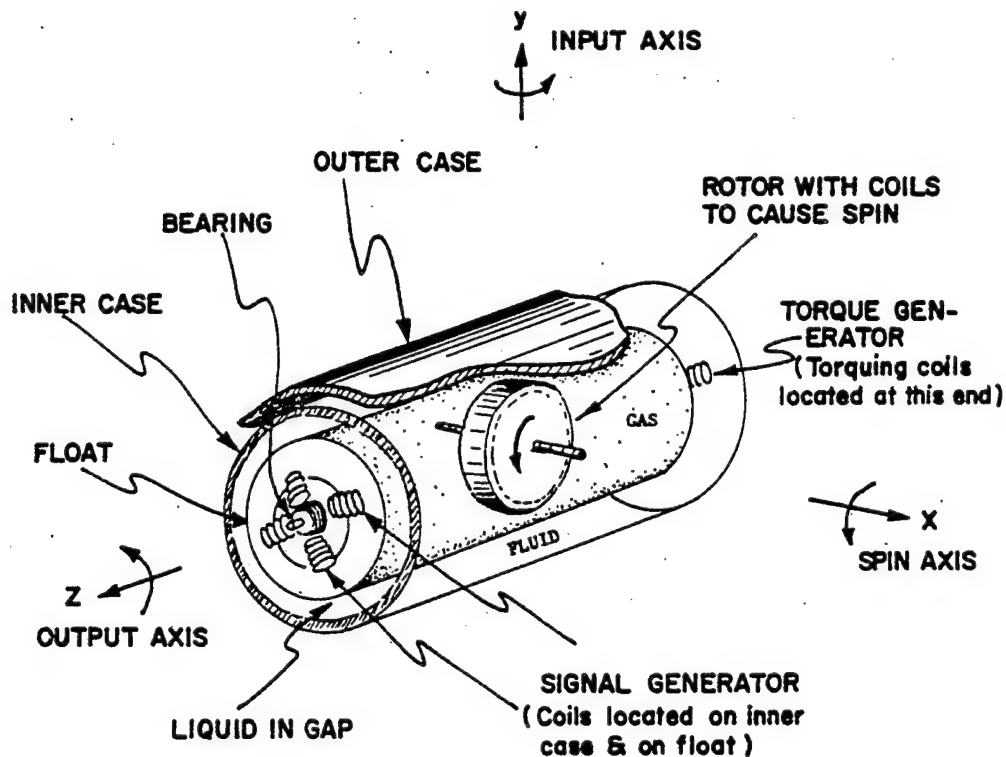
FIGURE 9.25. TYPICAL SINGLE DEGREE OF FREEDOM GYRO

9.42
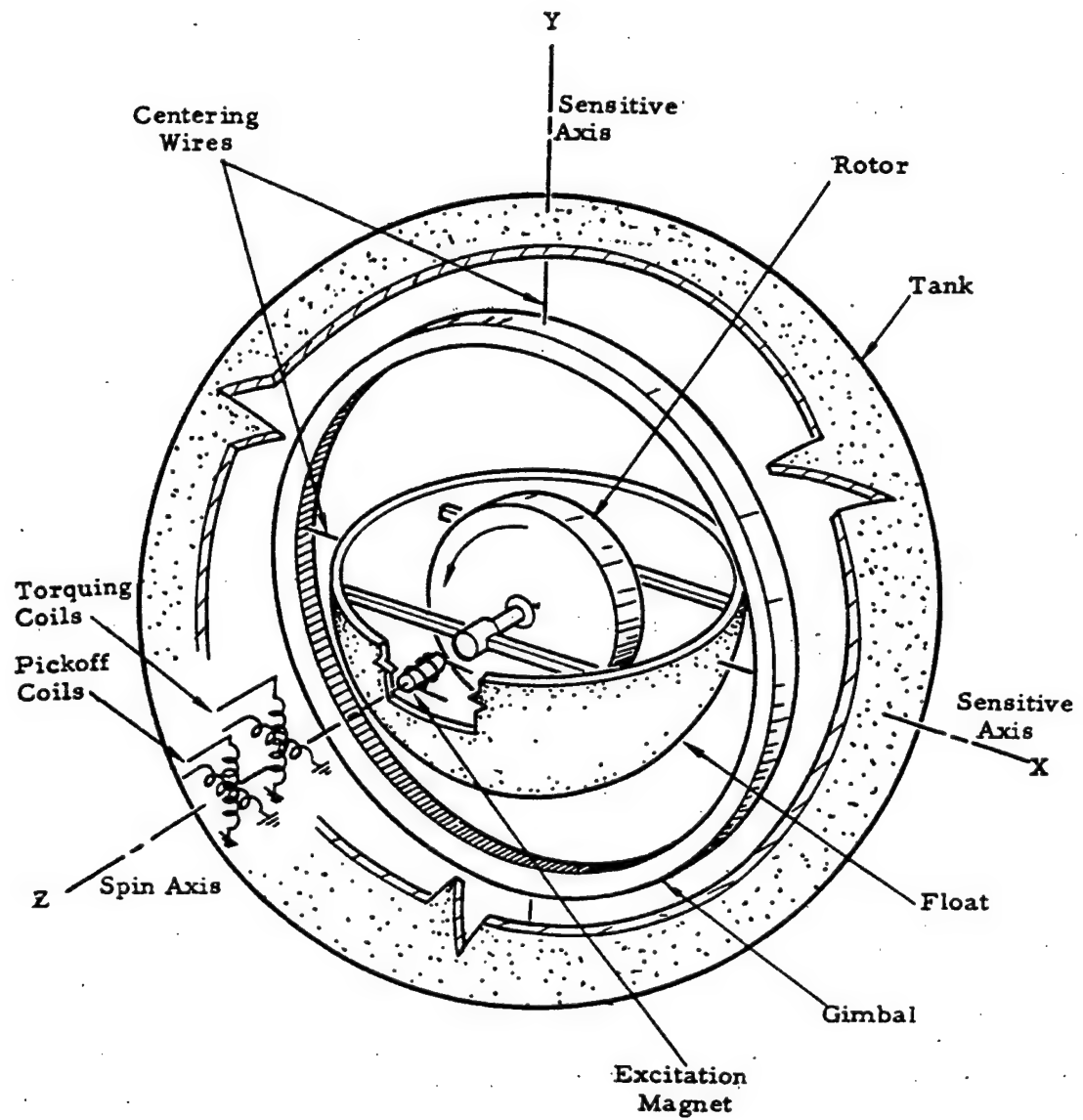
FIGURE 9.26.   ARMA–TYPE TWO DEGREE OF FREEDOM FLOATED GYRO
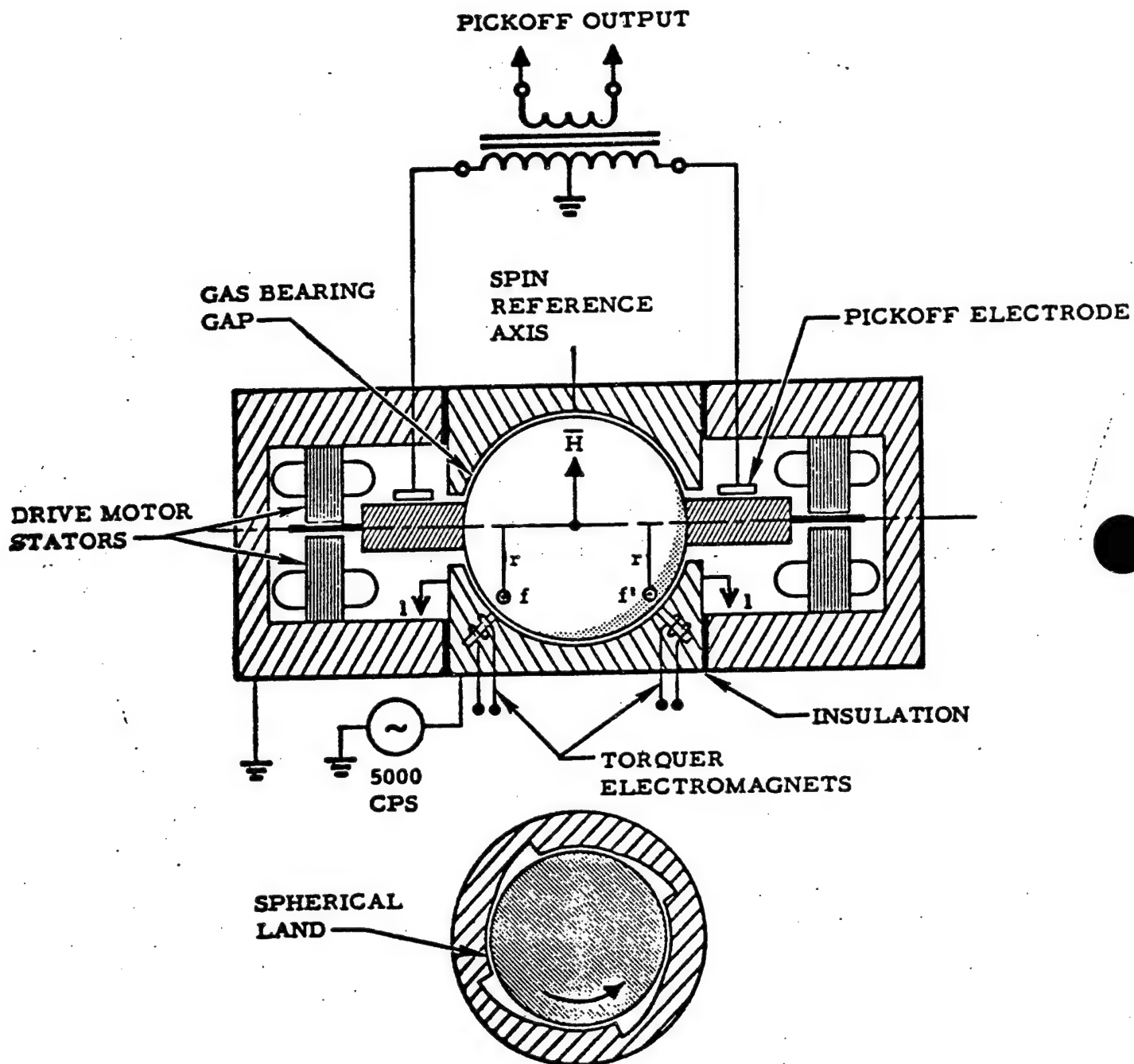
FIGURE 9.27.   ELEMENTS OF A GAS-SUPPORTED FREE-ROTOR GYRO

9.44

9.3.2.4 <u>Gyro Errors</u>. The errors in a gyro will depend upon its design, whether it is single degree of freedom or two degrees of freedom, floated or not floated and so on. Errors are normally expressed as drift rate, such as degrees per hour. Autopilot gyros found in missiles and aircraft have drift rates in the neighborhood of fifty degrees per hour; whereas precision gyros used in inertial guidance systems have drifts in the neighborhood of .05 degrees per hour. In guidance applications the actual drift of a gyro is not nearly as important as the randomness or unpredictability of the drift. This is because there are means of compensating for a known drift by using the computer of an inertial guidance system or through changing the environment to which the gyro is subjected. Examples of such changes are heating the gyro, or orienting the gyro with respect to the acceleration vector.

The spurious nongyroscopic torques which produce unwanted drift in the gyro can be categorized as:

1. Constant or fixed restraint drifts.
2. Mass unbalance or acceleration sensitive drifts.
3. Anisoelastic or compliance drifts (drifts proportional to the square of acceleration).
4. Gyro readout and torquer scale factor error.
5. Random drifts.

Non-acceleration sensitive or fixed restraint drifts are constant drifts and are generally caused by such factors as flex leads for power or signal transmission; the interaction of magnetic parts of the float with external magnetic fields (such as that of the earth); drifts caused by atmospheric changes; and drifts caused by manufacturing faults. The most common manufacturing faults take the form of sticking which occurs when dust or small hairs get trapped between the float and the case. Other manufacturing faults include air bubbles in the flotation fluid, damaged gimbal bearings and changes in the flotation fluid.

The gyro gimbal is never perfectly balanced about the output axis, so that any mass unbalance <u>along</u> the input axis or the spin axis will cause a torque about the output axis which is proportional to acceleration (including gravity). This is the predominant acceleration dependent gyro drift source (i.e. mass unbalance). Other acceleration dependent drifts result from buoyancy unbalance and changes in convective currents in the flotation fluids.

Torques (drifts) that are proportional to the square of acceleration arise from non-symmetrical compliance of the gyro gimbal along the input on the spin axis under the action of steady-state acceleration or vibration. This is also called anisoelastic drift since it is caused by the elastic deformation of the gyro under acceleration.

A gyro output is usually measured in terms of voltage or current values. These electrical values must in turn be related to the physical parameter of interest (turning rate for example in a rate gyro). This relationship is accomplished by a scale factor K, which is a constant determined by instrument design and/or calibration. Referring to the rate gyro example, the scale factor would have units of degrees per hour per volt (or amp) output. Any error in the scale factor will result in a corresponding error in the gyro measured quantity through the auxiliary computer processing.

After all the steady-state and predictable drifts are trimmed out, there remains an irregular drift of a random nature. Included in this classification of random drifts are all predictable drift uncertainties as well as noise.

The drift due to predictable errors is usually eliminated by applying an equal and opposite correction to the gyro output axis. The correction is applied through a torque motor which turns the gyro about its output axis at the same rate, but in the opposite direction to the precession caused by the error rate.

9.3.3 GYRO IMPROVEMENTS

Major efforts have been directed toward improving the accuracy, reducing the size and weight, and increasing the reliability of the individual compo- nents. The switch from analog to digital computers as well as the miniaturi- zation of accelerometers are good examples of this effort.

However, because the gyro drift error is the major source, most of the effort has been directed toward gyro design. This error is generated by friction along the precession axis and therefore the design effort has been toward controlling this friction. The practical applications to data are floated, gas, and dry bearings. The experimental attempts have been the cryogenic, the eletrostatic, the particle, and the laser gyro.

9.3.3.1 Floated Gyros. The floated gyro attempts to eliminate the friction by inducing a liquid between the rotor and the case. The advantage of this

9.46

bearing is that is does reduce the frictional forces thereby improving the accuracy of the gyro. The disadvantages are that the fluid is very temperature sensitive, requires a clean room atmosphere for construction and is large in size and weight.

9.3.3.2 Gas Bearing Gyros. The gas bearing gyro is also an attempt to eliminate the friction along the precessional axis. This is done by separating the rotor from the case and allowing the rotor to operate on a support of pressurized gas. This is accomplished by two methods called hydrostatic and hydrodynamic.

In the hydrostatic bearing the pressurized air is supplied by an external pump. The disadvantage being the requirement of an external pump, filter, and associated plumbing. This type of gyro is used on ballistic missiles, due to its large size and extreme accuracy.

The hydrodynamic bearing generates its own pressurized air through the relative motion between the rotor and the case. In order to pressurize the air sufficiently to lift the rotor from its mount, the rotor must be spinning in excess of a minimum velocity. Herein lies the problem with this gyro. Every time that it is started or stopped it will spin below the minimum velocity and cause wear between the rotor and the case. Therefore this gyro is only used in systems requiring a long continuous output such as in ships or space ships.

The major advantages of the gas bearing gyros are the absence of wear during continuous operation and relative insensitivity to temperature variations.

9.3.3.3 Dry Gyros. Dry bearing gyros have developed a different approach to problem of friction. Instead of trying to eliminate the friction, attempts have been made to measure and standardize the friction. If the frictional forces are known and repeatable, then the gyro can be biased by a compensating torque. Many different types of dry gyros have been developed and are in use today in aircraft systems. An example of this is the Gyroflex gyro. This particular type uses a rotating flexure suspension on one end of a shaft. This flexure supports the rotor. The major advantages of dry gyros are simplicity, low cost, ease of construction, reliability and small size.

9.3.3.4 Cryogenic Gyros. The cryogenic gyro attempts to eliminate the friction by suspending the rotor in a magnetic field, thereby eliminating the

9.47

need of a bearing. The magnetic field is created by passing electric current
through a super cooled matter and thereby takes advantage of the superconduc-
tivity of cryogenic materials. The major disadvantage of this type of gyro
are its sensitivity to temperature and magnetic fields and the problems
associated with working with super cooled materials. To date this type of
gyro has not been used operationally.

9.3.3.5 Electrically Suspended Gyroscope (ESG). The basic concept of the ESG
is a spinning sphere suspended in a vacuum by electric fields, thus
eliminating conventional gyro bearings with their unwanted spurious torques.
Forces of attraction are developed by servoed electric fields between each of
the electrodes and the rotor (Figure 9.28). The rotor mass then can be
supported is, therefore, limited to the maximum voltage gradient that can be
developed, between the electrodes and the rotor, without electrical breakdown.
To improve this a low vacuum is maintained. The position of the rotor is
maintained by feedback loops to each capacitive plate.
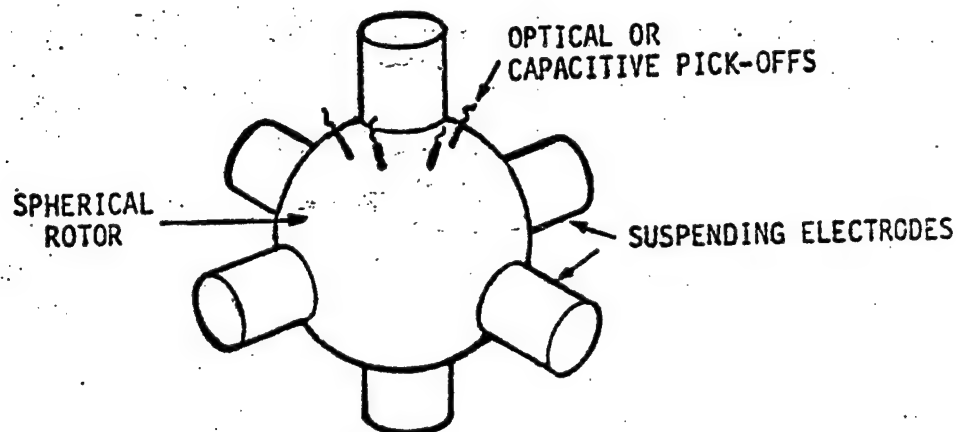
FIGURE 9.28. SIMPLE SCHEMATIC OF THE ELECTROSTATIC GYRO

After initial levitation the rotor is spun up to its operating speed by a rotating magnetic field produced by orthogonal spin coils. The rotor has a preferred spin axis, due to its internal geometry, which is likely to be removed from the actual spin axis, thus nutation is likely to occur. This nutation is damped to a suitable level by a magnetic field produced by applying a DC voltage to one of the coils. This has the effect of erecting the preferred spin axis to approximate coincidence to this coil, thereby defining the spin axis to starting position. When the rotor reaches the required speed, spin power is removed and the rotor allowed to coast. Operating in a near vacuum, the drag on the rotor is small, thus the change in rotor speed and angular momentum is small enough to be ignored.

The rotor, having reached operating speed, will be space stable so if the case is rotated there will be relative motion between the case and the rotor. This relative motion is detected by pick-offs, which may be optical or electrical. Thus, the ESG is a two degree of freedom displacement gyro.

The original test model was demonstrated in the late 1950s; it weighed 2,000 lbs, needed 24 hours to run up to its operating speed of 12,000 RPM, produced a real drift rate of 0.0004 deg/hr, and cost $60,000. However, since then considerable reductions in weight, run up time and cost have been made. These improvements had made possible the use of ESGs in airborne inertial navigators.

Two navigators, using ESGs, are currently under development, namely, the ASN-101 also known as the Gimbaled ESG Aircraft Navigation System (GEANS), and Micron (micro-navigator). Honeywell is producing the ASN-101 which employs a four gimbal stabilized platform and two ESGs. These ESGs use a hollow beryllium sphere that spins at approximately 60,000 RPM. The sphere is 1.5 ins in diameter, somewhat larger than the one cm sphere used in the North American Rockwell Micron system. Honeywell employs a larger diameter sphere to obtain lower drift rates and to enable the optical displacement pick-off to achieve the required precision. The sphere is hollow to reduce weight and thereby ease the load on the electrical suspension system.

The first three ASN-101 systems delivered to the USAF for evaluation each weighed 157 lbs, occupied 2.7 cu ft and consumed 862w. The company is working to optimize the design with the objective of reducing system weight to 138 lbs, size to 2.6 cu ft and power consumption to 555w. The target of the optimized design is to achieve a production price of approximately 125,000

dollars and an accuracy in the order of 0.1 nm/hr without updating.

Autonetics is the division of the North American Rockwell Corporation responsible for the development and production of the Micron system. The ESGs used in this system employ an electrical pick-off technique, involving mass unbalance modulation of the electrical suspension voltage. This permits the use of a much smaller, solid sphere. To achieve the required momentum, it is spun up to 150,000 RPM initially.

The Micron program, aims at producing a system capable of a 1 nm/hr accuracy, therefore, the gyro performance required is on the order of 0.01 deg/hr. Tests carried out have shown the gyros to have a real drift rate of 0.0095 deg/hr. The production cost of these gyros is approximately 5,000 dollars each, however the company is confident of reducing this to 2,500 dollars.

The development of small ESGs has opened the way to the use of strap-down inertial systems in fighter and other aircraft having a high maneuver capability. The strap-down system has always had considerable potential appeal for such applications because of its light weight and electro-mechanical simplicity. However, until the advent of the micro-miniature ESG it was only possible to implement strap-down systems using conventional rate integrating gyros. With such gyros, current pulses must be applied to the gyro torquers during aircraft maneuvers to keep the spin axes centered. These current pulses are continuously totaled by the associated computer to keep track of the aircraft attitude about all three axes. With this type of gyro it is extremely difficult to produce torque rates sufficiently high to cope with rapid rotation rates. In addition, if the aircraft maneuvers simulatan-eously about two or more axes, this results in a cumulative error, referred to as "coning error", which remains in the system until the aircraft lands.

The ESG being a free gyro (the spinning sphere retaining its spatial orientation regardless of aircraft maneuver) eliminates this error. A further advantage claimed for the ESG is that the electrical suspension isolates the gyro from the high vibration environment found in aircraft, which induced errors in more conventional gyros.

9.3.3.6 Gyroflex. The Gyroflex is a two degree of freedom, non-floated, free rotor gyroscope. The basic components are an inertial rotor, a synchronous-hysteresis motor, a two part flexure suspension, an E-bridge inductive pick-off, and DC torquers. Figure 9.29 shows, in simplified form, the layout of

these components. The unique feature of the Gyroflex is the suspension which
couples the rotor to the rotating shaft and provides the rotor with universal
freedom. Provided that the rotor's center of gravity coincides with the
center of the flexure support, there should be no torques due to
accelerations. However, whenever axis rotation of the gyro occurs, about a
sensitive axis, the rotor will be unaffected as it will move. This relative
motion is detected by the pick-offs, thus generating an electrical signal
which is fed to the appropriate gimbal torquer. These pick-offs are mounted
in pairs at 90 degrees, thus the gyro is capable of detecting rotations about
two axes.

The Gyroflex design principle was initially conceived in 1958. Extensive
testing at the Central Inertial Guidance Test Facility, Holloman AFB has
demonstrated real drift rates of 0.001 deg/hr.
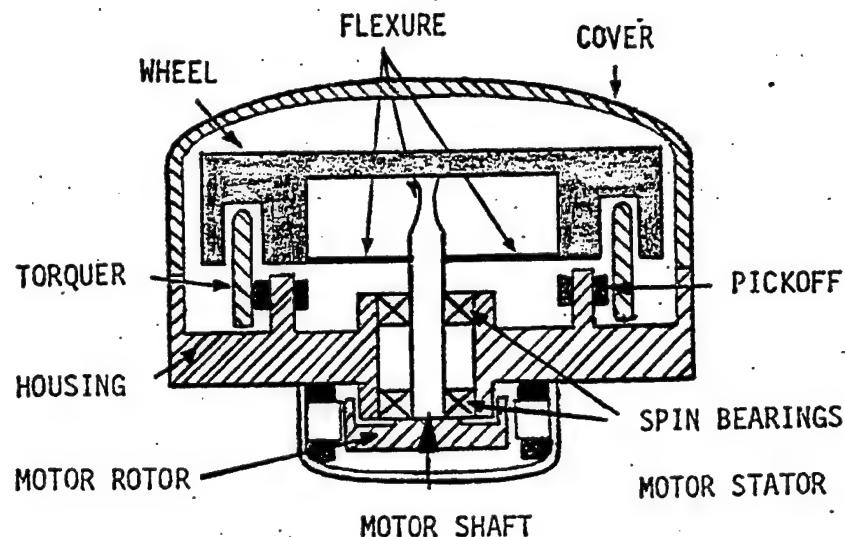
FIGURE 9.29.   SIMPLIFIED SCHEMATIC OF THE GYROFLEX GYRO

9.3.3.7 <u>Litton Multisensor</u>. The Litton Multisensor is an extension of the Gyroflex principle, the instrument being capable of acting as a two degree of freedom gyroscope and a two axis accelerometer. In this arrangement two rotors, attached by compliant joints (flexure supports), are driven by a common rotor (Figure 9.30). The rotor at one end acts as a gyro operating on the Gyroflex principle. However, the rotor at the other end is modified so as to be sensitive to accelerations. This is achieved by deliberately designing the rotor so that its center of gravity is displaced from the center of the compliant joint. This creates an unbalance, enabling the device to measure the effects of accelerations in a similar manner to a force balance accelerometer.

These Multisensors are 1.5 ins long, 1 in in diameter, weight 2.86 oz and require 1.25w of power. All the outputs of rotation and acceleration required by an IN can be provided by two of these instruments. Therefore, it is possible to achieve a considerable size reduction. Using Multisensors, Litton has produced a platform 3.15 ins in length and 2.8 ins in diameter. The 1.9 lb platform requires 25w of power. It is expected to produce similar accuracies to existing systems but should afford a considerable saving in cost.
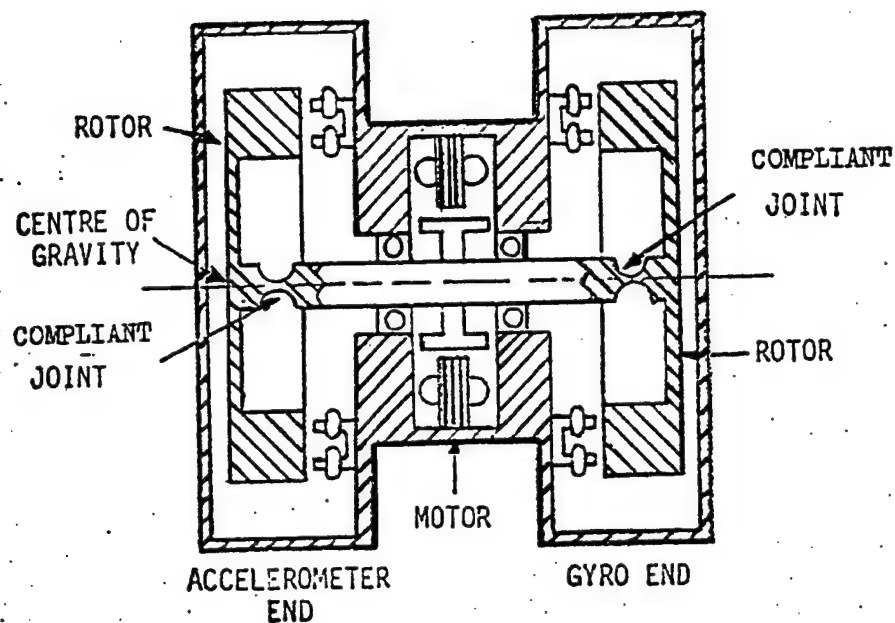
FIGURE 9.30. SIMPLE SCHEMATIC OF THE MULTISENSOR

The Multisensor has a number of potential advantages over other types of sensors, namely:

a.   Reduced size.

b.   The number of parts and manufacturing steps required is reduced compared to a normal gyro/accelerometer combination, resulting in cost savings.

c.   There is some commonality of the component parts.

d.   Difficulties in aligning gyro and accelerometer axes are avoided by presetting these during manufacture.

9.3.3.8 Laser Gyro. The possibility of using the properties of propagation of light as a means of measuring rotation occurred in 1962 with the advent of laser light sources of narrow spectral frequency bandwidths and high pulse stability. The principle of operation of a ring laser gyroscope is that continuous oscillation is obtained by directing waves around the complete optical ring. Although referred to as a ring, the normal shape is triangular (see Figure 9.31). The ring consists of gas laser inside gas tubes connected

by mirrors at each corner. In this way, a closed path optical ring (cavity) is effectively formed. Thus, continuous oscillation of the laser is obtained. The laser oscillation frequency is determined by the length of the ring. This is due to the fact that cavity path length is always equal to an integral number of wavelengths. Therefore, if the path length is altered, the wavelength must also alter.
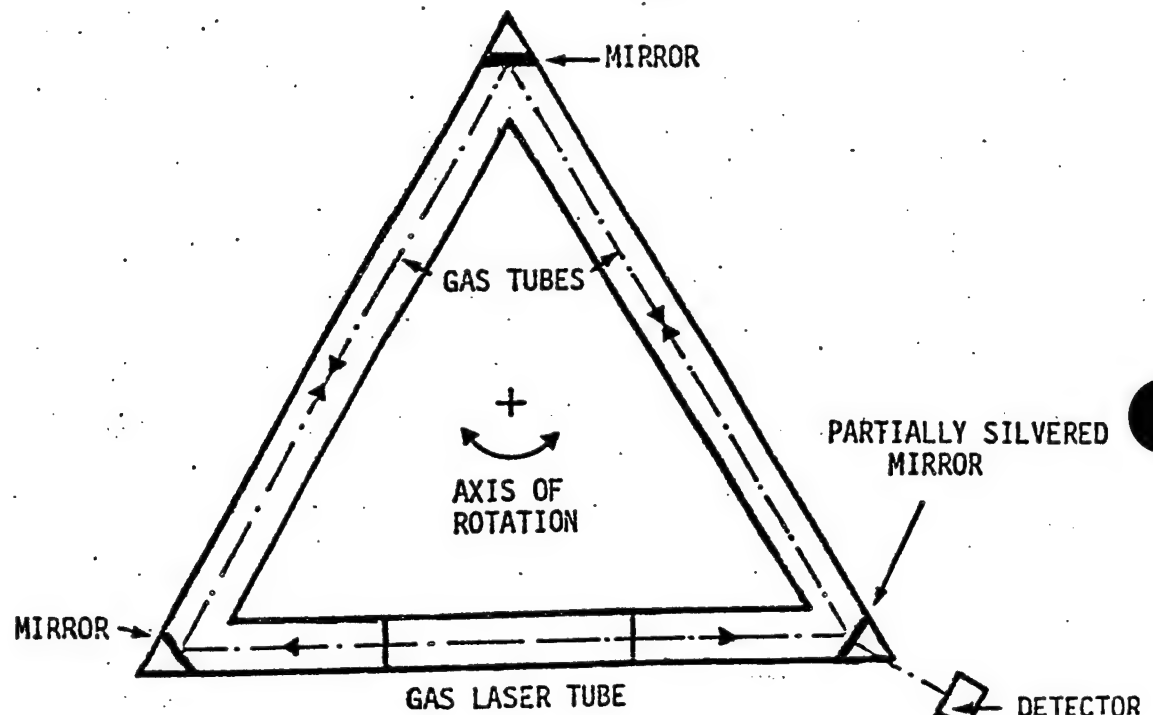
FIGURE 9.31. LASER GYRO

The laser is made to propagate two waves, one traveling clockwise around the ring, and the other counterclockwise. As the path length of each wave is identical, the frequency of each wave must be the same. If, however, the ring laser is rotated about an axis through, and at 90 degrees to, the ring, the effective path length of the two waves will be altered. The wave traveling in the direction of rotation will have its path length effectively lengthened, while the path length of the other wave will be effectively shortened. Thus a frequency difference will exist between the two waves.

9.54

The cavity path length change L is given by:

$$\Delta L = \pm \frac{2\omega A}{c}$$

where ω is the rotation rate, A is the projected area of the optical ring, and c is the velocity of light. As the frequency difference is related to change of path length, the rotation rate can be determined from that difference. Optical heterodyning techniques are used to extract the difference frequency. This can then be processed by frequency analysis to establish rotation rate, or by digital counting, to determine the integrated rotation or shift from an initial reference direction within an inertial co-ordinate frame.

Potentially, the laser gyro offers the following advantages:

a. It is insensitive to acceleration forces.

b. Operation over a wide dynamic range is possible.

c. There are no moving parts.

d. Manufacturing cost are low.

However, it also suffers several disadvantages, these include:

a. Short life.

b. Inconsistent warm up.

c. Frequency lock.

The MTBF currently being achieved is in the order of 100 hours, the main problem being the breakdown of seals. The problems associated with laser warm up are not fully understood. At the present time it is not possible to predict accurately the time required to achieve satisfactory operation. Frequency lock occurs when the laser is subjected to low rotation rates. At these rates the frequency difference between the two waves is small and the frequencies lock together, thus no output is obtained. In addition, in the vicinity of, but prior to frequency lock, distortions of the difference frequency occur. These problems are being overcome by biasing the gyro so that there is a frequency difference at low rotation rates. This can be achieved either by deliberately rotating the ring or by introducing a Faraday bias cell. Both of these methods have the effect of ensuring a difference in path length between the two waves.

9.55

THIS PAGE INTENTIONALLY LEFT BLANK

9.4 INERTIAL PLATFORMS

At this point we have seen how to determine inertial acceleration and then how to align the accelerometers through the use of gyroscopes. Any misalignment between the accelerometer input axes and the reference axes will result in erroneous acceleration sensing. In addition, the accelerometer must be isolated from accelerations caused by aircraft maneuvers.

In practice the accelerometers are mounted on a platform which is held in a gimbal system. The gimbal system allows the platform to be maintained in the required orientation and isolates the accelerometers from the effects of aircraft maneuvers. The most common arrangements are the conventional three and four gimbal systems.

Figure 9.32 depicts a three gimbal platform. It is a conventional gimbal system in that the gimbals surround the platform itself. The azimuth, or innermost gimbal carries the platform. The order of the remaining gimbals is governed by the mounting of the gimbal system in the aircraft. These gimbals are responsible for isolating the stable element from aircraft maneuvers in pitch and roll. Gimbals are named according to the function they perform, and are numbered from the stable element outward. In Figure 9.32, the gimbal order is azimuth (first), roll (second), and pitch (third) gimbal. In such a system all gimbals are controlled by gyroscopes and torquers.

9.4.1 Gimbal Lock

The major problem with the three gimbal system is that it is susceptible to an error called gimbal lock. This is possible because this gimbal system cannot isolate the stable element from all aircraft maneuvers.

From Figure 9.32, if the aircraft rolls through 90 degrees, the first gimbal axis becomes aligned with the third axis, and the stable element is no longer isolated from aircraft yaw maneuvers. (This condition is known as gimbal lock and limits operations about one axis to approximately 80 degrees.) Basically, after the aircraft is rolled 90 degrees and as a yaw is attempted, the platform will be forced to lose its orientation.

A solution to the problem of gimbal lock is to build a platform which has a fourth gimbal (Figure 9.33). The gimbal order of this system is azimuth (first), inner roll (second), pitch (third), and outer roll (fourth). Control of this system is accomplished by the use of a pick-off (between the

. 9.57

second and third gimbal) which determines the gimbal position, and a torquer. In such a system, gimbal lock is prevented by driving the fourth gimbal to keep the third gimbal perpendicular to the second at all times. This principle is shown in Figure 9.34. Any loss of orthogonality between the second and third gimbal is driven out almost instantaneously by the forth gimbal. Therefore, the second or inner roll gimbal does not require full physical freedom for the system to operate satisfactorily. In practice the inner roll gimbal movement is limited to about ±20 degrees.

STABLE ELEMENT

ROLL GIMBAL (SECOND)

AZIMUTH GIMBAL (FIRST)

PITCH GIMBAL (THIRD)

A/C LONGITUDINAL AXIS
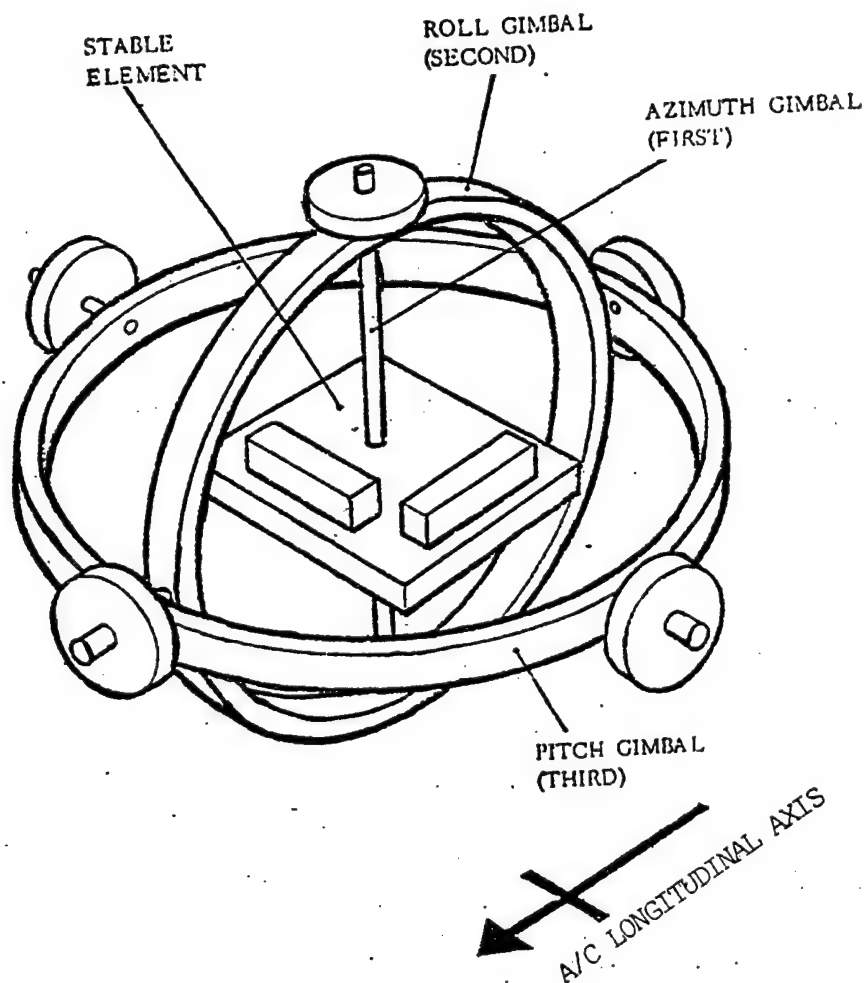
FIGURE 9.32   CONVENTIONAL THREE GIMBAL SYSTEM

9.58

OUTER ROLL
GIMBAL

INNER ROLL
GIMBAL

PITCH
GIMBAL

AZIMUTH
GIMBAL

A/C LONGITUDINAL AXIS
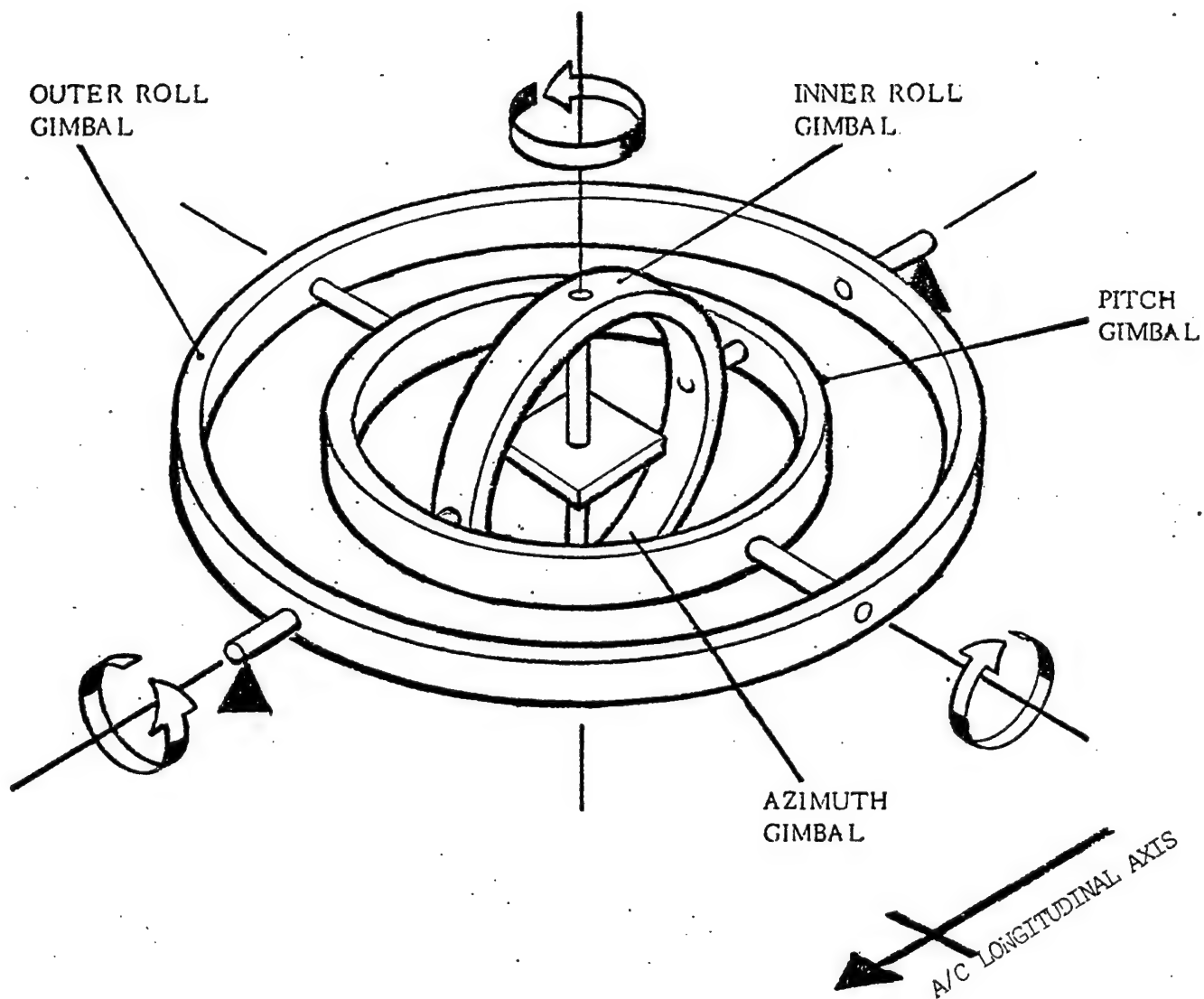
FIGURE 9.33   CONVENTIONAL FOUR GIMBAL SYSTEM

9.59

As the pitch angle increases the outer roll gimbal must move through larger angles to null the signal from the inner roll axis. In a vertical flight attitude no motion of the fourth gimbal would null the second gimbal and the entire assembly would rotate about the azimuth member. If the pitch angle passes through 90 degrees, then an opposite rotation about the fourth axis is required to null the second gimbal. To ensure orientation of the platform which provides the proper polarity for the follow-up servo, the outer roll gimbal "flips" through 180 degrees whenever the vehicle pitch angle passes the vertical.

Table 9.2 summarizes the advantages and disadvantages the two gimbal systems just discussed.

(a) STRAIGHT AND LEVEL FLIGHT

(b) IN A ROLL, GYRO STABILIZATION LOOP DRIVES SECOND GIMBAL TO KEEP PLATFORM LEVEL

(c) FOURTH GIMBAL DRIVES UNTIL SECOND GIMBAL IS CENTERED, THUS RETURNING THIRD GIMBAL PERPENDICULAR TO SECOND GIMBAL
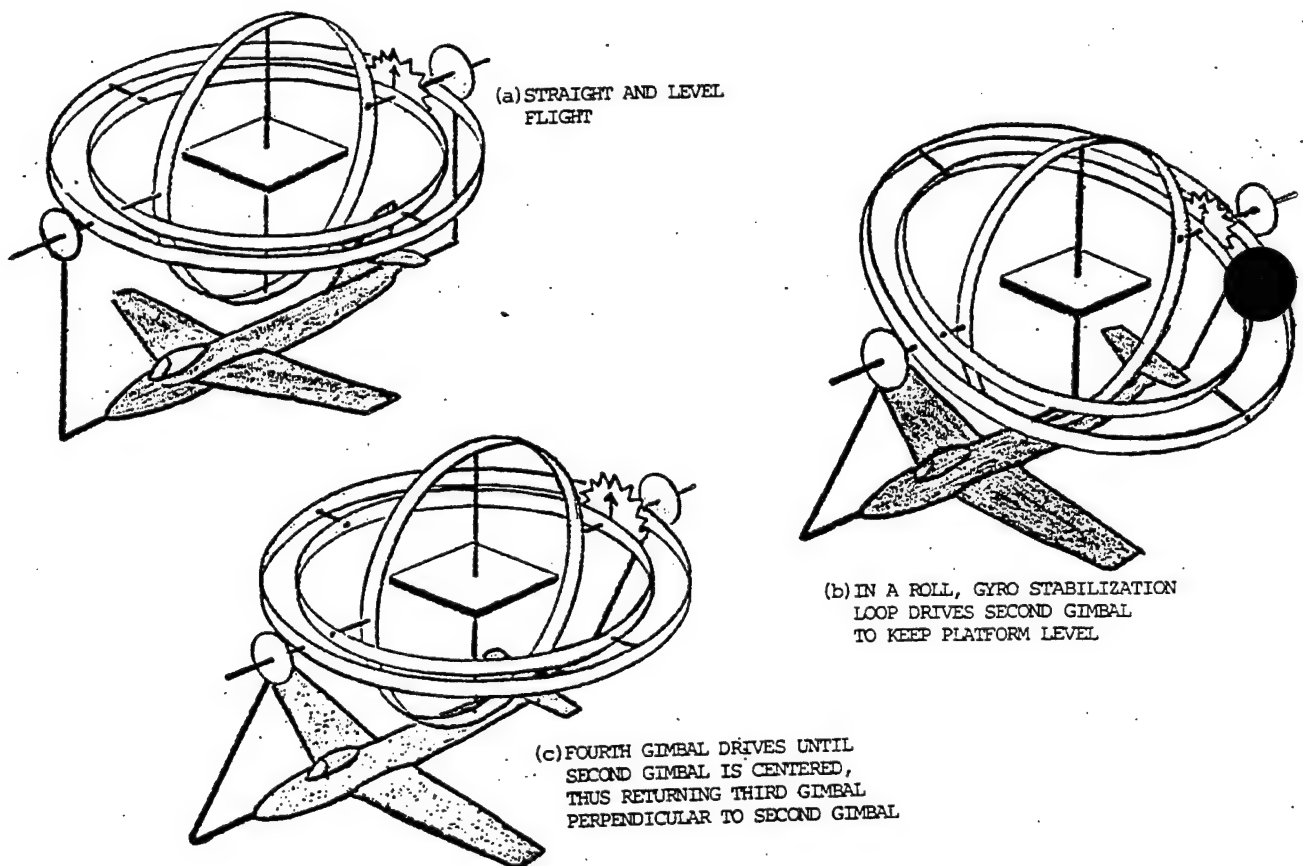
FIGURE 9.34   FUNCTION OF THE FOURTH GIMBAL

9.60

SYSTEM	ADVANTAGES	DISADVANTAGES
Three Gimbals	1. Smaller size and weight 2. Greater simplicity 3. Lower cost	1. Limited maneuverability of vehicle 2. Lower system accuracy 3. Higher susceptibility to effects of vibration
Four Gimbals	1. Unlimited maneuverability of vehicle 2. Higher system accuracy 3. Lower susceptibility to vibration 4. Magnitudes of inner roll gimbal errors are very small 5. Reduction of platform drift due to torque 6. Attenuation of effects due to gyro non-linearities 7. High system stability	1. Greater size and weight 2. Greater complexity 3. Higher cost

TABLE 9.2   COMPARISON OF THREE GIMBAL AND FOUR GIMBAL SYSTEMS

9.4.2   Platform Controllers:

The movement of platform gimbals due to disturbance torques is sensed by gyros. An output signal from the gyros activates torquers which return the gimbals to null position. Two kinds of torquers are presently being used:

1. A servo motor driving through a gear train,

2. A direct drive torquer.

Direct drive torquers are usually DC as opposed to AC because of their smaller size and greater efficiency. The disadvantage of the DC torquers is the requirement of brushes. Table 9.3 compares the advantages and disadvantages of the two types of torquers.

9.61

SYSTEM	ADVANTAGES	DISADVANTAGES
Direct Drive	1. High torque to inertia ratio 2. No gear train maintenance 3. No gear backlash nonlinearities 4. Lower friction torque 5. More accurate	1. No torque range 2. Higher cost 3. Larger size and power requirement 4. Requires brushes 5. Less reliable
Servo Motor	1. Wide range of torque available 2. Lower cost 3. Smaller size and power requirement 4. No brushes 5. More reliable	1. Low torque to inertia ratio 2. Requires gear train and maintenance 3. Gear backlash nonlinearities 4. Higher friction torque 5. Less accurate

TABLE 9.3   COMPARISON OF SERVO MOTOR AND DIRECT DRIVE TORQUERS

In general where extreme accuracies are required or where large torque requirements exist, the direct drive is used.

Figure 9.35 shows a typical arrangement of the gyros on a platform with their sensitive axes pointing in the directions about which rotation is to be detected. The East gyro has its sensitive axis pointing East, and is therefore able to detect rotations about East. On northerly headings, pitch maneuvers are detected by the East gyro which generates an error signal. This error signal activates the pitch gimbal, thereby maintaining the platform's alignment with the reference frame. Similarly, roll is detected by the North gyro which activates the roll gimbal motor, and yaw is detected by the azimuth gyro which activates the yaw gimbal motor. The action is summarized in Table 9.4.

9.62
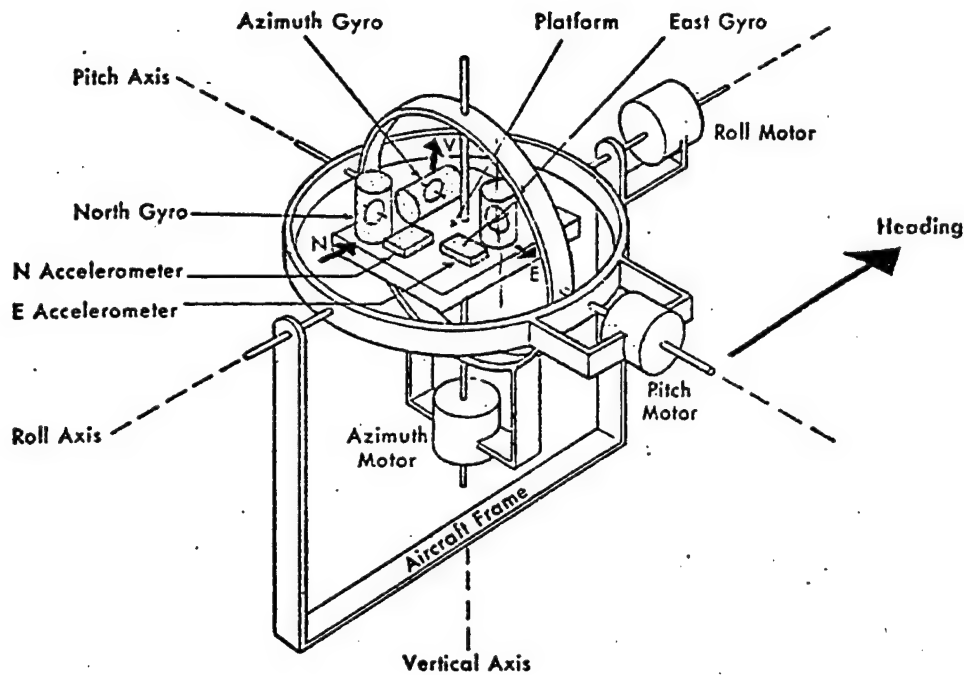
FIGURE 9.35   TYPICAL PLATFORM ARRANGEMENT (AC HEADING NORTH)

Heading	Maneuver	Sensing Gyro	Correcting Servo Motor
	Yaw	Azimuth	Azimuth
North	Pitch	East	Pitch
	Roll	North	Roll

TABLE 9.4   CONTROL ON NORTH

9.63

Figure 9.36 shows the same platform arrangement but on an easterly heading.   Table 9.5 summarizes the control action on East.
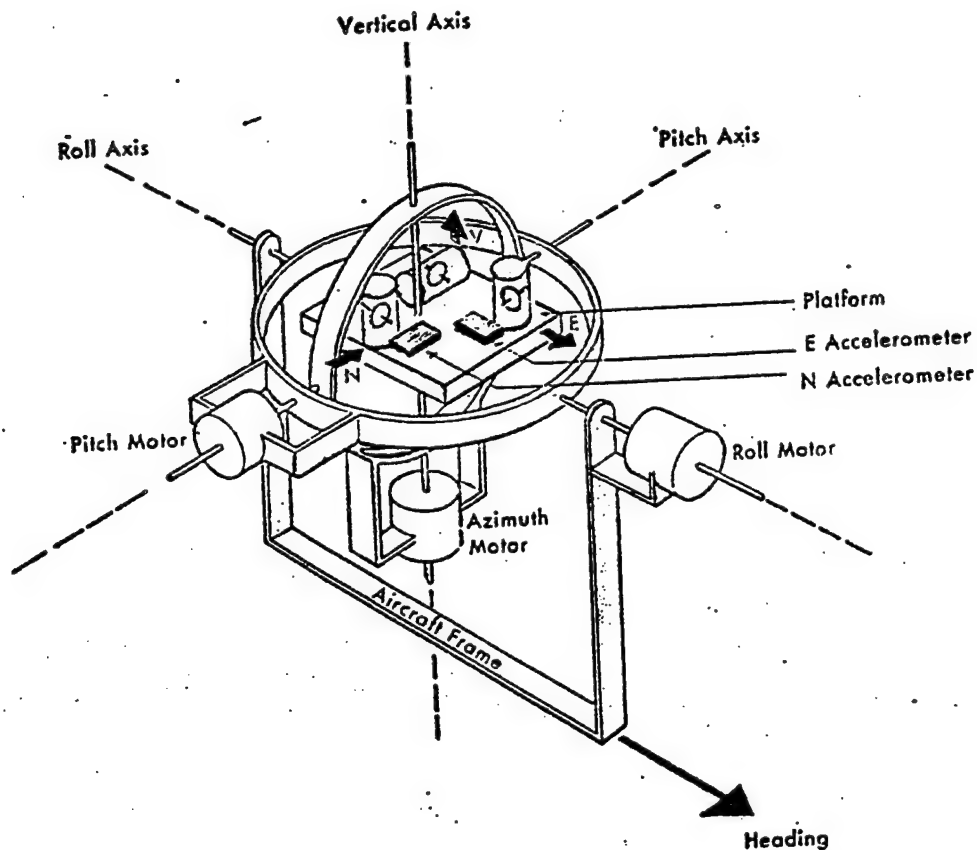
FIGURE 9.36   TYPICAL PLATFORM ARRANGEMENT (AC HEADING EAST)

Heading	Maneuver	Sensing Gyro	Correcting Servo Motor
	Yaw	Azimuth	Azimuth
East	Pitch	North	Pitch
	Roll	East	Roll

TABLE 9.5   CONTROL ON EAST

Two main conclusions may be drawn from Tables 9.4 and 9.5:

    a.   The azimuth gyro always controls the azimuth servo motor.

    b.   Control of the pitch and roll servo motors may be exercised by either the North or the East gyros or both, dependent upon aircraft heading.

Gimballed Inertial Navigation platforms do isolate the platform from the vehicle, but they have the four following disadvantages:

    a.   They add a lot of weight to the system

    b.   They occupy a large volume of space

    c.   They increase complexity and cost

    d.   They require a large number of servos, pick-offs, and transmission systems which tend to introduce errors and reduce overall system accuracy.

THIS PAGE INTENTIONALLY LEFT BLANK

9.5 INERTIAL SYSTEM MECHANIZATION

All of the elements of the INS must now be tied together so that it is possible to navigate from one point on the earth to another point. Simple changes in the mechanization of the system described in this chapter will allow for navigation between two points in space. Choosing the reference frame for the system accounts for the difference.

When traveling over the surface of the earth within the earth's gravitation field, it becomes necessary to make corrections to the inertially sensed acceleration to arrive at the true acceleration of the vehicle. Recall Equation 9.6 from Section 9.1:

$$\bar{A}_{P/E} = \bar{A}_I - 2(\bar{\omega}_{E/I} \times \bar{V}_{P/E}) - (\bar{\omega}_{E/I} \times \bar{\omega}_{E/I} \times \bar{r}_{P/E}) \qquad (9.10)$$

The sensed acceleration, $(\bar{A}_{P/E})_E$, is corrected for the gravitational acceleration, and for Coriolis and centripetal accelerations and is integrated twice to obtain velocity and position. This is shown below in Figure 9.37.
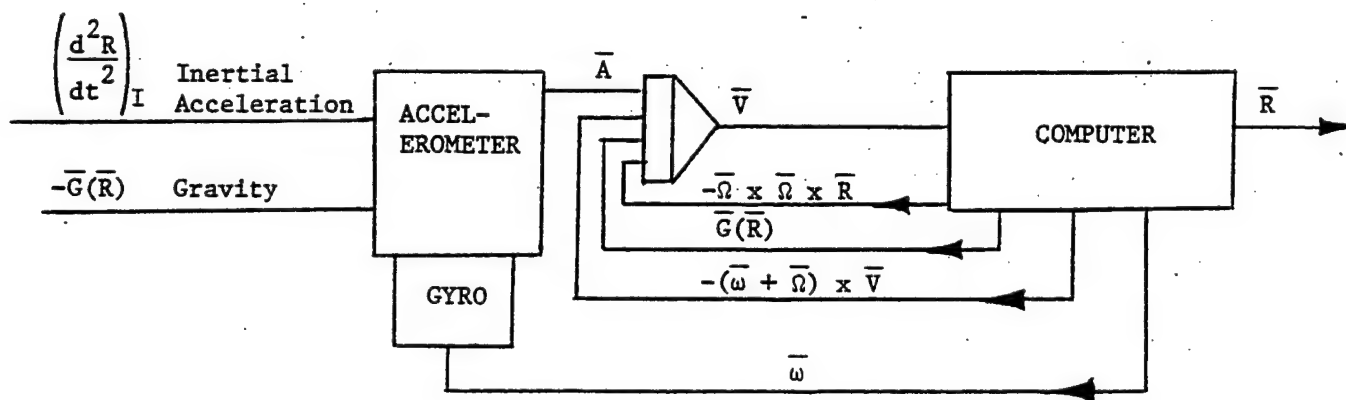
FIGURE 9.37 BLOCK DIAGRAM FOR SOLVING FOR R

The discussion to this point has assumed no specific earth reference system and is a general development for inertial space. In dealing with a specific reference system it is important to realize that corrections must be made not only to the sensed acceleration but also to the gyros which are trying to maintain the accelerometer inertial reference. Without both corrections the solution to the navigation problem, with good accuracy, is not

possible.

9.5.1 Local Vertical, Lat-Long Reference System

A local vertical reference frame is a geographic frame and has its orthogonal axes continually orientated in the directions of local North, local East, and local vertical (Figure 9.38). The local vertical system is the most commonly used reference frame in aircraft inertial navigation systems. It is usually chosen for an aircraft reference system because we can not only navigate using it but also get aircraft attitude information from the INS.
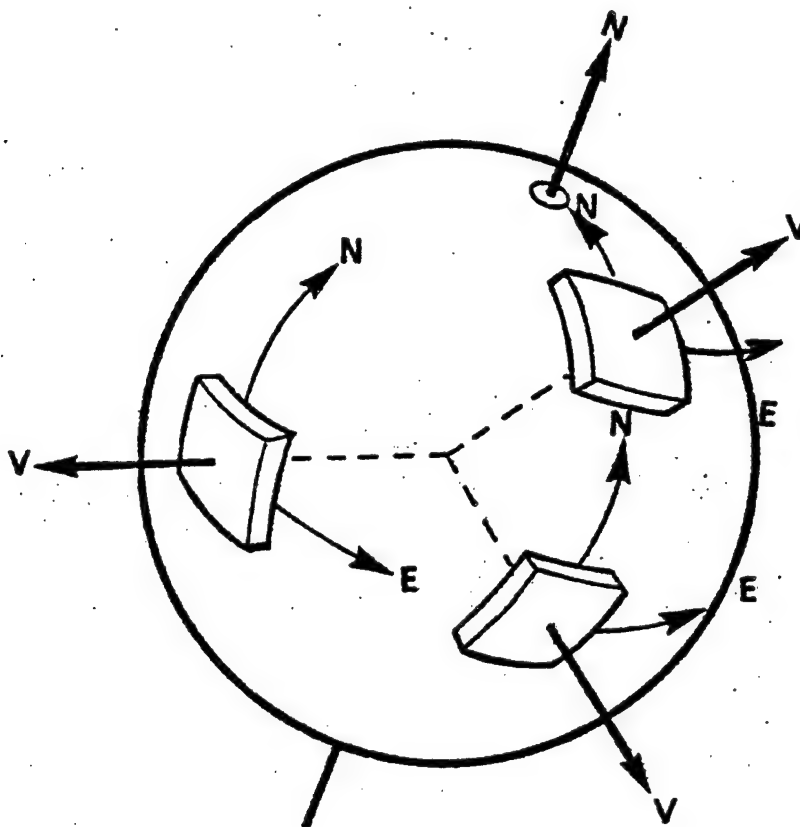
FIGURE 9.38 LOCAL VERTICAL REFERENCE FRAME

The basis of the local vertical reference frame is that the stable platform is perpendicular to the local gravity vector. This local gravity vector (g) is a compound function of mass attraction and centripetal acceleration and, but for the effect of local anomalies, would be perpendicular to the mean sea level surface. However, because of these anomalies, the surface which is everywhere perpendicular to g will be irregular and impossible to re-

9.68

present mathematically. This surface is called the geoid and is the one which a local vertical INS will follow. To correct the stable element for travel across the surface the radius at every point on the geoid must be known, and since the geoid cannot be represented mathematically this is impossible. To overcome this problem the best fitting mathematical ellipsoid to the geoid is used as the basis for calculating the radius R. This ellipsoid is known as the International Spheroid and its use introduces a maximum error, in R, believed to be within ± 600 feet.

9.5.1.1 Accelerometer Corrections

The stable element is rotated about all three axes to compensate for earth rate and transport rate. Thus in addition to normal aircraft accelerations, the accelerometers will sense accelerations caused by these rotations. An aircraft flying any track across the surface of the earth flies a curved path in space. Its accelerations relative to space must therefore be a compound of its accelerations relative to the earth (aircraft, Coriolis, and centripetal), and the acceleration of the earth relative to space (centripetal due to earth rotation).

By going back to equation 9.10 it is possible to show exactly what corrections must be made to accelerometers in the local vertical reference system.

$$\bar{A}_{P/E} = \bar{A}_I - 2(\bar{\omega}_{E/I} \times \bar{V}_{P/E}) - (\bar{\omega}_{E/I} \times \bar{\omega}_{E/I} \times \bar{r}_{P/E}) \qquad (9.10)$$

When coordinatized in the earth reference frame,

$$\bar{\omega}_{E/I} = f(\Omega, \lambda, \dot{\lambda}, \dot{L})$$

where

Ω = earth rotation rate
λ = latitude
$\dot{\lambda}$ = rate of change of latitude
$\dot{L}$ = rate of change of longitude

Earth rate is resolved into the components shown in Figure 9.39 The earth rate components there for each axis are:

9.69

$$\omega_x = \Omega \cos \lambda$$

$$\omega_y = 0$$

$$\omega_z = \Omega \sin \lambda$$
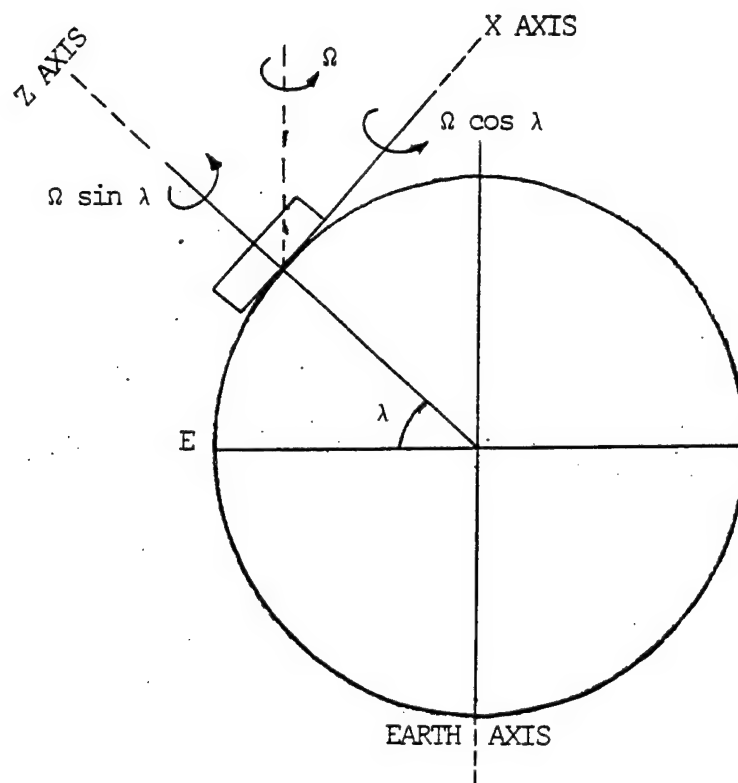
FIGURE 9.39   RESOLUTION OF EARTH RATE

9.70

The inertial rates about the platform axes are:

$$\omega_x = (\Omega + \dot{L}) \cos \lambda \tag{9.11}$$

where

$\Omega \cos \omega$ = earth rate, compensating for the rotation of the earth.

$\dot{L} \cos \lambda = \dfrac{Vy}{R}$ = platform transport rate, or compensation for traveling over the earth

$$\omega_y = \dot{\lambda} = \frac{Vx}{R} \tag{9.12}$$

$$\omega_z = (\Omega + \dot{L}) \sin \lambda \tag{9.13}$$

where

$\Omega \sin \lambda = $ earth rate

$\dot{L} \sin \lambda = \dfrac{Vy}{R} \tan \lambda$

now

$$V = \int_0^t [\bar{A} - (\bar{\omega} + \bar{\Omega}) \times \bar{V} + g(\bar{R})] \, dt \tag{9.14}$$

where

$$g(\bar{R}) = G(\bar{r}_{p/E}) + \bar{\omega}_{E/I} \times (\bar{\omega}_{E/I} \times \bar{r}_{p/E})$$

Substituting equations (9.11), (9.12), and (9.13) into (9.14) and writing the x and y components yields

$$V_x = \int_0^t [A_x + (2\Omega + \dot{L})(\sin \lambda) V_y - g(x)] \, dt \tag{9.15}$$

$$V_y = \int_0^t [A_y - (2\Omega + \dot{L})(V_x \sin \lambda) - g(y)] \, dt \tag{9.16}$$

9.5.1.2 Gyro Corrections

In the block diagram in Figure 9.37 is shown a correction ω that must go into the gyros. This correction is the same values shown in equations

(9.11), (9.12), and (9.13). What are these corrections for? Remember, the
gyros exhibit the property of rigidity in space. When gyros are used to
stabilize a platform relative to Earth axes, corrections must be applied to
overcome the effects of Earth rotation and the aircraft's movement over the
Earth relative to inertial space.

A little thought makes the reason for these corrections readily
apparent. If an aircraft sits on the ramp at Edwards with an INS istalled in
it that does not have earth rate compensation, what happens to the
apparent attitude of the aircraft over a 24 hour period? Because the gyro
alignment will not change relative to inertial space, it will appear that the
aircraft attitude is changing relative to the surface of the earth. By add-
ing earth rate compensation torques to the gyros we can keep the local verti-
cal and North axes of the platform aligned with the vertical and North. Once
the aircraft starts to move (gets a Velocity), we must make a transport
rate compensation through the gyros to the platform to keep the vertical and
North axes aligned.

Figure 9.40 illustrates an INS platform with two accelerometers (North
and East) and three gyros (North, East, and azimuth). Table 9.6 summarizes
those corrections necessary for navigating using a local vertical reference
frame.

Gyro Corrections:

	Earth Rate	Transport Rate
North Gyro	$\Omega \cos \lambda$	V_y/R
East Gyro	Φ	$-V_x/R$
Azimuth	$\Omega \sin \lambda$	$V_y/R \tan \lambda$

Accelerometer Corrections:

	Centripetal Accel.	Coriolis
North Accelerometer	$\dfrac{-V_y 2 \tan \lambda}{R}$	$-2\Omega V_y \sin \lambda$
East Accelerometer	$\dfrac{V_x V_y \tan \lambda}{R}$	$2\Omega V_x \sin \lambda$

TABLE 9.6   PLATFORM CORRECTIONS

A platform can also be built with a vertical accelerometer. In addition to correcting the vertical accelerometer for Coriolis and contripetal acceleration effects it must also be corrected for gravitational acceleration. The acceleration due to gravity decreases with height according to the formula $g_h = g_o \left(1 - \dfrac{2h}{R}\right)$ thus the correction to be applied is $-g_o \left(\dfrac{1-2h}{R}\right)$.
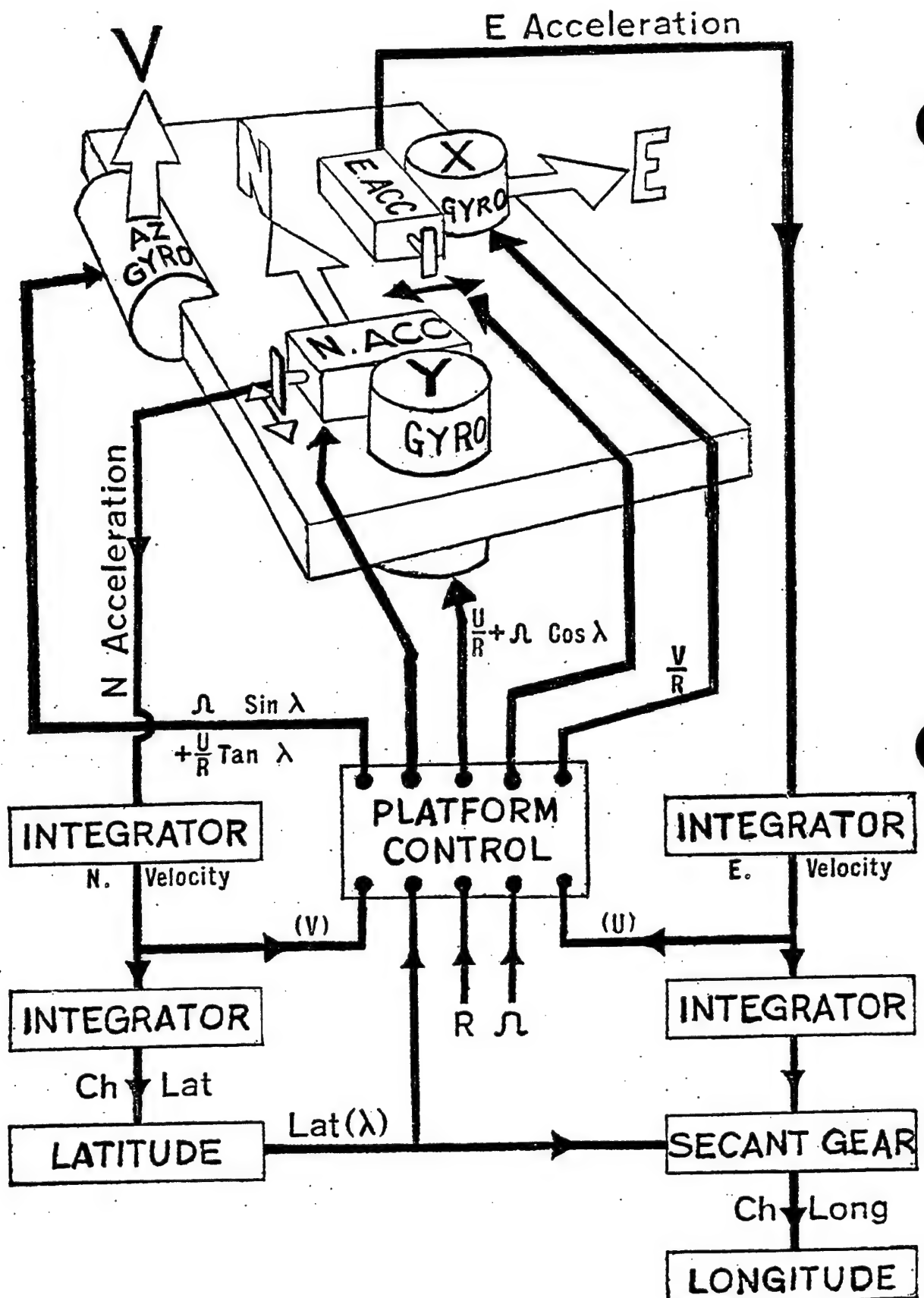
FIGURE 9.40   SIMPLE INERTIAL NAVIGATION SYSTEM

9.74

9.5.1.3 Control of the Local Vertical INS

As we have seen, the essence of a local vertical system is that the platform, through the gimbal system and torquers, must be continuously rotated about its horizontal axes to remain perpendicular to the local vertical. If the platform has groundspeed Vg, with earth radius R, then the local vertical is rotating at a rate Vg/R. To remain vertical the platform must be rotated about the horizontal at the same rate. This has been achieved by torquing the East and North gyro at transport rate $-Vx/R$ and Vy/R where Vx and Vy are the North and East components of Vg. This feedback loop for maintaining the platform perpendicular with the local vertical is called Schuler Tuning of the INS system.

The early gyro compass used in ships was a special form of gyro pendulum, and it was subject to excessive errors in the presence of horizontal accelerations which occurred during ship's maneuvers. This problem was studied by Dr. Maximilian Schuler who, in 1932, showed that the problem could be solved by adjusting the period of the pendulous gyro compass to a unique value determined by earth radius R and gravity g:

$$T = 2\pi\sqrt{\frac{R}{g}} = 84.4 \text{ mins} - \text{which is the period of a hypothetical}$$

pendulum of length R.

This hypothetical pendulum is known as the Schuler Pendulum and the associated period T as the Schuler Period – any system mechanized to have this period is said to be a Schuler Tuned System (See Figure 9.41).

This local vertical INS becomes a Schuler Tuned System. This is important because many of the errors associated with such a system are cyclic. They are therefore predictable and in some cases bounded.

9.75
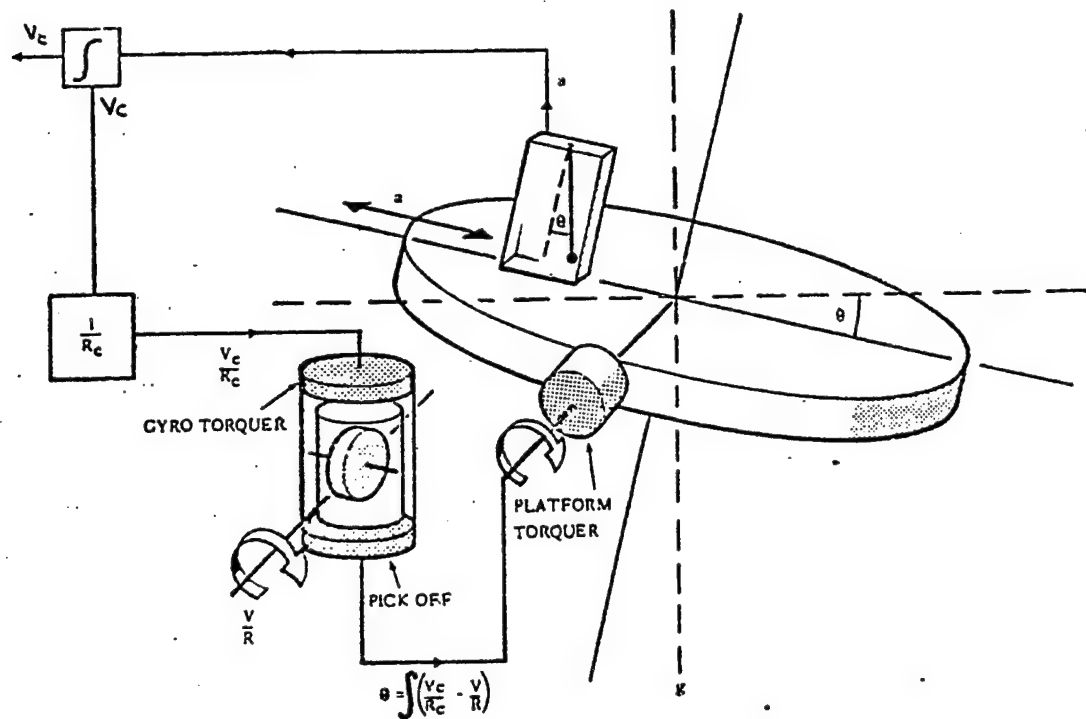
FIGURE 9.41 SCHULER TUNED INS

In Figure 9.41:

      a = applied acceleration

      V = actual velocity

      V_c = calculated velocity

      R = actual earth radius

      R_c = calculated earth radius

      g = acceleration due to gravity

      θ = platform tilt

9.76

9.5.1.4 Schuler-Tuned Local Vertical INS Mechanization

The objective of the Schuler Loop is to keep the platform level. Figure 9.41 shows a single axis of a Schuler Tuned two axis navigation system. If the calculated torquing rate $\frac{V_c}{R_c}$ is exactly correct, a level platform would be maintained level, i.e., $\theta = 0$. However, this is not likely in a practical system. If the platform is off level at all, the accelerometer picks up a component of gravity. Note that since this is the same accelerometer that is being used to sense vehicle acceleration, an acceleration error is introduced.

By carefully considering the platform dynamics it can be seen that a leveling error induces an acceleration which causes a torquing input to counter the leveling errors. (That is, the system is stable.) A leading edge down tilt causes a decrease in sensed acceleration, which results in a smaller $\frac{V_c}{R_c}$ torque, and a smaller error. Conversely, a leading edge up tilt causes the sensed acceleration to be greater than actual acceleration, and an increased $\frac{V_c}{R_c}$ is induced which reduces the tilt error. The error in sensed acceleration due to an accelerometer off-level by θ radians has a magnitude of g sin θ. If θ is small, this component can be approximated by gθ. When this component is sensed, the following sequence of operations (Figure 9.42) takes place:

9.77
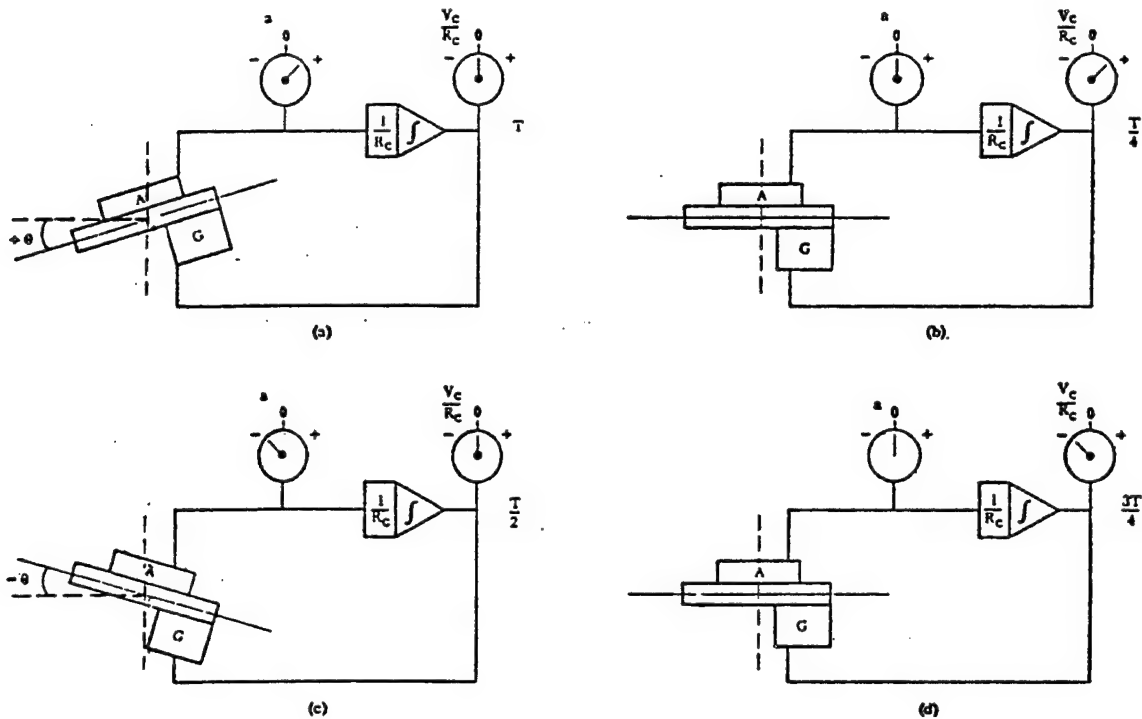
FIGURE 9.42   ERROR PROPAGATION IN AN INS

a.   The accelerometer senses $g\Theta$ and interprets it as an acceleration to the right, say $+v_e$. The signal is integrated and the platform rotates clockwise at a rate equal to computed torquing rate V_c/R_c.

b.   When the platform reaches the horizontal the apparent acceleration falls to zero. The integrator output is instantaneously constant. The platform thus continues to rotate clockwise at a rate V_c/R_c.

c.   On turning through the horizontal, the accelerometer senses an opposite gravity effect. This is interpreted as a $-v_e$ acceleration. This reduces the $+v_e$ velocity to zero, and at the angle $-\Theta$ the platform stops tilting.

d.   The accelerometer still signals a $-v_e$ acceleration and therefore a $-v_e$ velocity is built up. The platform is then rotated counterclockwise back towards the horizontal. The process continues with an oscillation of $+\Theta$.

9.78
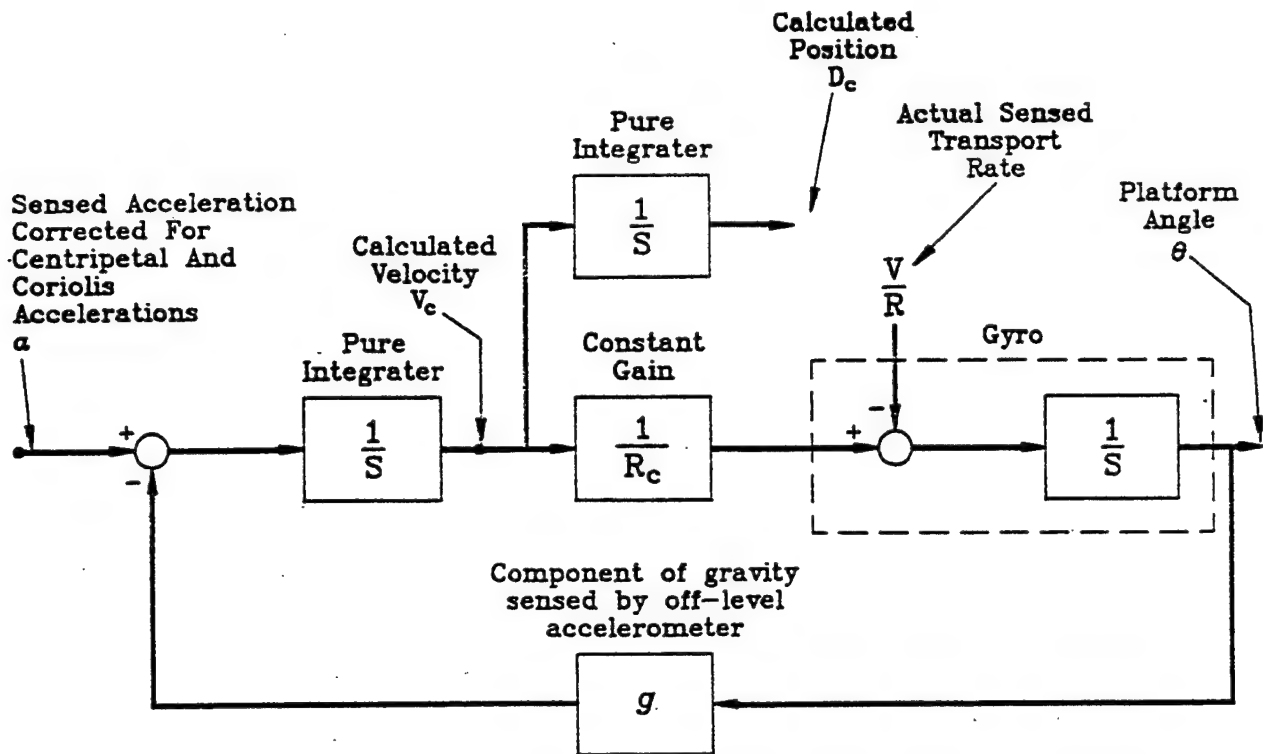
FIGURE 9.43   BLOCK DIAGRAM OF A SINGLE AXIS SCHULER TUNED INS

Figure 9.43 shows the block diagram of a single axis Schuler Tuned platform. Notice that in the forward loop, corrected acceleration is integrated twice to get position. As seen in the previous discussion about how gyros are used to stabilize the stable element, a transport rate correction must be made to the gyro or the vehicle motion around the earth will cause an apparent error in leveling. The transport rate correction, measured in radians per second, has a magnitude of $\frac{V}{R}$, that is, the angular rate at which the vehicle is moving.

In other words, the apparent precession that will be "felt" by the leveling gyros is equal to the ratio of actual aircraft velocity and actual earth radius. In order to counter the apparent precession, the system must provide an equal and opposite torque. The system's best estimate of its velocity V is the velocity V_c that it calculates based on sensed acceleration. For actual radius of the earth, the simple system in Figure 9.43 uses a constant value, R_c. The ratio $\frac{V_c}{R_c}$ is used to counter the $\frac{V}{R}$ apparent precession. Figure 9.43 represents the gyro as a summing junction and a pure integrator with angular

9.79

rates as input and an angle, Θ, as output. The calculated rate $\frac{V_c}{R_c}$ is applied as a torquing input to counter the apparent precession $\frac{V}{R}$ caused by movement over the earth's surface. This block diagram can be analyzed using standard analysis tools of linear control theory.

9.5.1.5 Latitude Restrictions

Restrictions using the local vertical north pointing INS system are encountered at the higher latitudes. These restrictions are summarized as follows:

a. The torquing rate to the azimuth gyro to compensate for transport rate (Vx/R tan λ) becomes excessively high as λ approaches 90° and tan λ approaches ∞. Depending on the velocity of the vehicle the limiting latitude is approximately $\pm$ 75°.

b. The calculation of longitude is a function of sec λ which also gets excessively high as λ approaches 90°; the limiting latitude is normally $\pm$80° to $\pm$85°.

c. As will be explained in Section 9.6, the magnitude of the error signal which is used to torque the azimuth gyro during the gyro compassing phase of alignment becomes very small as latitude increases. For practical purposes this limits gyro compassing to latitudes of less than $\pm$75° to $\pm$80°.

9.5.2 Strap Down Inertial Systems

All inertial navigation systems studied so far have consisted of a stable element either fixed in attitude with respect to inertial space, or fixed with respect to a moving navigational coordinate frame, such as an earth local vertical system. In these systems sensed accelerations are integrated to give velocities and distances along known directions, and the stable element is maintained in its known orientation by gyroscopic control.

It is possible, using digital computers and complex programming, to dispense with the gimbals and mount the inertial sensors directly on to the airframe (aircraft maneuvers are compensated for using mathematical equations so attitude and position can be calculated). Such a system is known as a strap down INS.

In a Strap Down System (SDS), the accelerometers are fixed to the vehicle, and their orientations with respect to the reference frame are computed. Information for this computation is obtained from the output of gyroscopes that are also directly mounted on the body of the vehicle.

The idea of an inertial navigation system using body-mounted sensors was described in a patent by W. Newell in 1956. However, development of such a system has only been possible since the development of digital computers; although analog computers could perform the required calculations their accuracy is not acceptable. In effect the computer in a SDS replaces the gimbals in a conventional system. The attractiveness of this trade off largely depends on the availability of a computer that is small, fast, and inexpensive. Recent developments in digital computers account for the widespread attention given to SDS within the last few years.

The basic configuration of a SDS is shown in Figure 9.44. In a SDS no control is exercised over the orientation of the accelerometers; they are fixed to the aircraft and are subjected to the full effect of all aircraft maneuvers. Thus, although a complex gimballing structure is not required to isolate the accelerometers, their outputs, which will be along aircraft axes, must be referred to the axes of an inertial reference frame for navigation. This coordinate transformation is achieved with the aid of information determined in an attitude computer that operates on the gyro outputs to continuously compute the orientation of the sensor package with respect to inertial space. Since the SDS may be readily made free of gimbal lock, it is equivalent to a four gimbal rather than a three gimbal platform system.

Two additional advantages are inherent in a SDS. First, sensors can be in any relative position with respect to one another. This eases the assembly and servicing of SDS and enables the system to be updated as more recent sensors become available. Secondly, changes in the reference frame, including those required for initial alignment, are not limited in speed by the necessity of physically moving the gimbals.

The accuracy of a SDS, like that of a gimballed INS, is usually limited by the accuracy of the inertial sensors. The contribution of other error sources such as computer error can be minimized. Since the effect of sensor error is the same in SD and gimballed systems, the total SDS error should be equivalent to that of a platform with the same sensors.

9.81
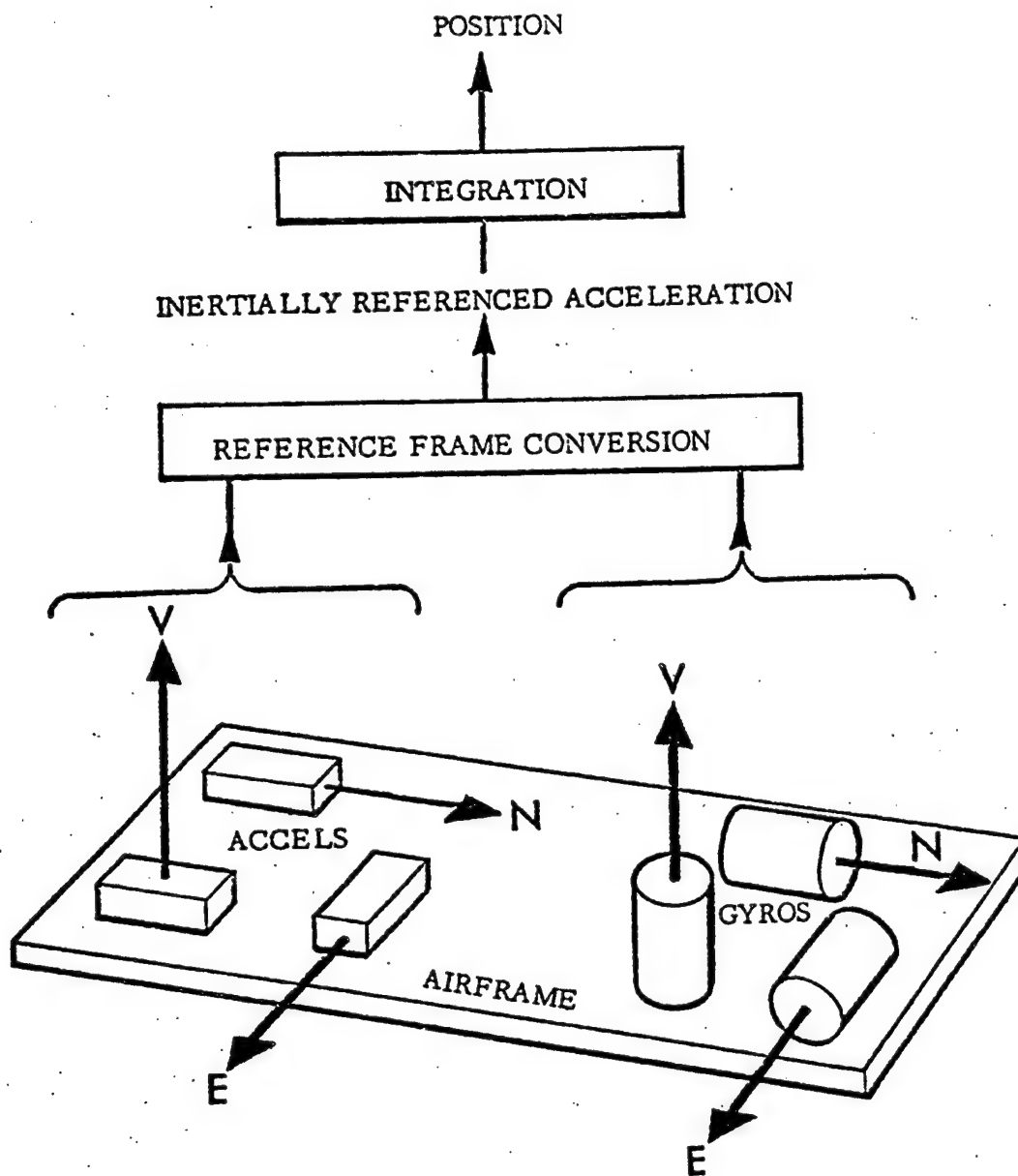
FIGURE 9.44   STRAP DOWN CONFIGURATION

9.82

9.5.3 <u>System Improvements</u>

Most attempts to improve the accuracy of inertial navigation systems
have been directed toward the addition of either speed, position, and/or
direction from an exter- nal source; however, one improvement has been
directed toward expending the operating envelope of the basic INS to cover the
polar regions. This system has been named the wander azimuth inertial system.
9.5.3.1 <u>Wander Azimuth System</u>. The basic fundamentals of a wander azimuth or
wander angle system, as it is commonly called, are the same as a basic INS
except that during alignment the x axis is aligned to the fuselage of the air-
craft. During the initial alignment, all the earth compensation rate is sent
to the x axis just as if it was pointing north. Since this is not true, the
platform will be torqued out of level and the accelerometer will sense a com-
ponent of gravity. This will cause the platform to precess in both the x and
y axes until it becomes level. The computer will then compute the wander
angle from the required torque necessary to produce the desired precession in
both axis. Once the computer determines the value of the wander angle, the x
and y axis are torqued at the proper rate to maintain the platform level with
the local vertical. Since there is no requirement to align the x axis with
true north, the z axis is torqued for earth's rate only. The results of this
are that the direction of the x axis varies with respect to true north, hence
the name wander angle system. This type of system is being used in the F-15.
The major advantage of this system is that it allows operation in the polar
regions. The biggest disadvantage is the inability to conduct conventional
flight testing. This problem has been circumvented by always aligning the
fuselage of the aircraft with true north prior to commencing the alignment
process.
9.5.3.2 <u>External Sources of Information</u>. There are three classes of external
sources of information available for updating the INS; speed, position, and
direction. The primary purpose of these inputs is to reduce the errors in the
INS.

1. Speed. Speed or velocity information can be added to the INS
in two manners, depending on its accuracy. In either case the velocity must
be of greater accuracy than the basic INS. In the simplest case the noniner-
tial velocity is algebraically added to the inertial velocity and a propor-
tional bias is applied to the accelerometer. The fact that the velocity is 90

degrees out of phase with the acceleration in a Schuler Tuned platform provides the damping characteristic. In the more sophisticated case where the accuracy of the noninertial velocity is far greater than the INS velocity, it can be used to correct the inertial velocity as well as damp the accelerometer. The noninertial velocity is used as a zero reference and the platform is torqued until the output of the accelerometer agrees with the reference. An example of this type of system is a Doppler – INS mix such as in the A-7 aircraft.

2. Position. Position data, if of a higher accuracy than the basic INS, can be used to update position and velocity errors. This is done by updating the actual position and/or velocity at that point in time. This data cannot be used to torque the platform. The problem associated with this type of update is the inability to account for the difference in the inertial parameters due to the Schuler Oscillations. LORAN, TACAN, VOR, and other types of radio systems are used to perform this type of update. This type of system has seen extensive use in civilian aviation.

3. Direction. Direction information is used to correct gyro drift errors by torquing the platform. This is accomplished by programming stars in the computer and at any given time, the computer will look at certain stars and torque the platform in order to have the correct alignment reference to the proper stars. This system has limitations of weather and in some cases daytime limits due to the light levels. However, the major limitation is the inability to damp the Schuler Period since the stellar tracker does not pro- de any indication of the earth's center. An example of this type of system is a stellar inertial tracker such as used in photo mapping C-141 and C-5 aircraft.

9.6 INS ALIGNMENT

Initial alignment consists of orientating the acceleration sensitive axes of the system within the navigation reference frame before it is required for use. The purpose of this chapter is to consider the various methods of accomplishing alignment. The choice of methods depends on operational factors. Alignment methods can be classified as follows:

      a. Self alignment

      b. Reference alignment

      c. At sea alignment

      d. Airborne alignment

9.6.1 Self Alignment

Self alignment normally consists of the following phases:

      a. Warm up and coarse alignment.

      b. Fine alignment

      c. Gyro compassing

9.6.1.1 Warm Up and Coarse Alignment

The course alignment phase consists of:

      a. Rapid heating to operating temperature and gyro run up.

      b. Leveling with reference to the aircraft frame.

      c. Setting azimuth by reference to a gyro magnetic compass.

All phases can be carried out concurrently and the time for the phase is limited by the platform heating (2 – 3 mins). Leveling and azimuth alignment by these means can be achieved to within about 1° of arc.

9.6.1.2 Fine Alignment

Vertical alignment is simply and speedily achieved by the application of the "accelerometer null" technique. With the aircraft stationary, there should be zero output from the horizontal accelerometers. However, a small leveling error of θ (rads) will result in a signal output of approximately $g\theta$.

This error signal is used to drive the appropriate leveling gyroscope until θ is reduced to zero. This process is illustrated in Figure 9.45 for both channels. In practice both gyro output signals would be resolved about the platform azimuth before being passed to the gimbal servo motors.
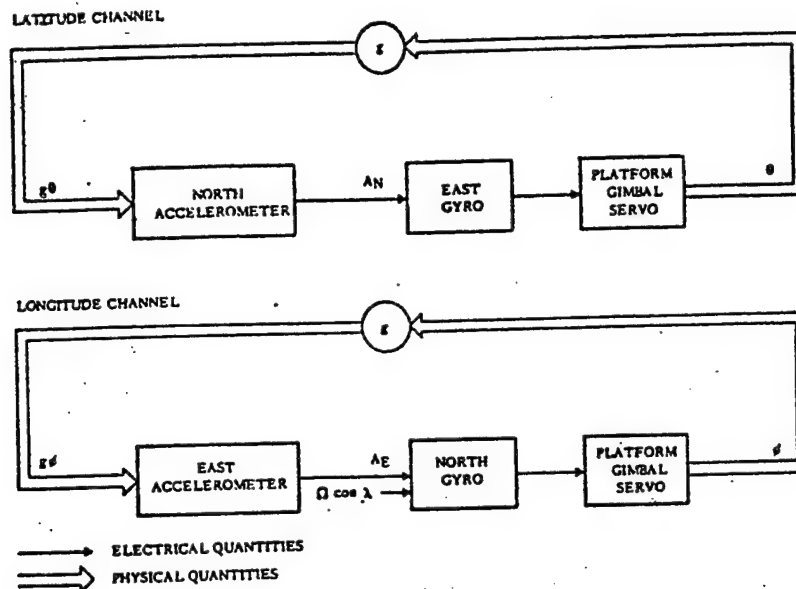
FIGURE 9.45 ACCELEROMETER NULL TECHNIQUE

9.6.1.3 Gyro Compassing

Gyro compassing is the name given to self alignment in azimuth, and is frequently referred to as normal alignment. It is based on the fact that the East gyro will sense a component of earth rotation $\Omega \cos \lambda \sin \psi$, or for small angles $\psi \Omega \cos \lambda$, Figure 9.46.

$$A_N = g \sin \theta = \Omega \cos \lambda \sin \psi$$

where

ψ = Azimuth Misalignment Angle
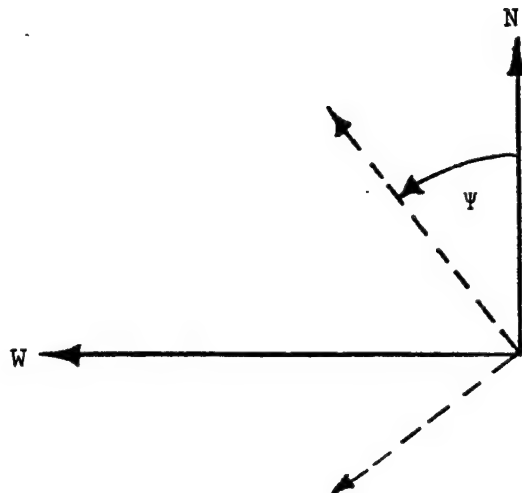
FIGURE 9.46   AZIMUTH MISALIGNMENT

In an alignment mode (Figure 9.47) this will result in a platform tilt to generate a compensating accelerometer signal. By using this accelerometer output signal through a high gain K_2 to torque the azimuth gyro, the platform can be rotated in azimuth until the error is driven to null. However, this takes time.

A typical system in US latitudes, starting at a temperature between 0 degrees C and 15 degrees C will carry out a complete alignment sequence in about 9 to 12 minutes.

9.6.2   Reference Alignment Methods

The gyro compassing phase of the self-alignment sequence consumes the most time. The use of some external reference produces a rapid method of alignment.

Methods so far developed are:

a. Transfer gyro alignment
b. Stored heading alignment
c. Head up display alignment
d. Runway alignment
e. Optical slave alignment

A_N = NORTH ACCELEROMETER OUTPUT
θ = PLATFORM LEVEL MISALIGNMENT ANGLE
g = GRAVITY
ψ = AZIMUTH MISALIGNMENT ANGLE
Ω = EARTH'S RATE OF ROTATION
λ = LOCAL LATITUDE
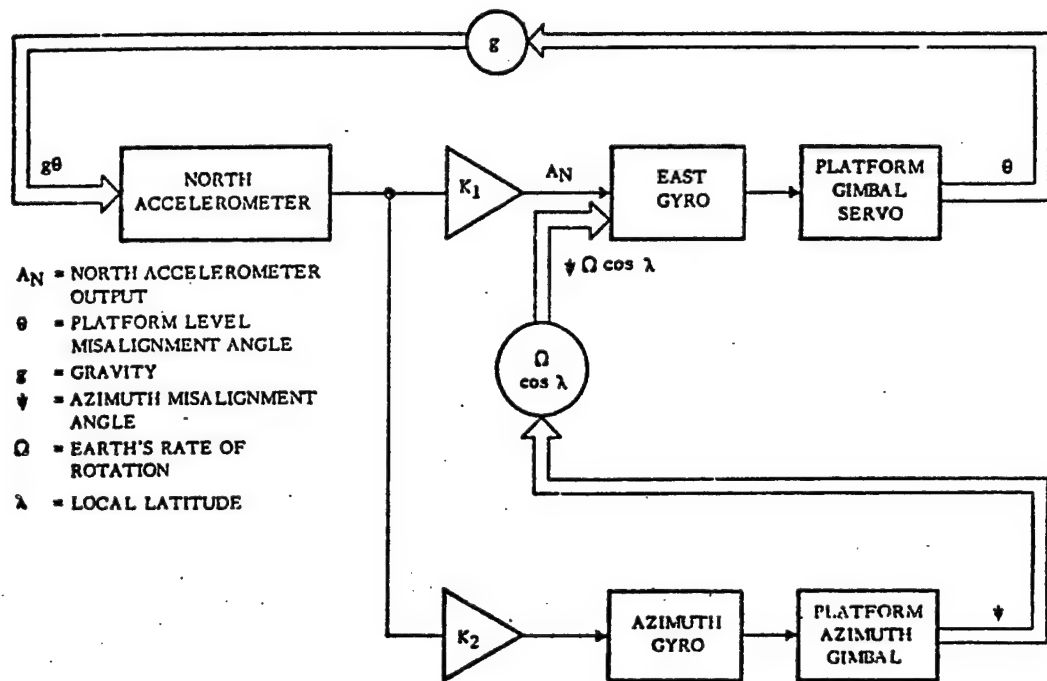
FIGURE 9.47   GYRO COMPASSING

9.6.2.1 Transfer Gyro Alignment

The transfer gyro comprises a datum gyro and a transfer gyro (Figure 9.48).

9.6.2.1.1 Datum Gyro. The datum gyro is used as a gyro-compass to establish an accurate North reference. The input rate $\Omega \cos \lambda \sin \psi$ about the input axis (East) drives a base plate in azimuth until ψ is zero.

9.6.2.1.2 Transfer Gyro. An azimuth gyro of the 'rotorace type' is located on the datum gyro base. The two gyros are matched, by matching of the stators of the two gyro synchros. The transfer gyro rotor is then servoed to the True North datum. It is then carried to the aircraft located on a mounting pad

leveled and connected to the aircraft platform by another synchro. The azimuth is then transferred. The complete sequence takes 75 seconds allowing for transport of the transfer gyro and attachment to the gyro requiring alignment.

9.6.2.2 Stored Heading Alignment

This is a simple and rapid process which utilizes servoing the azimuth to some preset synchro reference. This method assumes the aircraft has not moved during the 'power off' period as it relies on setting a reference which was noted on return from a previous sortie

9.6.2.3 Head Up Display Alignment

This technique is an extension of the stored heading alignment by using the HUD to record the true bearing of a suitable object in the middle distance. The platform is precessed until the correct bearing is measured against the known distant object.

9.6.2.4 Runway Alignment

9.6.2.4.1 Principle. In this technique, the aircraft's lateral displacement at the end of the take-off run is measured, by the INS. This displacement is assumed to be entirely due to platform misalignment in azimuth. The recorded values are used to realign the system.

9.6.2.4.2 Components. The system requires an analog computer with its associated controls in addition to normal INS components.

9.6.2.4.3 Method of Alignment. The platform is erected normally and the surveyed runway true bearing is set. A distance slightly less than the estimated take-off run is set into Comparator #1. The aircraft is then positioned on the center line and takes off. Normal take-off continues and when the aircraft has reached the end of take-off run, as set, a comparison between inertial datum and set datum will provide cross track error. Assuming the pilot remains on the center line the cross track error is a function of INS alignment error and can be used to realign the system.

9.6.2.5 Optical Slave Alignment

Optical Alignment. Final alignment can be done to a high degree of accuracy with optical autocollimating techniques. Essentially, this consists

9.89

of torquing the platform until an optical surface (which is mounted on the platform) is perpendicular to a reference beam of light. The beam of light used for the azimuth reference may be oriented by reference to a celestial azimuth or to a previously surveyed azimuth reference target.

The platform gimbals are usually torqued with automatic servo auto-collimating equipment such as an azimuth alignment theodolite. Optical alignment techniques are accurate to the order of a few seconds of arc.

9.6.3 At Sea Alignment

The problem of alignment at sea is aggravated by further accelerations being present due to the ship's velocity, pitch, roll, and yaw. An accurate ship's position for any specific point of time is difficult to obtain.

Any of the following alignments can be carried out at sea:

a. Insertion. Where the INS is readied and aligned at a central position and then carried to the aircraft for insertion, it may be subjected to gross accelerations during the transit. Some form of transit power pack will be required.

b. Transfer Alignment. A transfer gyro will "remember" a datum azimuth which may have changed during transit, because of ship's movement. Alternatively, initial conditions may be relayed by transmission cables from the SINS, but such a system will increase the clutter on the already crowded flight deck.

c. Gyro-Compassing. This requires complex computing, to cope with the variable inputs connected with ship's movement. Alignment times are thus longer than for ground based gyro-compassing. About 25 minutes will be required to achieve an accurate alignment.

d. Aided Gyro-Compassing. Aided gyro-compassing can be achieved by the use of a portable velocity sensor to transfer azimuth from the SINS and update local velocity information.

9.6.4 Airborne Alignment

It is highly desirable to be able to airborne align an INS, both from the initial alignment aspect, and for subsequent recalibration during long flights. This is NOT possible with pure INS. It is possible however, with aided systems which provide a continuous velocity reference with which to monitor the INS outputs.
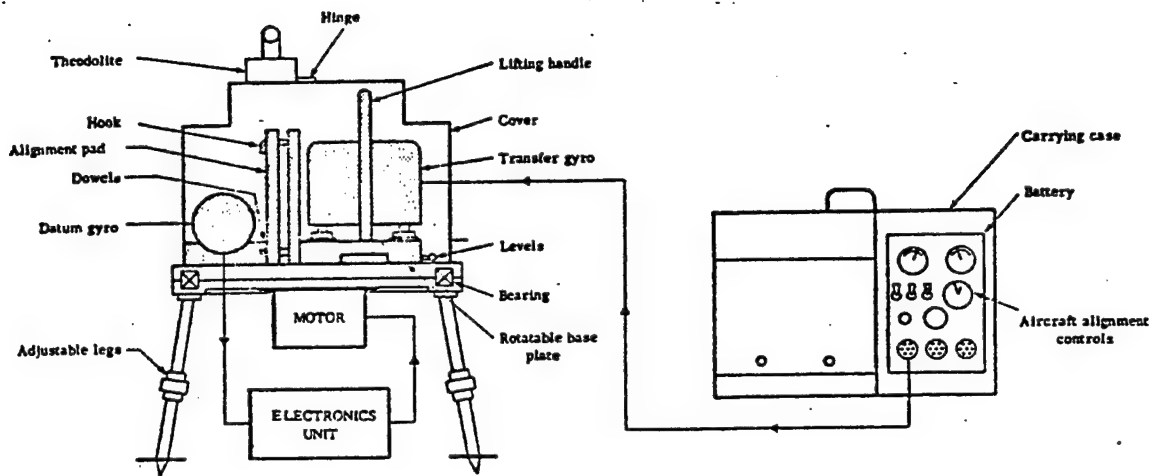
FIGURE 9.48   TRANSFER GYRO ALIGNMENT

9.7 ERROR ANALYSIS

From the discussion about Schuler Period (Reference Figure 9,43) it can be shown that any time $V_c/R_c - V/R \neq 0$, the platform will be torqued out of level. This will cause a false acceleration $g\theta$ to be sensed, and a Schuler oscillation will commence. Thus any factor which can cause V_c/R_c to be different from V/R is a source of acceleration error (EA), a velocity error (EV), and a distance error (ED). It is essential to examine these errors as knowledge and measurement of them will form much of the work in the test programs of INS testing.

9.7.1 Error Sources

The factors which can cause these errors are:

    a. Instrument errors in gyros, accelerometers, integrators, and torquers.

    b. Errors in initial alignment, both level and azimuth.

    c. Errors in mechanizing the calculated Earth radius and the accelerometer and gyro correction terms.

    d. The effects of vibration, accelerations and maneuvers on a real platform and its components.

9.7.2 Effects of Errors

The effects of these factors will be reflected as one or more of the fundamental error sources:

    a. Errors within the leveling loop.

        (1) Acceleration errors (ε_a).

        (2) Velocity errors (ε_v).

        (3) Initial tilt (θ_o).

        (4) Leveling gyro drift (δ_L).

    b. Cross-coupling effects of errors in the azimuth loop.

        (1) Azimuth misalignment (ψ).

        (2) Azimuth gyro drift (δ_ψ).

The system errors (θ, E_A, E_V, E_D) due to each of these fundamental sources in the leveling loop will now be examined using block diagram algebra.

The dynamics of the Schuler Loop can be seen in Figure 9.49 (a repeat of Figure 9.43). The technique which will be used for this examination will be to investigate the relationship between the two relevant points of the Schuler Loop using the FUNDAMENTAL error as the input, and the SYSTEM error as the output. The transfer function of output to input will then be obtained. The equation will then be solved in the time domain, using Laplace transforms.
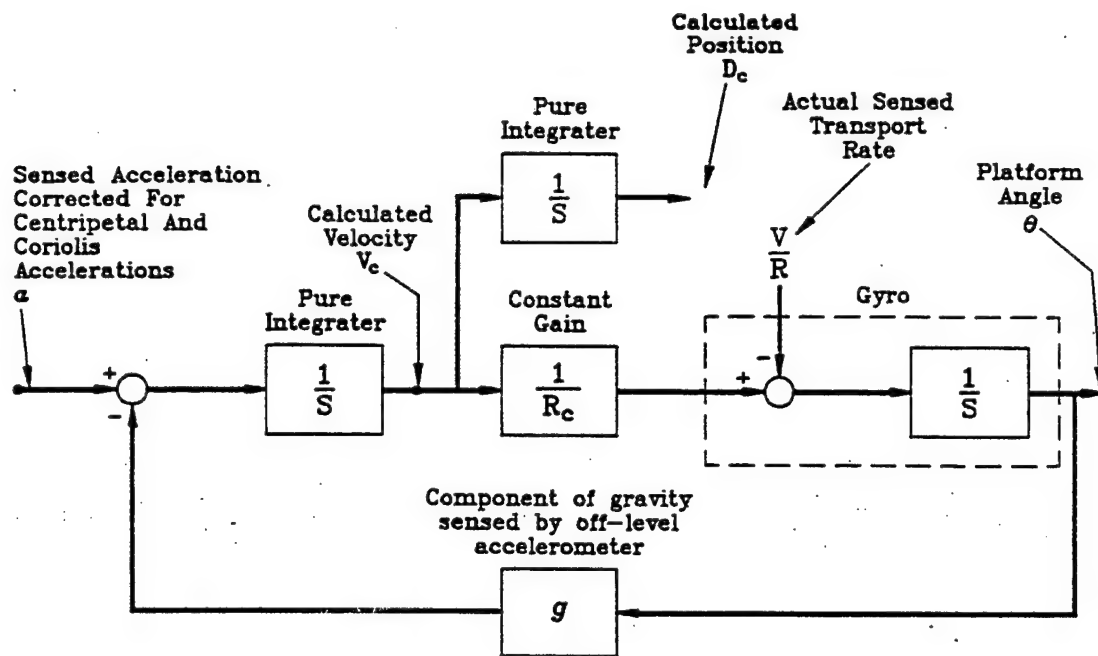
FIGURE 9.49   DYNAMICS OF THE SCHULER LOOP

9.7.2.1 Effect of Acceleration Errors (ε_a)

Acceleration errors are first integrated into an error velocity which, through the Schuler Loop, torques the platform out of level. The accelerometer will then sense a component of gravity opposite in direction to the acceleration error. The sum of the acceleration error and the component of gravity oscillates at the Schuler frequency with E_V and E_D being the first and second integrals of this acceleration signal E_A. θ equals E_A/g. To illustrate the effect of ε_a, the loop at Figure 9.49 may be redrawn as in Figure 9.50.

9.93
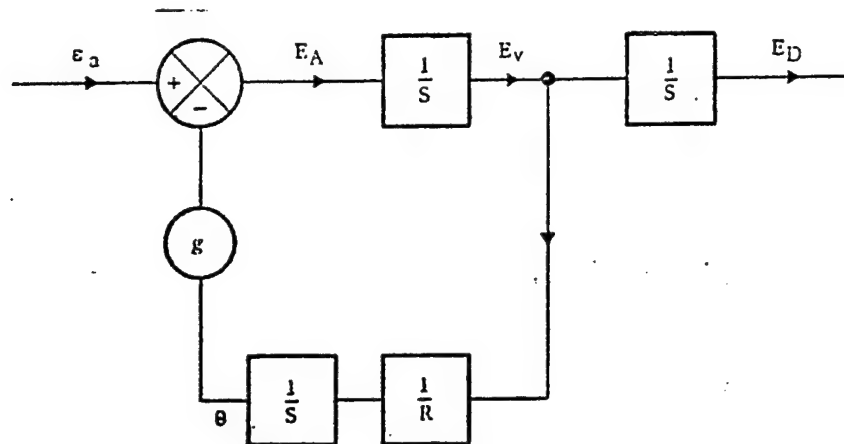
FIGURE 9.50   EFFECT OF ε_a

Determination of E_D.   From Figure 9.50 using block diagram algebra:

$$\frac{E_D}{a} = \frac{\dfrac{1}{S^2}}{1 + \dfrac{g}{RS^2}} = \frac{1}{S^2 + \dfrac{S^2 g}{RS^2}} = \frac{1}{S^2 + \omega_s^2}$$

Where $\omega_s = \sqrt{\dfrac{g}{R}}$, the Schuler Frequency.

For a step input ε_a

$$E_D(S) = \frac{\varepsilon_a}{S} \cdot \frac{1}{S^2 + \omega_s^2} = \frac{\varepsilon_a}{\omega_s^2} \cdot \frac{\omega_s^2}{S(S^2 + \omega_s^2)}$$

and transforming into the time domain

$$E_D = \frac{\varepsilon_a}{\omega_s^2} (1 - \cos \omega_s t)$$

E_V, E_A and Θ may be similarly obtained, or arrived at by successive differentiation to give:

9.94

$$E_V = \frac{\varepsilon_a}{\omega_s} \sin \omega_s t$$

$$E_A = \varepsilon_a \cos \omega_s t$$

The curves and approximate values of θ, E_A, E_V, and E_D for an ε_a of 3×10^{-4} g are in Figure 9.51.
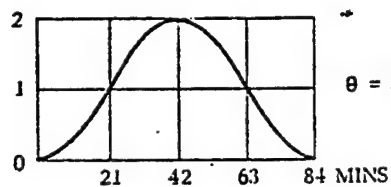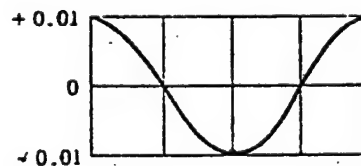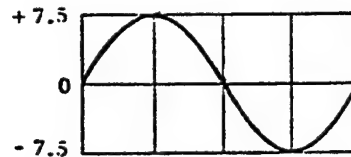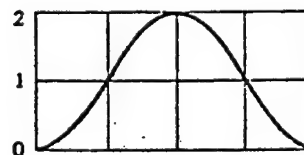
FIGURE 9.51   SYSTEM ERROR CURVES DUE TO ACCELERATION ERROR

9.95

9.7.2.2 Effects of Velocity Errors (ε_v)

Velocity errors may be considered as errors in the first stage integrator. ε_v will therefore cause an error in the level gyro torquing rate causing the platform to torque out of level. The out of level accelerometer now senses $g\theta$ which it interprets as an acceleration. This signal is integrated into a velocity of the opposite polarity to that of the initial ε_v. The sum of these velocities oscillates at the Schuler Frequency. To illustrate the effect of ε_v the loop in Figure 9.49 may be redrawn as in Figure 9.52.
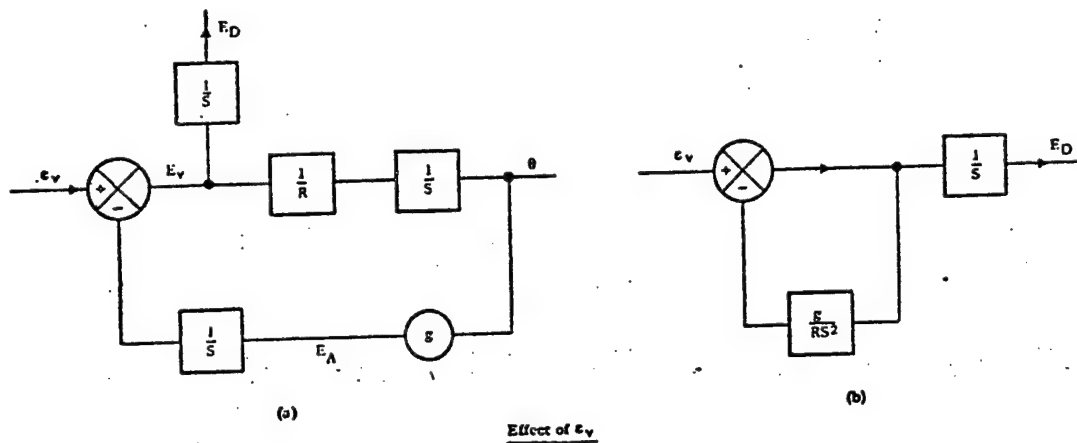
Effect of ε_v

FIGURE 9.52   EFFECT OF VELOCITY ERRORS

Determination of E_D, E_V, E_A, and θ may be determined in exactly the same way as outlined in the paragraph on Acceleration Errors. They are:

$$E_D = \frac{\varepsilon_v}{\omega_s} \sin \omega_s t$$

$$E_V = \varepsilon_v \cos \omega_s t$$

$$E_A = \varepsilon_v \omega_s \sin \omega_s t$$

$$\theta = \frac{\varepsilon_v \omega_s}{g} \sin \omega_s t$$

The curves and appropriate values of θ, E_A, E_V, and E_D for an ε_v of 1 ft/sec are in Figure 9.53.

θ
PLATFORM
TILT
(MINS ARC)
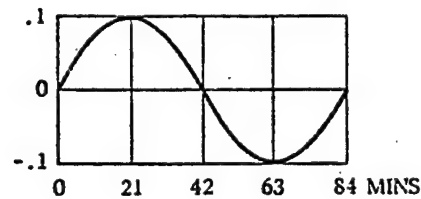
$$\theta = \frac{\varepsilon_V \, \omega_S}{g} \sin \omega_S t$$

E_A
ACCELERATION
ERROR
(FT/SEC^2)
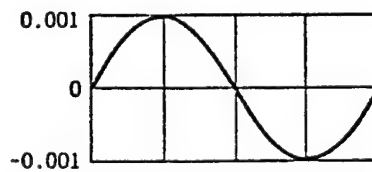
$$E_A = \varepsilon_V \, \omega \sin \omega_S t$$

E_V
VELOCITY
ERROR
(FT/SEC)
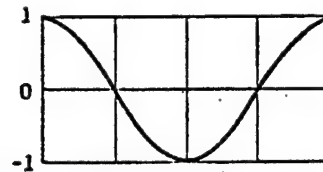
$$E_V = \varepsilon_V \cos \omega_S t$$

E_D
DISTANCE
ERROR
(FT)
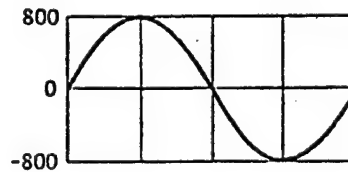
$$\varepsilon_D = \frac{\varepsilon_V}{\omega_S} \sin \omega_S t$$

$$\varepsilon_V = 1 \text{ FT/SEC}$$

FIGURE 9.53   SYSTEM ERROR CURVES DUE TO VELOCITY ERROR

9.7.2.3   Effect of Initial Tilt (θ_o)

The effect of initial tilt θ_o can be obtained by redrawing the Schuler Loop as in Figure 9.54.

9.97
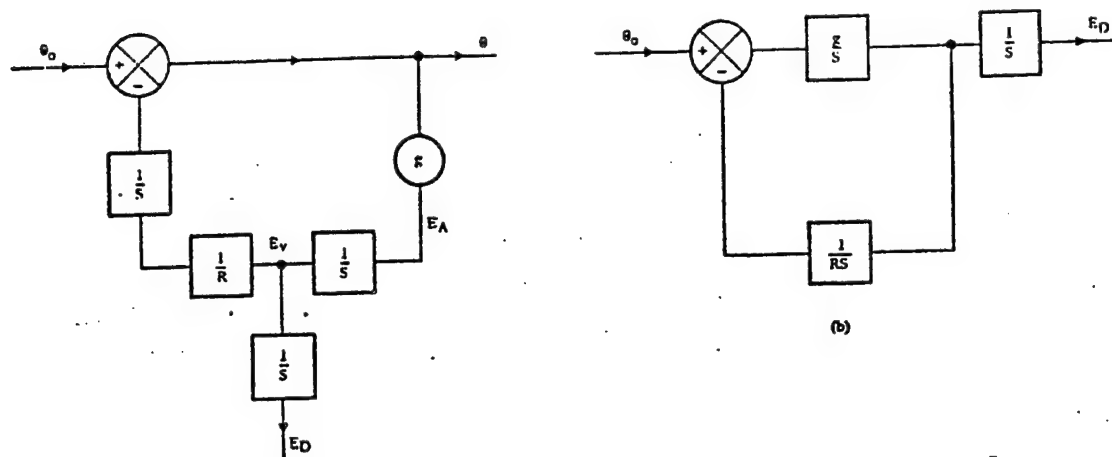
FIGURE 9.54   EFFECT OF θ_o

The errors of E_D, E_V, E_A, and θ may be determined as indicated in the previous paragraphs. They are:

$$E_D = \frac{g\Theta_o}{\omega_s^2} (1 - \cos \omega_s t)$$

$$E_V = \frac{g\Theta_o}{\omega_s} \sin \omega_s t$$

$$E_A = g\Theta_o \cos \omega_s t$$

$$\theta = \Theta_o \cos \omega_s t$$

The curves and approximate values of θ, E_A, E_V, and E_D for an initial leveling error of 1 min are in Figure 9.55.

9.7.2.4 Effect of Leveling Gyro Drift (δ_L)

A drift of the leveling gyro causes an error in the applied torquing rate which means that the platform will be torqued out of level. The acceler-

9.98

ometer now picks up a component of gravity which is integrated as a velocity. Through the Schuler Loop the erroneous velocity torques the leveling gyro in opposition to the error signal. However, the erroneous torquing overshoots the gyro drift, and the resulting velocity error oscillates about a mean value equivalent to the difference between the two rates. The resulting distance error oscillates as a negative sine wave at the Schuler Frequency about an average value which is a RAMP function of TIME.

θ
PLATFORM
TILT
(MINS ARC)

$\theta = \theta_0 \cos \omega_s t$

E_A
ACCELERATION
ERROR
(FT/SEC^2)

$E_A = g\theta_0 \cos \omega_s t$

E_v
VELOCITY
ERROR
(FT/SEC)

$E_v = \dfrac{g\theta_0}{\omega_s} \sin \omega_s t$

E_D
DISTANCE
ERROR
(N.M.)

$E_D = \dfrac{g\theta_0}{\omega_s{}^2} (1 - \cos \omega_s t)$

$\theta_0 = 1$ min arc
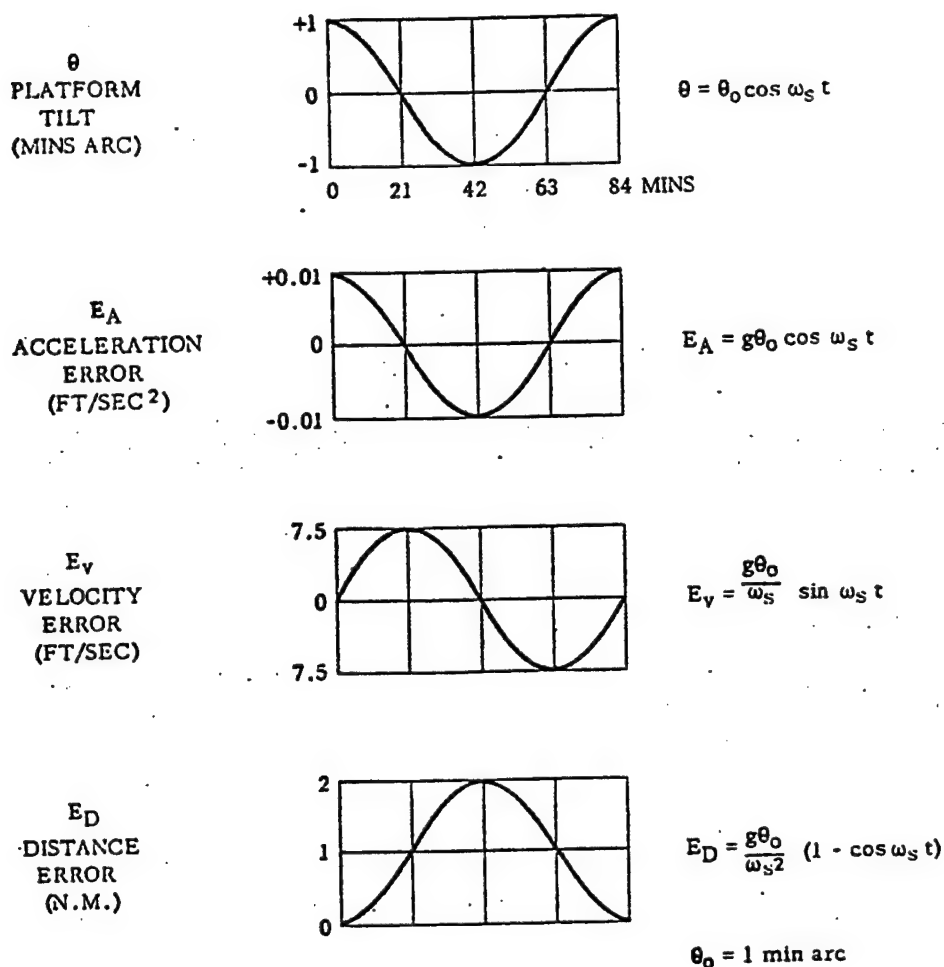
FIGURE 9.55   SYSTEM ERROR CURVES DUE TO INITIAL TILT ERROR

9.99
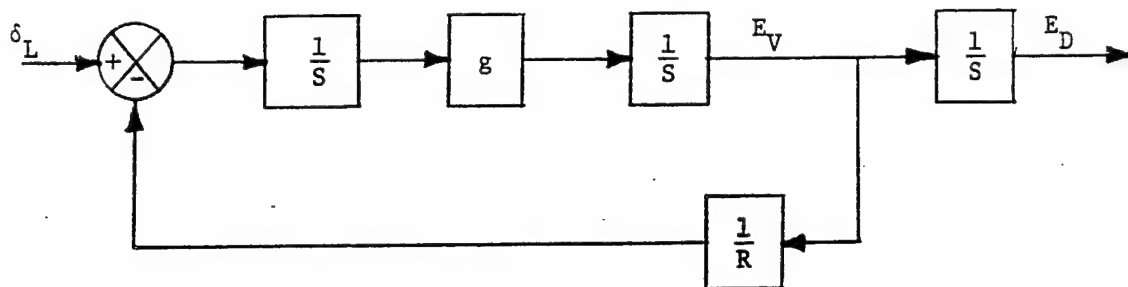
FIGURE 9.56. EFFECTS OF GYRO DRIFT δ_L

Now for the determination of E_D, E_V, E_A, and θ. The Schuler Loop may be redrawn as in Figure 9.56 to illustrate the effects of δ_L. The system errors are:

$$E_D = \delta_L\ R\left(t - \frac{\sin \omega_s t}{\omega_s}\right)$$

$$E_V = \delta_L R(1 - \cos \omega_s t)$$

$$E_A = \frac{\omega_L\, g}{\omega_s} \sin\ \omega_s t$$

$$0 = \frac{\delta_L}{\omega_s}\ \sin \omega_s t$$

The curves and approximate values of θ, E_A, E_V, and E_D for a leveling gyro drift of .01°/hr are shown in Figure 9.57.

9.100

PLATFORM TILT (MINS ARC)
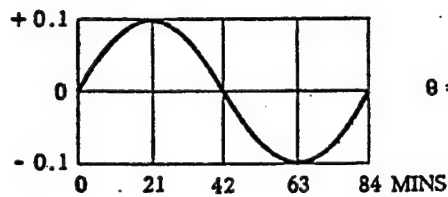
$$\theta = \frac{\delta_L}{\omega_s} \sin \omega_s t$$

ACCELERATION ERROR (FT/SEC²)
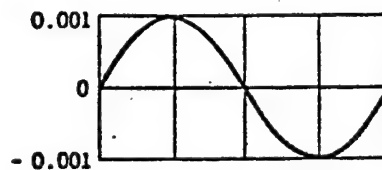
$$E_A = \frac{g \, \delta_L}{\omega_s} \sin \omega_s t$$

VELOCITY ERROR (FT/SEC)
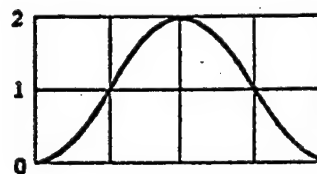
$$E_V = \delta_L R (1 - \cos \omega_s t)$$

DISTANCE ERROR (N.M.)
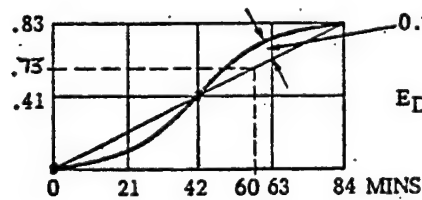
$$E_D = \delta_L R \left(t - \frac{\sin \omega_s t}{\omega_s} \right)$$

$$\delta_L = 0.01^\circ/\text{hr}$$

FIGURE 9.57   SYSTEM ERROR CURVES DUE TO LEVELING GYRO DRIFT

9.101

9.7.2.5 Effect of Azimuth Misalignment ψ

If an INS is properly aligned the East gyro will sense no component of earth rotation and the North gyro will sense $\Omega \cos \lambda$ (where Ω is the angular velocity of the earth, λ is the latitude). If the INS is misaligned by an angle ψ then the East gyro will sense $\Omega \cos \lambda \sin \psi$ and the North gyro will sense $\Omega \cos \lambda \cos \psi$ (See Figure 9.58).
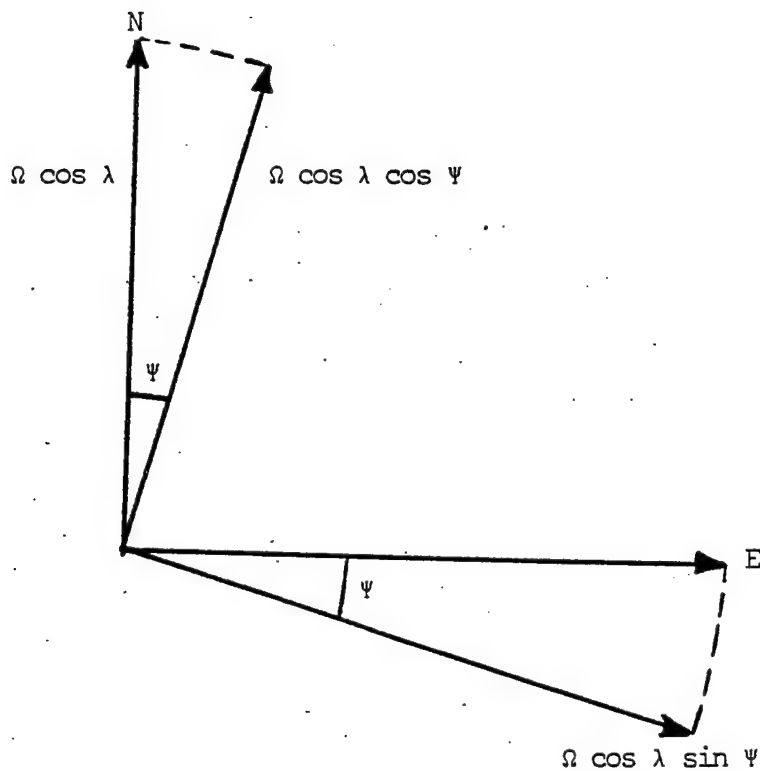
FIGURE 9.58 EFFECTS OF AZIMUTH MISALIGNMENT

For the North gyro, already being torqued by $\Omega \cos \lambda$, the torquing will be in error by:

$$\Omega \cos \lambda - \Omega \cos \lambda \cos \psi = \Omega \cos \lambda (1 - \cos \psi)$$

which is approximately zero for small values of ψ. ($\cos 1° = .998$). Thus errors in the longitude channel may be disregarded.

For the East gyro the sensed error will be $\Omega \cos \lambda \sin \psi$ which becomes $\psi \, \Omega \cos \lambda$ for small angles. This will manifest itself as a drift of the East leveling gyro.

$$\delta_L = \psi \, \Omega \cos \lambda$$

for a latitude of 45° and an ψ of 5 min of arc

$$\delta_L = .018°/hr.$$

This error is small but the unbounded nature of the error makes it essential that the initial azimuth alignment error be kept as small as possible. An additional effect of $\dot{\psi}$ is that the misaligned accelerometers will sense slightly incorrect accelerations. This error could become significant in conditions of prolonged acceleration, e.g. turns.

The equations for the determination of E_{DN}, E_{VN}, E_{AN} and θ_N are similar to the leveling gyro drift case, but the $\psi \, \Omega \cos \lambda$ substituted for δ_L.

9.7.2.6 Effect of Azimuth Gyro Drift (δ_ψ)

The most significant cross coupling error is azimuth gyro drift δ_ψ. An error entering the system here is integrated in the azimuth stabilization loop to give a misalignment ψ. As with azimuth misalignment, this will register as a leveling gyro drift where $\delta_L = \psi \, \Omega \, \cos \lambda$. In this case ψ (and therefore, $\psi \, \Omega \cos \lambda$) is growing and so the velocity error will oscillate about a mean which is increasing linearly with time.

For the determination of E_{DN}, E_{VN}, E_{AN}, and θ_N, the Schuler Loop may be redrawn as in Figure 9.59 The system errors are:

$$E_{DN} = \delta \, \psi \, R \, \Omega \, \cos \lambda \, \frac{t^2}{2} - \frac{1- \cos \omega_s t}{\omega_s^2}$$

$$E_{VN} = \delta \, \psi \, R \, \Omega \, \cos \lambda \quad t - \frac{\sin \omega_s t}{\omega_s}$$

9.103

$$E_{AN} = \delta \psi R \Omega \cos \lambda (1 - \cos \omega_s t)$$

$$\theta_N = \frac{\delta \psi \Omega \cos \lambda}{\omega_s^2} (1 - \cos \omega_s t)$$

Figure 9.60 shows the propagation of E_{DN} for a δ_ψ of .01°/hr at 60° North latitude.
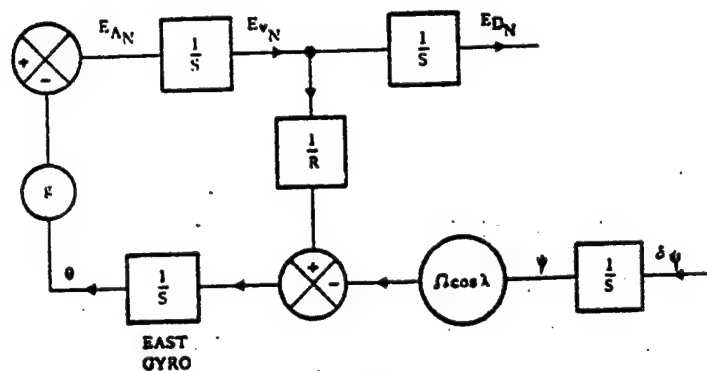
(a)

Effect of Azimuth Gyro Drift
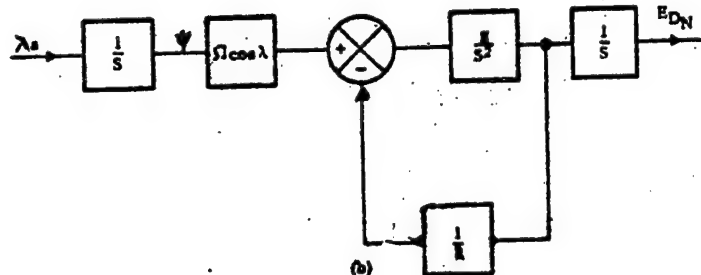
(b)

FIGURE 9.59   EFFECT OF AZIMUTH GYRO DRIFT

9.104

Effect of Azimuth Gyro Drift

$$\delta \Psi = 0.01^{\circ}/hr$$

Fig 16
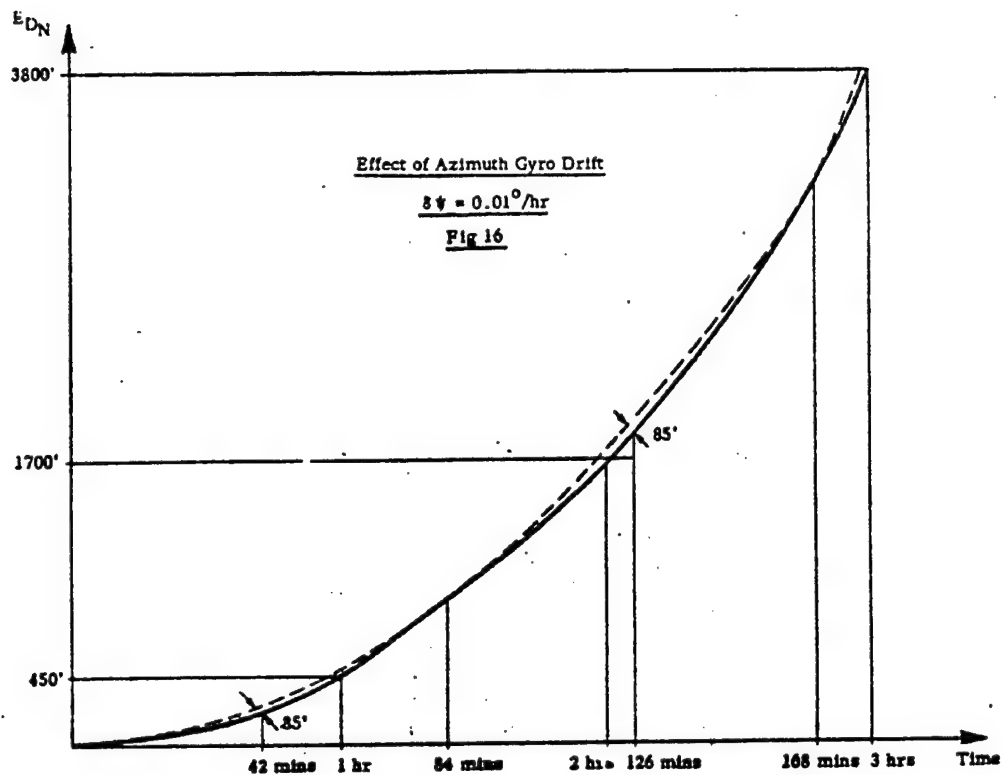
FIGURE 9.60   EFFECT OF AZIMUTH GYRO DRIFT

9.7.2.7   Summary of Errors

An examination of the equations derived in the previous paragraphs
and their curves show that error sources ε_a, ε_v and θ cause the system velo-
city error E_v to oscillate about a zero mean. This results in the distance
error E_D being BOUNDED by fixed values. However, for error sources δ_L, ψ, and
$\delta \psi$, the system velocity error E_v oscillates about a NON ZERO mean. Thus the
resulting oscillations of E_D are UNBOUNDED and will progressively increase
with time.

9.7.3   Errors in the Vertical Channel

A number of errors in the leveling channels are bounded by the
Schuler Oscillations. This is not the case in the vertical channel.

The vertical accelerometer must be corrected for acceleration due
to gravity (g_h) at the particular height before its output can be integrated
twice to give altitude change. However, gravity decreases with altitude
according to the law,

9.105

$$g_h = g_o - f(h)$$

and hence, errors in determining h (E_h) will affect the calculation of g_h. Errors in the altitude channel are not self limiting and the channel is unstable. It can be shown that

$$E_h = \frac{\varepsilon_v}{2a} e^{at}$$

For an ε_v of 0.1 ft/sec, E_h is 670 ft after 30 mins, but this increases to 15,000 ft after 1 hr (See Figure 9.61).
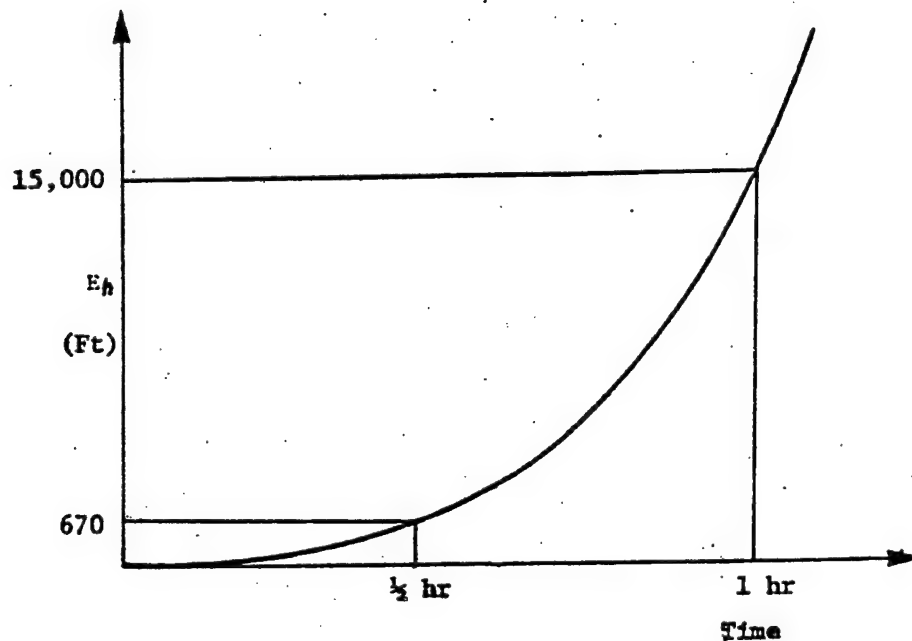
FIGURE 9.61 ALTITUDE ERROR DUE TO VERTICAL VELOCITY ERROR

9.106

9.7.4   Conclusion:

It has been shown that by mechanizing the leveling channels of an INS such that they are ANALOGS of the Schuler Pendulum, the platform will maintain itself perpendicular to the local vertical, even in the presence of accelerations.

It has also been shown that errors within the Schuler Loops will cause the platform to oscillate about the local vertical, and produce oscillatory velocity and distance errors as shown.

Input Error	Velocity Error Oscillations	Distance Error Oscillations
ε_a	Zero Mean	Bounded
ε_v	Zero Mean	Bounded
θ_o	Zero Mean	Bounded
δ_L	Non Zero Mean	Unbounded
ψ	Non Zero Mean	Unbounded
δ_ψ	Increasing Mean	Unbounded

It is possible to reduce these errors by:

a.   Making θ_o and ψ as small as possible by careful INITIAL ALIGNMENT.

b.   Reducing δ_L, ε_a, ε_v, and δ_ψ by careful design of components.

c.   Using the output of another reference to damp the platform oscillations or bound the errors.

9.8 INERTIAL NAVIGATION SYSTEM FLIGHT TESTS

9.8.1 INTRODUCTION

Testing of new INS systems within the Air Force is handled in two test phases. First, verification testing is accomplished by the 6585th Test Group Combined Inertial Guidance Test Facility (CIGTF) at Holloman AFB, New Mexico. These tests are flown in specially instrumented test bed aircraft. The second test phase is to evaluate the INS in the actual aircraft in which it is to be flown operationally. Testing of this nature is usually performed by the Combined Test Force (CTF). Operational suitability and accuracy are the two areas that are specifically checked by the CTF. This section provides details of the testing performed by the CTF, and then gives an overview of verification testing.

Inertial navigation system testing is often accomplished in conjunction with other aircraft tests. This approach is appropriate and cost effective, but INS data should not be considered completely "free" because the need to know actual aircraft position data is a requirement that can affect mission profile considerations.

If you find yourself in the position of being an INS project manager, the checklist in Table 9.7 may prove to be a useful aid.

9.8.2 TEST PLANNING

9.8.2.1 Requirements Definition

The INS test planning process begins with the definition of test requirements. Often this question is best approached by considering the reporting requirements.

ASCC Air Standard 53/11B (Ref 1), which specifies requirements for INS position error reporting, can help you establish the number of sorties, number of flying hours, and number of ground tests required, as well as the instrumentation and ground support requirements. Sufficient ground testing should be accomplished to establish the relationship of the ground accuracy to the inflight accuracy and to validate the ground maintenance procedures specified in the tech orders.

For inflight tests, plan on at least eight sorties of INS error data for every alignment method and navigation mode. Some flights, or portions of flights, should be dedicated to straight-and-level, non-maneuvering profiles, and some should be dedicated to operational profiles.

TABLE 9.7
INS PROGRAM MANAGER'S CHECKLIST

VERIFICATION (ACCURACY) TESTS:

    1. Ensure tracking facilities or airborne reference systems are available to provide time-space-position information to the accuracy required for determining spec compliance. Facilities available include cinetheodolites, radar, and laser tracking. Airborne reference systems include astro-inertial systems, CIRIS (see section 7.8.5), global positions system, photography, and air combat maneuvering (ACMI) ranges. The system or facility selected will be dependent upon budget, time constraints, location, and accuracy requirements.

    2. Ensure that flight profiles are designed to identify all error sources (see section 9.8.5).

    3. Are sufficient flights dedicated for INS testing to insure that the required statistical confidence levels can be met?

SUITABILITY TESTS:

    1. Do the flight profiles cover the entire operational envelope?
        a. G limits - both positive and negative
        b. Airspeed/Mach
        c. Maneuvers
        d. Environmental - temperature, size, electrical power, weight
        e. Time constraints
            1) alignment time vs scramble requirements
            2) length of flight vs allowable errors

2a. Are the intended operational uses sufficiently tested?

    a.   DISPLAYS

    b.   INPUT TASK AND LOCATION

    c.   READABILITY AND LOCATION

2b. Does the system properly integrate with the other systems?

    a.   AUTOPILOT

    b.   BOMB NAV

    c.   NAV COMPUTER

3. Is the MEANTIME between failures (MTBF) acceptable and operationally arrived at?

   4. Is the mean time between repair (MTBR) acceptable and operationally arrived at?

The following considerations should be addressed during the test:

    1. Is the maintenance being performed by Air Force personnel?

    2. Are the technical orders provided sufficient both for the maintenance and operational people?

    3. Are all types of alignments being tested?

    4. Are all degraded alignments which represent operational requirements being tested?

    5. All alignments should be made on different headings to ensure a good check on the alignment feature of the system.

    6. Is the alignment position on the ramp free from magnetic disturbance?

    7. Sufficient time between runs should be allowed for system cool down. Usually 12 hours.

    8. Ground runs should be made prior to and after a flight using one alignment. This allows identification of static errors.

    9. Data should be taken every 5 minutes during the flight. This data must be taken from the INS as well as the tracking facility. This allows a very accurate plot of system errors.

    10. All legs of the flight should either be 84.4 minutes of fractions of this time, i.e. 21.1, 42.2, etc.

    11. Are there any differences between operating on ground power and aircraft power?

12. Does the operational environment require a time delay on power interruptions?

13. Are operator errors minimized?

14. Have environmental aspects been addressed during the program? This is especially true if the aircraft with its INS must operate in either arctic or other harsh environments.

9.8.2.2 Test Method

The INS test method must be based on sound theoretical considerations. Since modern inertial navigation systems can take a variety of forms, as test director or test planner you must know your system: gimballed or strapdown platforms, mechanical or laser gyros, augmented or unaugmented. Each of these system implementations has its own characteristics and its own problem areas. Knowledge of the system will allow you to write a better test plan, one that will adequately exercise the system in the areas where its performance can be expected to be marginal.

Normally, the Flight Test Center does not test an INS that does not have a considerable amount of test data already available on it. That test data may be from the INS manufacturer's development testing, from testing conducted by the CIGTF, from the avionics development and integration test program of the airframe contractor, or from test reports on other aircraft with the same inertial system installed. Any system test should include consideration of data available from earlier tests. These data sources can be extremely helpful as you determine specific test objectives and methods, as well as for later comparison with your own data.

A key element in the proper design of any test is to understand the characteristics of the error. A conventional, unaugmented local vertical inertial navigation system exhibits bounded and unbounded errors which vary with the Schuler oscillation. Augmentation is often employed in an attempt to bound the error. The INS designer or system integrator establishes an "error budget," which identifies error sources and assigns a maximum error rate with each. Knowledge of the error budget for a given system is of great importance to anyone planning a test because it helps focus on particular system characteristics. In general, you should test for the

effects of temperature, accelerations, acrobatic flight, and alignment heading on position and velocity error. In some systems, moving from one hemisphere to another may present a problem, either in alignment or navigation, or both. This should be investigated if possible.

A major consideration in testing an inertial navigation system is how well it interfaces with the many other systems in the aircraft that require INS inputs. For example, sensors require attitude stabilization, ground speed, true ground track, etc. Additionally, the displays used to present INS data are usually separate subsystems, often designed and built by a company other than the INS manufacturer. Individual subsystems can be "hard wired" together with discrete connections for each parameter, or they can be tied together over a multiplex bus. In either case, the human factors assessment takes on increased importance when multiple subsystems are integrated. Finally, there is the possibility that the displayed data is not in agreement with calculated internal values. If INS data is acquired directly from within the INS, additional verification of the actual cockpit indications must be done.

Strapdown inertial platforms are becoming increasingly common in today's weapons systems. Although a strapdown platform has the same charac- teristic gyro and accelerometer errors as a gimballed platform, these errors act along the aircraft body axis only. As a result, the clear correlation between the error source and the position, velocity, and azimuth errors is reduced. Additionally, a strapdown system can be expected to have a larger share of its error budget allocated to computational errors than a gimballed system. Avionics systems have evolved to the point where the inertial measurement system is but one component of an integrated navigation system. This approach allows the use of less precise (and less expensive) inertial platforms, which, when combined in a Kalman state estimator with other navigation sources such as GPS, Doppler, air data, etc., can yield highly accurate navigation information. The idea is that if error sources such as gyro drift, accelerometer errors, etc., can be accurately estimated, they can also be compensated for and the overall system can yield accurate results.

An important consideration in data reduction is the accuracy of the tracking data. The Air Force Flight Test Center has tracking radars for measuring and recording aircraft actual position. Three instrumentation radar systems are available with accuracies suitable for some INS testing. The 6521 Range Capabilities Handbook (Ref 2) describes each system in detail. For tests of highly accurate navigation systems, the AFFTC tracking radars may not be sufficiently accurate. In this case, alternate methods of determining aircraft position, such as Global Positioning System (GPS) satellites, dedicated transponders, or photographic methods should be investigated. Bear in mind that the contractor may challenge the source of your truth data. For example, if the position of the system is fixed by flying over a surveyed point and taking a picture, the contractor will want to know how the data is arrived at from the picture and the associated proven accuracies of the photo system.

A final consideration in planning your test method is to decide on how the data will be gathered. ASCC 53/11B specifies that position data be taken every 5 minutes, not to exceed 10. An automatic data recording system is highly desirable for INS testing. Besides relieving the operator of the burden of recording parameter values at frequent intervals, an automatic system offers distinct advantages: (1) the possibility of automated data reduction because the data is already in machine-readable form, and (2) the possibility of recording additional parameters besides just position and velocity. For automatic systems, ensure that the recording system is capable of recording data for the full duration of the flight. In addition, some method of correlating the onboard data with the truth data is essential. This generally takes the form of continuously recorded IRIG time and/or audio tones that serve as event markers on both tapes. For manual systems, it generally becomes necessary to dedicate one crewmember to the data taking function. In accordance with ASCC 53/11B, results from at least eight complete sorties are required to make up a statistically valid sample.

All tests will require some form of data card, both to record data and to aid in cataloging and organizing results. Some sample cards for alignment and inflight data are contained in Figure 9.62 through 9.64.

1. Align mode _____

2. Instrumentation recorder ON

3. Function switch to align   Time _____

4. Enter coordinates and reset

5. Heat light out   Time _____

6. Record outside air temperature

    TEMP _____

7. Alignment complete   Time _____

8. System heading

    HDG _____

9. System magnetic variation

    MAG VAT _____

10. Select NAV position   Time _____

11. Instrumentation recorder OFF

FIGURE 9.62   ALIGNMENT TEST CARD – INSTRUMENTED AIRCRAFT

INERTIAL TEST CARD

1. At 5 minute intervals, turn instrumentation recorder ON
2. Record time
3. Wait a minimum of 15 seconds and transmit to SPORT "This is record number_____". Them activate the Tone and Event button for 3 sec.
4. Instrumentation recorder OFF

Record No.	Time
1	
2	
3	
4	
5	
6	
7	
etc.	

FIGURE 9.63   INFLIGHT TEST CARD INSTRUMENTED AIRCRAFT

INS FLIGHT LOG

DATE	FLIGHT NUMBER	TYPE ALIGNMENT	NAV TIME	LATITUDE ERROR	LONGITUDE ERROR	RADIAL ERROR	VELOCITY ERROR	DRIFT RATE	REMARKS

AFSC FORM 1858
JAN 61   PREVIOUS EDITION OF THIS FORM MAY BE USED.

GENERAL PURPOSE WORK SHEET (17" X 11")

AFSC (AAFB)

FIGURE 9.64   FLIGHT LOG (MANUAL DATA)

9.116

9.8.3 TEST CONDUCT

9.8.3.1 Ground Tests

INS ground testing generally has two parts: alignment tests and baseline position accuracy tests. For alignment tests, the objective is to exercise all available alignment modes. Results from a number of like tests can be combined to determine the mean time to align for a given mode. Record the timing of align phases under different conditions of initial aircraft heading and ambient temperature. Allow the system to thoroughly cool (at least 12 hours) between alignment tests. After shutdown, move the aircraft to a new heading to fully exercise the self-alignment capability. Document local wind conditions and any buffet or movement of the aircraft during align. Also note whether the aircraft is inside or outside of the hangar, and clear of large metal objects such as ground power units which could affect the alignment. Finally, assess the suitability of the system for any special mission requirements that may exist (i.e., helicopter operations, scramble, etc.).

Ground navigation tests should consist of at least eight runs of 42 minutes in NAVIGATE mode while stationary. Accomplish ground testing on both internal and external power, if possible. Park the aircraft over surveyed coordinates and record system position and velocity every 5 minutes. In addition, postflight ground runs should be accomplished in conjunction with inflight tests to identify system errors. Plan on at least a 21-minute postflight run time for the ground tests, using the same alignment as the inflight tests (i.e., Do not shut down after flight). Reduce the data in the same way as inflight data is reduced. Finally, evaluate the Built-In-Test/System Integrated Test (BIT/SIT) features of the system, with emphasis on capability for simple external verification of internal fault analysis.

9.8.3.2 Inflight Tests

Inflight tests should consist of both non-maneuvering and operationally-representative profiles. For non-maneuvering tests, attempt to limit excitation of errors to one axis only by flying east/west and north/south runs on separate missions. This will help establish a baseline

error profile which can be compared with ground data as well as operationally representative mission profiles. Fly at least eight missions, with data taken at 5 minute intervals.

One of the most important elements in the testing of integrated systems is the qualitative assessment of operational suitability. This evaluation is primarily a human factors evaluation. Assess the operator/system interface, including displays and controls, data entry and extraction, and location and functional grouping of components. Qualitatively evaluate the INS interface with other systems, such as Head Up Display (HUD), weapons computer, autopilot, etc. Establish some method of quantifying your qualitative data by using questionaires, workload analysis, or some other suitable means.

9.8.3.3 Maintaining Control of Your Test

As test planner or test conductor, you must maintain the integrity of your test against outside influences. The following discussion will identify areas of concern, but concrete solutions to these problems will vary depending on the particular situation.

The most common factors which oppose your control of the test fall into the following categories:

a. Control of Test Conditions By Advocates of the System Under Test (Contractors). A legitimate test must be independent and free of the influence of those with preconceived opinions about the test article. For an inertial navigation system test, alignment procedures and flight profiles are two areas which should be carefully controlled. If alignment data is to be accurate, the system must thoroughly cool (normally for 12 hours or more) prior to beginning the alignment. This can be difficult to ensure, especially if maintenance personnel are cleared to work on the system overnight, as is often the case in time-limited test programs. Additionally, the aircraft heading must be changed after system shutdown to fully exercise the alignment capability. These requirements are particularly important for gimballed platforms in which internal temperature gradients can vary with platform orientation. Airborne tests should include baseline non-maneuvering profiles as well as operationally representative profiles.

Guard against restrictions placed on allowable maneuvers or flight conditions. If INS tests are conducted too early in a program, i.e., during envelope expansion, the flight profiles may not be operationally representative. Insure that enough flights are flown for the data to be statistically valid.

b. Control of Midstream Maintenance. Quick-response repair capability is a must for system tests, particularly new or prototype systems which can have a relatively high failure rate. Midstream maintenance, however, often leads to problems of configuration control which can invalidate much of your data. This is particularly true in a developmental test in which changes can occur rapidly. Establish a rigorous procedure for configuration control early in your program, and stick with it. Establish a comprehensive cataloging procedure for tracking data products, and avoid the tendency to collect vast amounts of unidentifiable data.

c. Accommodating the Requirements of Unrelated Tests. INS testing is usually done in conjunction with other tests in order to maximize sortie productivity. This requirement can have an impact on aircraft availability, alignment procedures, and inflight profiles. You can attack this problem during the test planning process. Maintain the integrity of INS testing by establishing certain minimum dedicated INS tests, both ground and inflight. With this core of mandatory tests points, INS testing can proceed in conjunction with other tests without sacrificing data quality.

d. Control of Data Reduction. Do not allow an advocate of the system to reduce the data. If you are in charge of the test, you are in charge of data reduction. The contractor may want to independently reduce the data. Be prepared to defend your data reduction method if differences arise.

e. Ensuring Repeatability. Repeatability is fundamental to any test. The way to ensure repeatability is to thoroughly document the test procedures and be disciplined in the taking of data. Follow your configuration control procedures. If the test extends over a long period of time, the chances of losing control of configuration and of losing data integrity increase.

9.8.4 DATA REDUCTION

9.8.4.1 GM/RMS Method

ASCC Air Standard 53/11B explains the data reduction for position error using the so-called "GM/RMS method." The method is as follows:

1. Determine radial error as a function of time for at least eight test sorties. This error is found by comparing measured INS position with actual position. Computer routines are available at the Air Force Flight Test Center to perform this computation automatically. The result is a set of eight or more curves of radial error vs time, as shown in Figure 9.65.

2. Calculate the GM/RMS value for the ensemble at discrete times. A program which can be used in the Hewlett-Packard HP-41 programmable calculator to compute GM/RMS for a collection of radial errors in found in Figure 9.66.
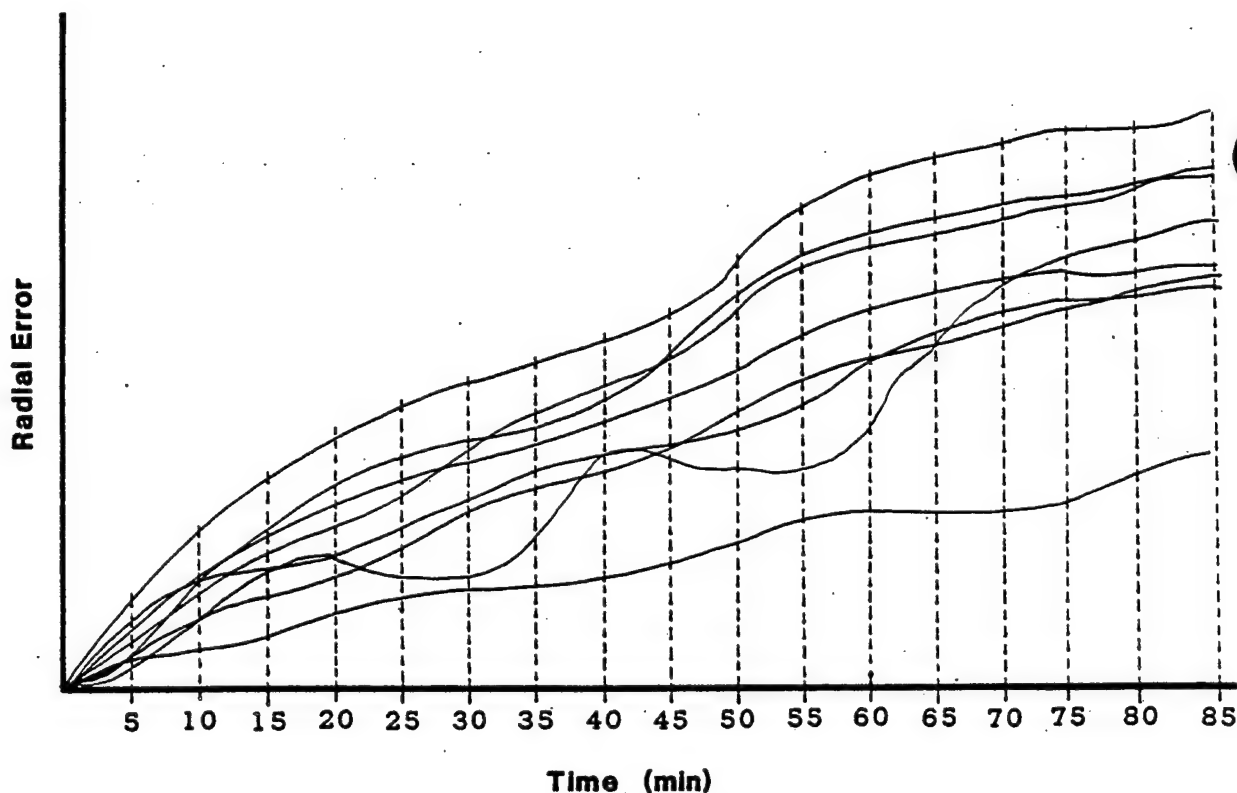

FIGURE 9.65 TYPICAL TIME HISTORIES FOR AN ENSEMBLE OF ERRORS

9.120

```
PRP "GM/RMS"

01◆LBL "GM/RMS"              28◆LBL 03
   02 1                      29 RCL 02
   03 STO 01                 30 RCL 01
   04 STO 02                 31 1/X
   05 0                      32 Y↑X
   66 STO 04                 33 STO 03
                            34 RCL 04
   07◆LBL 01                 35 RCL 01
   08 "ERROR "               36 /
   09 FIX 0                  37 SQRT
   10 ARCL 01                38 STO 05
   11 PROMPT                 39 /
   12 ST* 02                 40 STO 06
   13 X↑2                    41 FIX 2
   14 ST+ 04
   15 "N"                    42◆LBL 05
   16 ASTO Y                 43 "GM/RMS="
17 "MORE? Y/N"               44 ARCL 06
   18 AON                    45 PROMPT
   19 PROMPT                 46 "RMS="
   20 AOFF                   47 ARCL 05
   21 ASTO X                 48 PROMPT
   22 X=Y?                   49 GTO 05
   23 GTO 03                 50 END

   24◆LBL 02
   25 1
   26 ST+ 01
   27 GTO 01
```

FIGURE 9.66   GM/RMS COMPUTATION OF HP-41

3. Determine R(p)/RMS from Figure 9.67 for whatever percentile is desired. This value, R(p)/RMS, is the "normalized pth-percentile level of error", the Circular Error Probable (CEP) at the discrete time of calculation. Commonly, the 50th or 90th percentile level is specified. This normalized value should be converted to linear distance by multiplying by the RMS value. The result, R(90), the "90th percentile level of error," means that the position error in a given flight will be less than this value on 90% of flights (if the number of flights is large). It is also correct to say there is a 90% probability that the position error in a given flight will be less than this value.

4. Compute the 90th percentile level of error, R(90), for discrete times throughout the mission. Plot R(90) vs. time and fare a curve through the individual points. This represents the accuracy of the system to a 90% confidence level.

5. Most inertial navigation system contractural guarantees are expressed in terms of R(50). For determining specification compliance, compute and plot the R(50) value for the same data set. Plot the specified or guaranteed accuracy on the same plot.
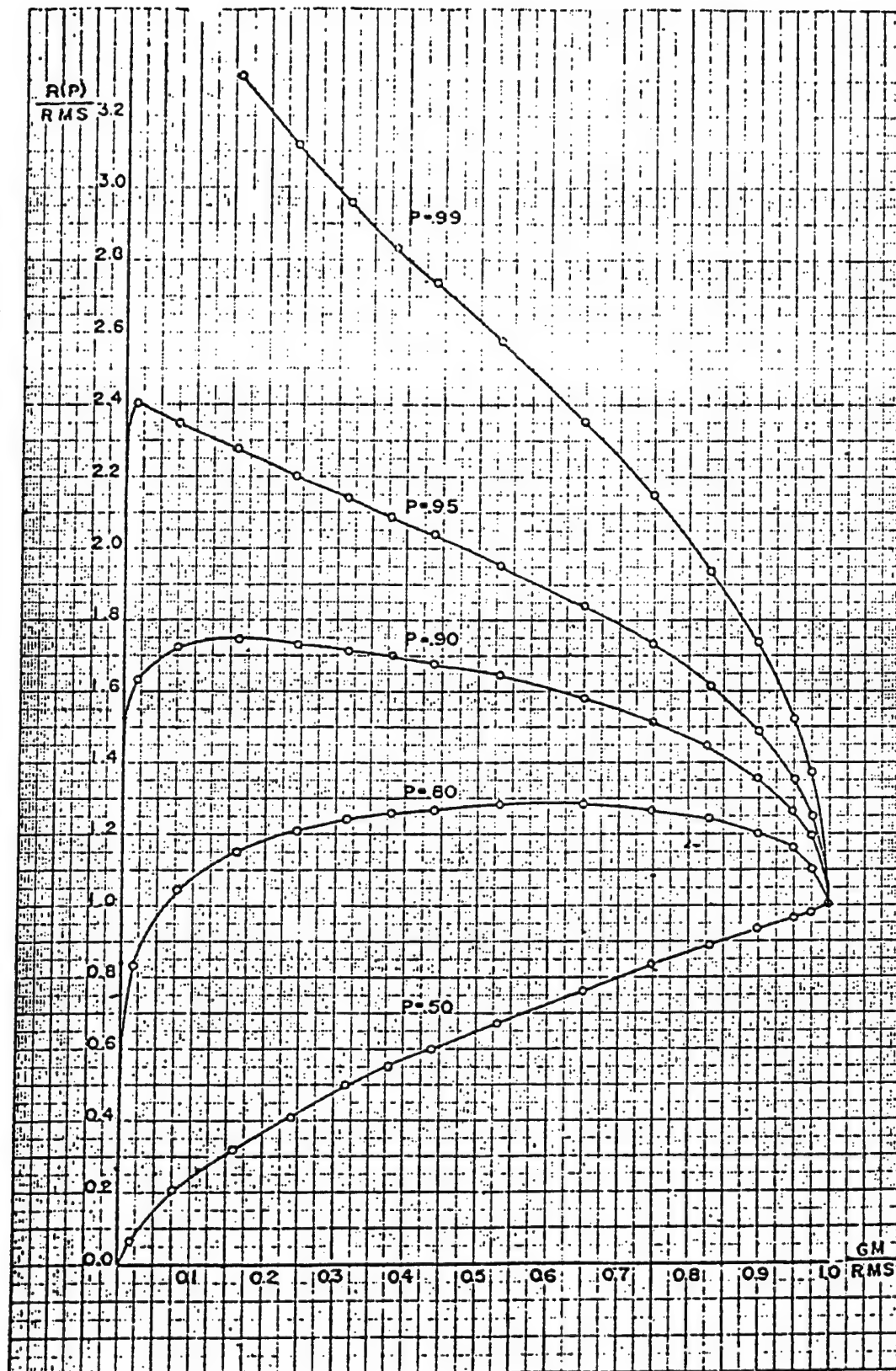
FIGURE 9.67   ERROR PERCENTILE CURVES

9.123

9.8.4.2 Circular Error Probable

The direct Circular Error Probable (CEP) plot of normalized terminal error is a method of data presentation that is sometimes requested. Radial error at the end of a flight is determined by comparing INS position with known coordinates of the aircraft parking spot. This value of radial error is normalized to some value of time, usually one hour of mission time. Limits must be placed on what constitutes a suitable sortie duration for this calculation. Sortie durations which vary from the desired duration by more than a specified percentage should not be accepted. This percentage limit must be specified in the test planning phase if this method of data presentation is planned. A large number of data points is required for this method to yield meaningful results.

A sample Terminal Error CEP plot is shown in Figure 9.68. A circle with radius equal to the specification CEP is overlaid on the plot of normalized latitude and longitude errors. Analysis of this data is best done by computer. The computer forms the ratio of points within the circle to total points. After the initial calculation, the computer should examine the distribution of error points with respect to the value of the calculated CEP. If the terminal error from any of the flights exceeds a three-sigma value of the CEP, that data point is temporarily suppressed and the CEP calculation is repeated.

9.8.5 VERIFICATION TESTING

Verification testing of any new INS is accomplished by the 6585th Test Group at Holloman AFB, New Mexico. The primary purpose of verification testing is to provide a basis for comparative analysis of the performance and operational suitability characteristics of a series of theoretically similar navigation systems. This is done by obtaining comparative results under nearly identical test conditions in a minimum amount of time. At the same time reliability testing is being accomplished to verify that system or component reliability is equal to or better than a specified minimum value. ADTC-TR-75-70 (Test Planning Information and Procedures for Testing Aircraft Navigation Systems) is the generalized test planning guide written by the 6585th Test Goup to help in the planning of all tests conducted by

them. The basic verification test outline from this guide is shown in
Figure 9.69. The objective of the verification is to establish a level of
statistical confidence in the performance of the system for its primary
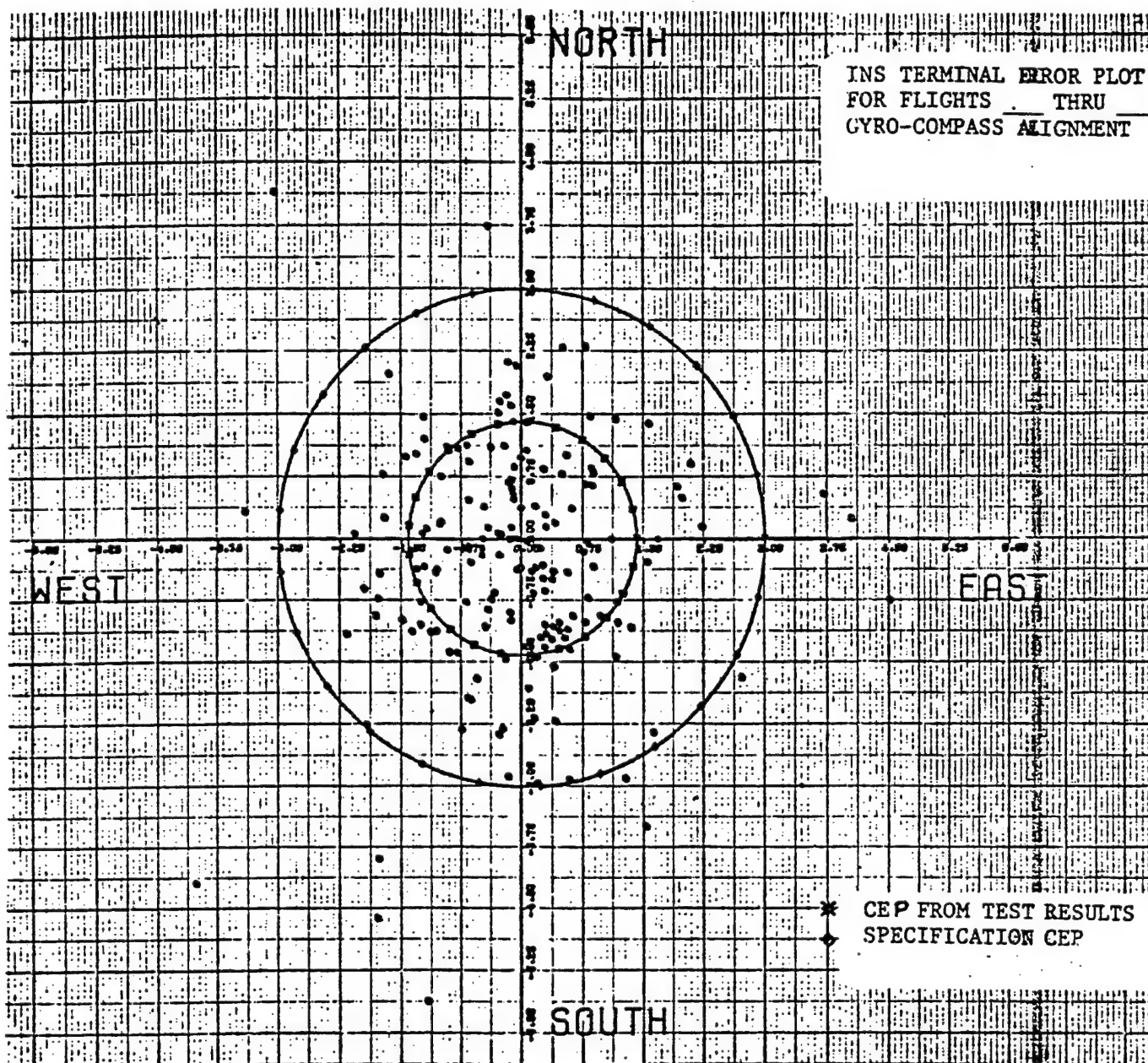operating mode in a typical operational environment.

FIGURE 9.68   TYPICAL TERMINAL ERROR CEP PLOT

PHASE 0

Predelivery Ground Tests
2 - Static Nav Tests

PHASE I-A

I-A Standard Ground Tests
1-2 Functional Checkout Tests
2 Static NAV Tests
3 Scorsby Tests
1 Heading Sensitivity Tests

PHASE I-B

I-B Special Ground Tests
0-3 Special Analysis Tests
0-3 Special Application Tests

TOTALS:
7-15 Tests
4-8 Weeks

PHASE II

II Standard NC-141A Flight Tests
1-2 Functional Checkout Flights
6 West 84 Min Cruise Profile and Return
6 North 84 Min Cruise Profile and Return
3 East 84 Min Cruise Profile and Return
1-2 Terminate at a Distant Point/R.O.N./& Return
0-3 Special Analysis

TOTALS:
17-22 Flights
54-72 Flying Hours
8-12 Weeks

SPECIAL MISSION APPLICATION FLIGHT TEST PHASE

PHASE III

PHASE III

III-A UH-1H Helicopter Flight Tests
1-2 Functional Checkout Flights
6 East 42 Min Cruise Profiles and Return
6 North 42 Min Cruise Profiles and Return
6 East Terrain Mapping Missions
0-6 Special Analysis Flights

TOTALS:
19-26 Flights
29-39 Flying Hours
8-10 Weeks

PROGRAM TOTALS:
69-97 Tests
115-218 Flying Hours
32-50 Weeks
8-12 Months

PHASE III

III-B RF-4C Fighter Flight Tests
1-2 Functional Checkout Flights
6 West 42 Min Cruise Profiles and Return
6 West 42 Min Cruise/Simulate Ordnance
       Delivery Profiles and Return
6 West 42 Min Cruise/Simulate Air Combat
       Maneuvers and Return
2-4 Special Analysis Flights

TOTALS:
21-24 Flights
36-41 Flying Hours
8-12 Weeks

PHASE III

III-C Extended NC-141A Cargo Flight Tests
0 Functional Checkout Flights
2-3 West/NW 168 Min Cruise Profiles & Return
2-3 East 168 Min Cruise Profiles & Return
1 East/SE/terminate at distant point/
       R.O.N./& Return
0-3 Special Analysis Flights
2-3 North 168 Min Cruise Profiles & Return

TOTALS:
7-13 Flights
48-84 Flying Hours
5-9 Weeks

FIGURE 9.69   BASIC VERIFICATION TEST OUTLINE

9.8.5.1 Verification Test FLight Profiles

The perfect verification flight profile would accomplish the following:

1. It would provide a constant readout of the acceleration, velocity, and position errors.

2. It would identify the various error sources.

3. It would insure that no errors were masked or lost during the conduct of the test due to flight paths.

4. It would be general enough that all systems could be flown over it in order to provide a comparison between all systems.

Before this perfect profile can be flown, certain real life constraints must be considered. They are:

1. The inability to measure acceleration without biasing it.

2. The difficulty of determining the source of an error.

3. The limitations on the ability to accurately determine the position of the behicle by an independent source.

4. The fuel restraints of various aircraft.

When these constraints are imposed on the perfect flight profile, the actual flight path takes on the following dimensions:

1. The flight profile becomes very important when testing to establish system performance. In the past, radar tracking facilities were used to establish the position and velocity of the test aircraft and thus the INS system. The accuracies of such a method for tracking the aircraft was limited (approximately 200 ft at 30,000 ft altitude). Data turnaround was 2 to 3 days. Surveyed checkpoints that are photographed in the air is another method used to establish the aircraft position. Accuracies for this method vary with altitude and data is available within 24 hours. The latest system for flight profile control is the Completely Integrated Reference Instrumentation System (CIRIS). CIRIS provides a highly accurate position, velocity, and altitude reference over a long flight path for real-time use. CIRIS is carried as an instrumentation pallet on the NC141A or center-line pod on F-4 test beds. Reference data from CIRIS is accurate to 13 feet in the horizontal axes for position and to .1 ft/sec for velocity. The only flight path limitation placed on CIRIS is the availability of surveyed sites

for the placement of specialized ground based transponders required by the system.

    2. Ideally 84.4 minutes legs would be flown, however some aircraft particularly fighter aircraft, cannot fly that long. Therefore a fighter profile usually has 21.1 minute legs and the multi-engine aircraft usually have 84.4 minute legs or multiples thereof.

    3. Since error analysis is a very complicated process, the profile must help isolate the various error sources. This is accomplished by exciting only one channel of the platform at a time, and assuming that the non-excited channel is good thereby forcing all the errors to occur in the excited channel and by conducting ground runs to determine the static errors. Hence, the verification flight profile would look like the following:

    a. One profile would go North-South along a route depicted in Figure 9.70, with either 84 or 168 minute outbound legs.

    b. One profile would go East-West along a route depicted in Figure 9.70, with either 84 or 168 minute outbound legs.

    c. Both routes would start with a ground alignment.

    d. Next the flight would proceed in a cardinal direction for 84 minutes at an operational altitude. This would identify errors sensitive to horizontal motion.

    e. A 180° turn would then be made and the path would repeat itself. THis is done to see if the errors cancel themselves out.

    f. Finally a 21 minute ground run would be performed after the flight. This provides quality data at the end of the flight for analysis.
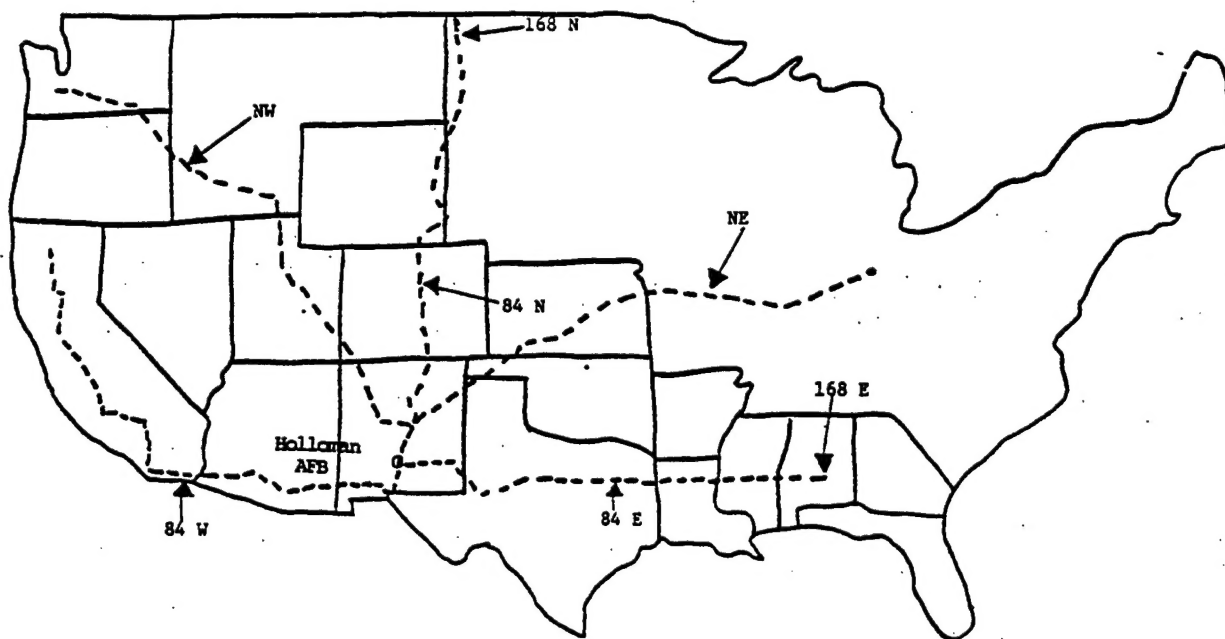
FIGURE 9.70   INS VERIFICATION FLIGHT PROFILES

REFERENCES

1. ASCC Air Standard 53/11B, 15 August 1968.

2. 6521 Range Capabilities Handbook, Air Force Flight Test Center, 15 June 1985.